

# Trends in micropollutant biotransformation along a solids retention time gradient

---

## SUPPORTING INFORMATION

Stefan Achermann,<sup>1,2</sup> Per Falås,<sup>1,3</sup> Adriano Joss,<sup>1</sup> Cresten B. Mansfeldt,<sup>1</sup> Yujie Men,<sup>1,4</sup> Bernadette Vogler,<sup>1</sup> Kathrin Fenner\*,<sup>1,2,5</sup>

<sup>1</sup>Eawag, Swiss Federal Institute of Aquatic Science and Technology, 8600 Dübendorf, Switzerland.

<sup>2</sup>Institute of Biogeochemistry and Pollutant Dynamics, ETH Zürich, 8092 Zürich, Switzerland.

<sup>3</sup>Department of Chemical Engineering, Lund University, 221 00 Lund, Sweden. <sup>4</sup>Department of Civil and Environmental Engineering, University of Illinois at Urbana-Champaign, Urbana, IL 61801, USA.

<sup>5</sup>Department of Chemistry, University of Zürich, 8057 Zürich, Switzerland.

\*Corresponding author (email: [kathrin.fenner@eawag.ch](mailto:kathrin.fenner@eawag.ch) )

This supporting information (SI) is organized in 8 sections (S1-S8) with a total of 73 pages and comprises 9 figures (Figure S1-S9) and 22 tables (Table S1-S22). In section S8, measured spectra are provided for 27 transformation products.

20    **Contents**

21	S1	Inoculation and operation of sequencing batch reactors.....	3
22	S2	TSS, pH, nitrogen and COD measurements .....	5
23	S3	Substance selection.....	8
24	S4	Biotransformation batch experiments.....	12
25	S5	Chemical analysis using LC-HRMS.....	15
26	S6	Biotransformation rate constants .....	17
27	S7	Transformation products.....	23
28	S8	MS2 spectra .....	44
29		References .....	72

30

31

## S1 Inoculation and operation of sequencing batch reactors

**Inoculation:** The sequencing batch reactors were inoculated with activated sludge collected from the nitrification tank (operated at 10 d SRT) of a Swiss full-scale wastewater treatment plant (WWTP Niederglatt, dimension: 40,000 population equivalents) receiving mostly municipal (and approximately 5% industrial) wastewater.

**Operation:** The sequencing batch reactors (SBRs) were operated in 4 h cycles comprising the following phases: a) A settling phase: 30 min, (b) a discharge phase: 10 min (discharge of supernatant until a volume of 8 L remained in the reactors), (c) a feed phase: 20 min (wastewater was pumped into the reactors to reach again a total volume of 12 L), and (d) an aerated reaction phase: 3 h. To adjust the different SRTs, different portions of activated sludge were withdrawn from the six reactors according to Table S1. The sludge was withdrawn from the stirred reactors at the end of a cycle (between the aerated reaction phase and a settling phase). The startup phase of 48 days allowed all reactors to acclimatize for more than 3 times their operational SRT which previously has been applied as criterion to reach steady state.<sup>1</sup> In total, the six reactors were operated for 360 days. A picture of the reactor setup is provided in Figure S1.

**Table S1:** Activated sludge withdrawal to adjust the different SRTs.

Reactor	SRT [d]	Reactor volume [L]	Sludge withdrawal [L/d]	Number of sludge withdrawals per day	Volume per withdrawal event [L]
R1	1	12	12	6	2
R2	3	12	4	2	2
R3	5	12	2.4	2	1.2
R4	7	12	1.7	1	1.7
R5	10	12	1.2	1	1.2
R6	15	12	0.8	1	0.8



**Figure S1:** Photograph of the reactor setup.

## S2 TSS, pH, nitrogen and COD measurements

**Measurements during sequencing batch reactor operation:** During the initial reactor startup phase until Exp1 was started (48 days after start of reactor operation) and before Exp2 was conducted (started on day 187), total suspended solids (TSS) was measured at several time points (Table S2). Additionally, during the reactor startup phase, COD and nitrogen species were measured (Table S3) by filtering (0.45 µm regenerated cellulose syringe filters, C. Roth) and analyzing AS samples using the following methods: Ion chromatograph 881Compact IC Pro (Metrohm) for  $\text{NO}_2^-$  and  $\text{NO}_3^-$ , FIAstar 5000 Analyzer (FOSS) for  $\text{NH}_4^+$  and Hach Lange test cuvettes (LCK314) for chemical oxygen demand (COD). On day 14, pH was measured: 7.7 (1 d SRT), 7.7 (3 d SRT), 7.6 (5 d SRT), 7.6 (7 d SRT), 7.5 (10 d SRT), and 7.5 (15 d SRT).

**Table S2:** TSS measured during startup phase and prior to Exp2.

day	TSS <sup>a</sup> [g/L]					
	SRT 1 d	SRT 3 d	SRT 5 d	SRT 7 d	SRT 10 d	SRT 15 d
0	3.40	3.40	3.40	3.40	3.40	3.40
7	0.20	1.33	1.70	1.96	2.88	3.14
14	0.85	1.37	2.34	3.19	4.06	4.72
21	0.42	0.63	1.20	1.32	2.29	3.26
42	0.84	0.69	0.79	1.80	2.01	3.36
48	0.22	0.55	0.62	1.49	2.11	2.70
Exp1: 48						
176	0.17	0.28	0.64	1.21	1.39	0.95
182	0.12	0.34	0.55	1.06	1.16	1.92
184	0.24	0.48	0.77	1.05	1.57	2.29
Exp2: 187						

<sup>a</sup>For TSS measurements, AS was sampled (1 d SRT: 150 mL, 3,5 d SRT: 100 mL, 7,10,15 d SRT: 50 mL) and the filtered solids dried (105 °C) to determine the dry weight per sampled AS volume as described elsewhere.<sup>2</sup>

**Table S3:** Nitrogen ( $\text{NH}_4^+$ ,  $\text{NO}_2^-$ ,  $\text{NO}_3^-$ ) and COD measurements during the reactor startup phase.

	day	influent	SRT 1 d	SRT 3 d	SRT 5 d	SRT 7 d	SRT 10 d	SRT 15 d
NH <sub>4</sub> -N (mg/L)	14	18.6	16.8	5.9	3.3	3.7	1.9	1.6
	21	31.2	25.3	18.8	2.6	0.65	0	0
	28	15.9	11.7	3.4	0	0	0	0
	42	30.6	27.3	18.7	4.9	0.2	0	0
	47	29.6	25.6	26.8	20.6	0	0	0
NO <sub>2</sub> -N (mg/L)	14	<0.2	<0.2	<0.2	1.8	1.9	0.6	0.9
	21	<0.2	<0.2	1.7	4.2	2.2	0.3	<0.2
	28	<0.2	0.72	5.7	3.5	<0.2	<0.2	<0.2
	42	<0.2	<0.2	<0.2	8.5	1.6	1	<0.2
	47	<0.2	<0.2	<0.2	0.6	3.8	0.6	<0.2
NO <sub>3</sub> -N (mg/L)	14	<0.2	<0.2	2.8	13.1	12.7	16	14.8
	21	<0.2	<0.2	0.2	10	14	17.8	17.5
	28	<0.2	0.38	0.73	6.4	9.1	11.1	11.2
	42	<0.2	0.47	2.7	7.3	17.4	17.9	21.2
	47	<0.2	0.23	0.55	2.2	16.5	22.1	23.9
COD (mg/L)	14	239	49.9	42.4	26.9	29.1	23.1	22.7
	21	148	41.5	37.1	31	28.1	23.9	27
	28	118	27.9	29.5	24.5	20.4	17.9	18.3
	42	125	34.3	28.9	35.1	20	18.5	18.1

**Measurements during Experiments:** During the biotransformation batch experiments Exp1 and Exp2, measurements of TSS, pH, nitrifying activity and oxygen uptake rate (OUR) were conducted (Tables S4 and S5). Measurements of  $\text{NH}_4^+\text{-N}$ ,  $\text{NO}_2^-\text{-N}$  and  $\text{NO}_3^-\text{-N}$  during ExpOx are shown in Figure S2. During ExpOx, the pH remained in the range between 7.5 and 8.5.

**Normalization of biotransformation rate constants:** Previous comparisons of TSS and volatile suspended solids (VSS) measurements have shown that fractions of non-active cell material (organic or inorganic) can vary substantially and typically increase with increasing SRT.<sup>3</sup> This could potentially lead to an underestimation of positive effects of SRT on  $k_{\text{bio}}$  when normalizing rate constants with TSS. Therefore, we performed VSS measurements for Exp1 (Table S4), which confirmed the expected increasing differences between TSS and VSS values at higher SRTs. However, since these differences were always below 10%, they were not deemed relevant for the purpose of our study and we remained with TSS normalization. As an alternative to normalization by suspended solids, rate constants could be normalized by measures of microbial activity. In membrane bioreactors (MBRs), Maeng *et al.*<sup>4</sup> showed that the ATP concentration per gram VSS decreased with increasing SRT, potentially leading to a further underestimation of positive effects of SRT on  $k_{\text{bio}}$  if normalized with TSS instead of measures of biomass activity.

**Table S4:** TSS, VSS, pH, nitrifying activity and OUR measured during Exp1.

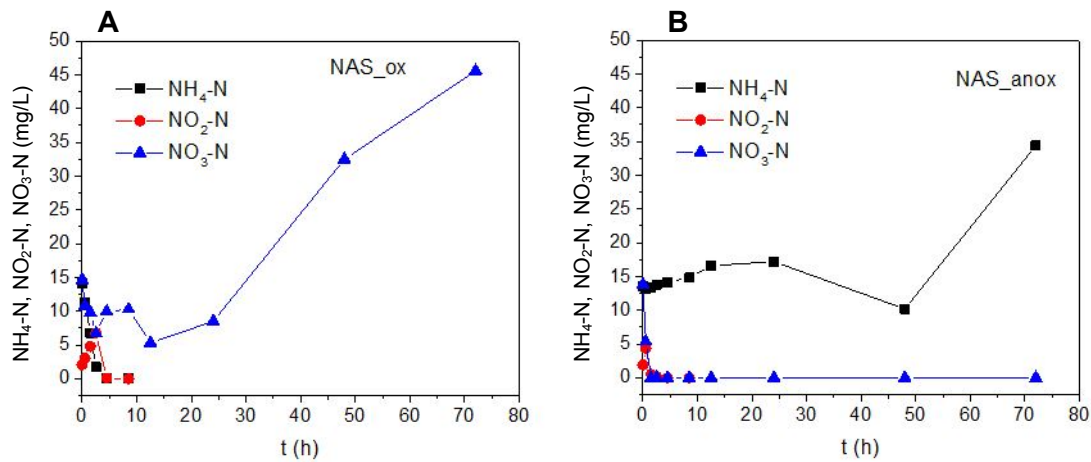
SRT [d]	solids concentration			pH <sup>b</sup>			Nitrification (0-4h) [mg( $\text{NO}_2\text{-N}+\text{NO}_3\text{-N}$ )/(h g <sub>TSS</sub> )] <sup>c</sup>	OUR (2 h) [mg O <sub>2</sub> /(h g <sub>TSS</sub> )] <sup>d</sup>	Temperature <sup>e</sup> [°C]
	TSS <sup>a</sup> [g/L]	VSS [g/L]	VSS/TSS	-1.5 h	7 h	49 h			
1	0.43±0.03	0.42±0.03	0.98	7.65	7.96	7.72	0	13.37	18.5 ± 0.7
3	1.1±0.05	1.04±0.05	0.94	7.63	7.88	7.55	0.17	11.07	18.0 ± 0.7
5	1.23±0.03	1.16±0.02	0.94	7.66	7.84	7.58	0.44	9.46	17.9 ± 0.8
7	1.49±0.02	1.44±0.02	0.97	7.54	7.65	7.47	2.2	21.93	17.9 ± 0.6
10	2.11±0.06	1.95±0.06	0.92	7.57	7.61	7.37	2.23	12.86	18.1 ± 0.7
15	2.7±0.04	2.43±0.03	0.90	7.56	7.58	7.35	1.79	11.21	18.4 ± 0.7

<sup>a</sup>For TSS and VSS measurements (means and standard deviations from triplicate measurements), AS was sampled (1 d SRT: 150 mL; 3, 5 d SRT: 100 mL; 7, 10, 15 d SRT: 50 mL) and processed as described elsewhere.<sup>2</sup> In short, for the measurement of VSS, the loss on ignition (at 550 °C) of the mass of measured TSS was quantified, so the inert matter is not considered. <sup>b</sup>pH was measured 1.5 hours prior to and 7 and 49 hours after the chemicals were spiked to the reactors. <sup>c</sup>Measures for the nitrifying activity were obtained by calculating linear regression coefficients for the formation of the summed  $\text{NO}_2^-\text{-N}+\text{NO}_3^-\text{-N}$ . <sup>d</sup>The OUR was determined as the slope of the O<sub>2</sub> decline with time measured by the dissolved oxygen (DO) sensors of the 12 L reactors. <sup>e</sup>Temperature was continuously recorded within the two weeks before Exp1 was started. Here, the mean and standard deviation of these records is given.

**Table S5:** TSS, pH, nitrifying activity and OUR measured during Exp2.

SRT [d]	solids concentration		pH		Nitrifying activity (0-4 h) [mg(NO <sub>2</sub> -N + NO <sub>3</sub> -N)/(h × g <sub>TSS</sub> )] <sup>b</sup>	OUR (1 h) [mg O <sub>2</sub> /(h × g <sub>TSS</sub> )] <sup>c</sup>	Temperature <sup>d</sup> [°C]
	TSS <sup>a</sup> [g/L]		12h	28.5h			
1	1.47 ± 0.15		8.11	8.15	0.35	57.52	19.6 ± 0.8
3	2.02 ± 0.22		8.06	8.00	2.62	35.97	19.0 ± 0.9
5	1.93 ± 0.1		8.04	8.16	2.81	20.76	19.0 ± 0.9
7	2.46 ± 0.09		8.09	7.94	3.66	27.7	19.1 ± 1.0
10	2.15 ± 0.12		8.23	8.18	3.61	21.29	19.2 ± 1.0
15	2.11 ± 0.13		8.25	8.21	3.28	21.65	19.7 ± 0.9

<sup>a</sup>For TSS and VSS measurements (means and standard deviations from triplicate measurements), AS was sampled (10 mL) and processed as described elsewhere.<sup>2</sup> <sup>b</sup>Measures for the nitrifying activity were obtained by calculating linear regression coefficients for the formation of the summed NO<sub>2</sub><sup>-</sup>-N + NO<sub>3</sub><sup>-</sup>-N. <sup>c</sup>The OUR was determined as the slope of the O<sub>2</sub> decline with time as described elsewhere.<sup>5</sup> <sup>d</sup>Temperature was continuously recorded within the two weeks before Exp2 was started. Here, the mean and standard deviation of these records is given.



**Figure S2:** Under aerobic conditions (A), nitrifying activity was observed (i.e., the available NH<sub>4</sub><sup>+</sup> and NO<sub>2</sub><sup>-</sup> at the beginning of the experiment was converted to NO<sub>3</sub><sup>-</sup>). With suppression of oxygen supply (B), NO<sub>2</sub><sup>-</sup> and NO<sub>3</sub><sup>-</sup> present at the beginning of the experiment were rapidly depleted in the first hours of the experiment. Thereafter, anaerobic conditions (absence of electron-accepting nitrogen or oxygen species) prevailed until the end of the experiment.

### S3 Substance selection

Reference standards were obtained from Sigma-Aldrich GmbH, Dr. Ehrenstorfer GmbH, HPC Standards GmbH, Honeywell Specialty Chemicals, and Toronto Research Chemicals. Stock solutions in ethanol or methanol with a concentration of 1 g/L were prepared for each compound. For the biotransformation experiments, the individual stock solutions were combined and mixed. First, in an intermediate step, 6 mixes (Mix 1-6, each comprising 10–20 MPs, Table 1) were prepared and thereafter combined as the final mix used for spiking. To minimize the addition of organic solvents (final concentration after spiking <20 mg/L), the majority of the organic solvent was evaporated using a gentle airstream of nitrogen, and the concentrated MP solution was diluted with water prior to addition to the biotransformation reactors. In Table S6, all investigated micropollutants are listed and the internal standards used for quantification are indicated. Additionally, initial biotransformation reactions predicted by EAWAG-PPS are indicated as biotransformation rule numbers, which are further explained in Table S7. Molecular structures and analytical details are provided in section S7 on transformation product analysis. Finally, for a subset of substances biomass-normalized second-order rate constants  $k_{\text{bio}}$  are given in Table S6. Details on their calculation are given in the main text, in section S6 and in the footnote of Table S6.



128 **Table S6:** List of all substances spiked and analyzed.

MP name	Mix <sup>a</sup>	allocated ISTD	triggered btrules <sup>b</sup>	Exp1 <sup>c</sup>	r <sup>2</sup> <sub>d</sub> (Exp1)	Exp2 <sup>c</sup>	r <sup>2</sup> <sub>d</sub> (Exp2)
Acesulfame		Acesulfam-D4	144	A	0.46-0.99	A	0.30-0.99
Acetamipride	MIX 4	Dimethoat-D6	028,350	A	0.75-1.00	A	0.42-0.98
Alachlor	MIX 2	Alachlor-D13	022,023,242,243	A	0.99-1.00	A	0.97-1.00
Amisulpride	MIX 5	Amisulpride-D5	023,063,065,067,243	B		A	0.31-0.96
Asulam	MIX 6	Atenolol-acid D5	144,318			C1	
Atenolol	MIX 1	Atenolol-D7	002,023,027,063	A	1.00-1.00	A	0.94-0.99
Atrazine	MIX 2	Atrazin-D5	330,339	B		B	
Azoxystrobin	MIX 2	Bezafibrat-D4	024,030	A1	0.48-0.99	A1	0.25-0.99
Bezafibrate	MIX 1	Bezafibrat-D4	051,067,243	A	0.92-0.98	A	0.80-0.93
Bicalutamide	MIX 6	Bicalutamid-D4	030,065,067			B	
Boscalid	MIX 1	Bezafibrat-D4	067	C3	0.13-0.75	C3	0.29-0.83
Bromoxynil	MIX 5	Bicalutamid-D4	030	A	0.85-1.00	A	0.81-0.98
Capecitabine	MIX 4	Atrazin-D5	002,318	A	0.98-1.00	A	0.90-0.99
Carbendazim	MIX 4	Carbendazim-D4	318	B		A	0.37-0.93
Carbetamide	MIX 1	Furosemid-D5	067,318,334	C1		C1	
Chlortoluron	MIX 1	Chlortoluron-D6	036,068,243	A	0.05-0.97	A	0.27-0.97
Cilastatin	MIX 3	Clothianidin-D3	051,063,067,162,241,259	B		B1	
Citalopram	MIX 4	Citalopram-D6	030,063,073	C3	0.56-0.90	C3	0.60-0.77
Clofibric acid	MIX 4	Clofibrinsaeure-D4	005,051	A	0.90-0.98	A	0.23-0.99
Clomazone	MIX 4	Naproxen-D3	243	B		C3	0.01-0.31
Clozapine	MIX 6	Clozapin-D8	065,350			C3	NA
Crotamiton	MIX 6	Dimethenamid-D3	036,243			B	
Cyclamate		Cyclamat-D11	144			B1	
Cyromazine	MIX 2	Morphin-D3	330,339	B		B	
Deprenyl	MIX 5	Diazinon-D10	063	C3	0.50-0.98	C3	0.68-0.96
Diazepam	MIX 1	Diazepam-D5	243,391	B		B	
Dicamba	MIX 5	Bicalutamid-D4	023,072	B		B	
Diclofenac	MIX 4	Diclofenac-D4	065			B	
Dimefuron	MIX 6	Diuron-D6	068,243			A	
Dimethenamide	MIX 5	Dimethenamid-D3	022,023,036,162,243	A	0.98-1.00	A	0.85-0.99
Diuron	MIX 1	Diuron-D6	068,243	A	0.65-0.99	A	0.34-0.96
Doxylamine	MIX 5	Sulfapyridin-D4	023,063	C3	0.62-0.83	C3	0.09-0.69
Ethofumesate	MIX 2	Bezafibrat-D4	023,158	C3	0.55-0.84	C3	0.16-0.57
Fenhexamid	MIX 5	Terbutylazin-D5	067	A	0.85-1.00	A1	0.80-0.99
Fenoxycarb	MIX 4	Terbutylazin-D5	318,334,374			B1	
Fipronil	MIX 4	Mecoprop-D6	030,193	C1		B	
Flonicamid	MIX 6	Saccharin-13C6	030,067,243			B	
Flufenacet	MIX 2	Terbutylazin-D5	023,065,162,243	A	0.97-1.00	A1	0.91-0.99
Fluoxetine	MIX 2	Fluoxetine-D5	023,063	C3	0.29-0.98	C3	0.28-0.85
Furosemide	MIX 3	Furosemid-D5	063,144,359,375	A	0.56-1.00	A	0.47-0.96
Gemfibrozil	MIX 4	Diazinon-D10	023,036,242	A	0.86-0.95	A	0.89-0.97
Hydrochlorothiazide	MIX 3	Acesulfam-D4	063,144	B		B	
Ibuprofen	MIX 4	Ibuprofen-D3	051,241,242,333	C3	0.00-0.97	C3	0.05-0.99
Imidacloprid	MIX 4	Imidacloprid-D4	420	B		B	
Indomethacin	MIX 4	Indomethacin-D4	023,036,242	B		C2	
Iprovalicarb	MIX 6	Terbutylazin-D5	067,318			A1	0.27-0.97
Irgarol	MIX 6	Irgarol-D9	330,339			A1	0.50-0.98
Isoproturon	MIX 1	Isoproturon-D6	068,241,243	B		A	0.64-0.96
Ketoprofen	MIX 4	Atrazin-D5	353	A	0.00-0.99	A	0.77-0.97
Kresoxim-methyl	MIX 6	Diclofenac-D4	024,036			C2	
Levamisole	MIX 3	Atrazin-D5	063,162,259	C3	0.61-0.88	C3	0.72-0.97
Levetiracetam	MIX 1	Levetiracetam-D3	027,242,243,334	A	0.45-0.98	A	0.72-0.97
Lidocaine	MIX 3	Lidocain-D10	063,067	C3	0.16-0.89	C3	0.52-0.89
Lovastatin	MIX 6	Fenofibrate-D6	002,024			C3	NA
Mecoprop	MIX 4	Mecoprop-D6	023,036	B		C2	
Metalaxyl	MIX 6	Bicalutamid-D4	024,036,243			B	
Metolachlor	MIX 2	Metolachlor-D6	022,023,036,242,243	A	0.94-1.00	A	0.87-0.99
Metoprolol		Metoprolol-D7	002,023,063	A	0.86-0.98	A	0.68-0.89
Metoxuron	MIX 6	Carbamazepin-10-11-epoxid-13C,D2	023,068,243			A	0.09-0.91
Mianserin	MIX 3	Pirimicarb D6	063,065	C3	0.52-0.98	C3	0.14-0.83

Monuron	MIX 6	Atrazin-D5	068,243			C1	
N,N-dimethyl-4-chlorobenzamide (MMclB)	MIX 6	Clotrimazol-D5	243			A	0.60-0.97
Napropamide	MIX 1	Terbutylazin-D5	023,243	C3	0.74-0.92	C3	0.90-0.96
Naproxen	MIX 2	Naproxen-d3	023,241	A	0.88-1.00	A	0.60-0.99
N-butyl-N-ethyl-4-chlorobenzamide (BEclB)	MIX 6	Terbutylazin-D5	242,243,334			A	0.82-0.97
N-N-diethyl-3-methylbenzamide (DEET)	MIX 1	DEET-D10	036,243	A	0.95-0.99	A	0.94-0.99
Oseltamivir	MIX 2	Clodogrel-(+/-)-D4	021,024,067,243	B		C3	0.74-0.88
Pargyline	MIX 3	Diazinon-D10	063,353	A1	0.64-0.99	A1	0.54-0.90
Perindopril	MIX 5	Atomoxetin-d3	024	B		B	
Pheniramine	MIX 3	Levetiracetam-D3	063,241	C3	0.79-0.91	C3	0.60-0.94
Propachlor	MIX 2	Atrazin-D5	022,065,243	A	1.00-1.00	A	0.98-0.99
Propranolol	MIX 4	Citalopram-D6	002,023,063	C3	0.46-0.91	C3	0.61-0.76
Propyzamide	MIX 1	Terbutylazin-D5	067	B		C1	
Ranitidine	MIX 3	Ranitidin-D6	063,162,259	A	0.99-1.00	A	0.95-0.99
Rufinamide	MIX 1	Clothianidin-D3	027	A	0.73-1.00	A1	0.92-0.99
Saccharin		Saccharin-13C6	005,144,425			B1	
Simeton	MIX 5	Sulfamethoxazol-D4	330,339	B		B	
Sulfadiazine	MIX 3	Sulfadiazin-D4	144	A	0.93-0.99	A	0.84-0.95
Sulfamethazine	MIX 3	Sulfamethazine-13C6	144	A	0.94-0.99	A	0.88-0.98
Sulfamethoxazole	MIX 3	Sulfamethoxazol-D4	144	A	0.89-0.97	A	0.81-0.96
Sulfapyridine	MIX 3	Sulfapyridin-D4	005,144	A	0.91-0.95	A	0.80-0.95
Sulfathiazole	MIX 3	Sulfathiazol-D4	144	A	0.87-0.97	A	0.69-0.98
Tebufenozide	MIX 5	Terbutylazin-D5	067	C3	0.50-0.86	C3	0.85-0.93
Tebutam	MIX 1	Tebutam-D4	243	B		B	
Terbutryn	MIX 6	Chlortoluron-D6	330,339			A	0.13-0.98
Terbutylazine	MIX 2	Terbutylazin-D5	330,339	B		B	
Thiacloprid	MIX 4	Morphin-D3	028,162,259,350	C3	0.61-0.97	C3	0.09-0.90
Ticlopidine	MIX 3	Pirimicarb D6	005,063,162			C1	
Trimethoprim	MIX 2	Trimethoprim-D9	023,242	C3	0.39-0.82	C3	0.53-0.91
Trinexapac-ethyl	MIX 2	Diuron-D6	024,044,071	A	1.00-1.00	A	0.91-0.97
Valsartan	MIX 1	Valsartan-13C5-15N	051,241,242,243,334	A	0.67-0.99	A	0.97-0.99
Venlafaxine	MIX 5	Venlafaxin-D6	023,063,241	C3	0.70-0.85	C3	0.56-0.89
Zonisamide	MIX 3	Phenazon-D3	005,144	B	0.46-0.99	C1	0.30-0.99

<sup>a</sup>The column "Mix" describes how the substances were spiked together as an intermediate step between the individual stock solutions and the final spike mix. Note that Mix6 was not spiked in Exp1, and a few substances were analyzed although not spiked (present in local wastewater). <sup>b</sup>trule numbers for initial biotransformation reactions of parent compounds as predicted by Eawag-PPS (<http://eawag-bbd.ethz.ch/predict/>). <sup>c</sup>For both Exp1 and Exp2, all analyzed substances were assigned to categories A-C according to their concentration-time series and results from control experiments as follows: C1 indicates sorption >30%, C2 abiotic transformation >20%, C3 are substances for which a flattening out of the concentration-time series was observed (mostly amine compounds as described by Gulde *et al.*<sup>7</sup>) or for which no monotonic decline in concentration was observed by visual inspection. For these compounds, the  $r^2$ -values of the first-order fits were generally lower than for compounds assigned to category A. The degree of sorption was estimated using the sorption control experiments with AS from the reactor operated at 10 d SRT. Comparable results were obtained for sorption experiments with AS cultivated at different SRTs. B are substances for which no or very slow biotransformation was observed (see methods section in the main text), and B1 indicates extremely fast biotransformation (concentrations below LOQ after 2 hours). A and A1 indicate substances which were considered for further analysis (e.g., in Figure 2 in the main text). A1 indicates substances for which the fraction adsorbed to AS solids was estimated between 30%-50% but for which the bias introduced by sorption was expected to be low (in Exp1, fold-changes between highest and lowest  $k_{bio}$  were >5 for MPs assigned A1). <sup>d</sup>For substances that were classified A, A1 or C3, first-order rate constants were calculated and the range of observed  $r^2$ -values is provided (low  $r^2$  were obtained in reactors with low values for the observed rate constants, in most cases corresponding to a removal between 10-30%).

148 **Table S7:** List of triggered btrules.

btrule number <sup>a</sup>	btrule count	btrule description
243	26	N, N-disubstituted Amide -----> N-substituted Amide + Aldehyde or Ketone
23	20	aromatic-aliphatic Ether -----> Phenol derivative + Aldehyde
63	19	primary Amine -----> Aldehyde or Ketone
67	13	secondary Amide -----> Carboxylate + primary Amine
144	12	Sulfamate -----> Amine
36	10	aromatic Methyl -----> primary Alcohol
242	9	secondary Aliphatic -----> secondary Alcohol
24	7	Ester -----> Alcohol + Carboxylate
65	7	1-Amide-2-unsubstituted aromatic -----> vic-Dihydroxyaromatic + Amide
162	7	disubstituted Sulfide -----> disubstituted Sulfoxide
241	7	tertiary Aliphatic -----> tertiary Alcohol
30	6	Nitrile -----> Carboxylate
68	6	N,N-disubstituted Urea derivative -----> N-substituted Carbamate + primary Amine
318	6	Carbamate -----> Amine
330	6	1-halo or 1-pseudohalo-s-Triazine -----> 1-hydroxy-s-Triazine
339	6	N-aliphatic-s-triazine -----> Amino-s-triazine
2	5	secondary Alcohol -----> Ketone
5	5	vic-unsubstituted Aromatic -----> vic-Dihydroxyaromatic
51	5	2- or 3- substituted Carboxylate -----> RH + CO2
334	5	aliphatic Methyl [H2] -----> primary Alcohol
22	4	Dihalomethyl derivative -----> 1-Halo-1-methylalcohol derivative
259	4	Monoalkylthiol -----> Aldehyde + H2S
27	3	primary Amide -----> Carboxylate
350	3	Formamidine -----> Amide + Methyl or Amine derivative
28	2	Cyanamide -----> Urea derivative
353	2	mono-carbon-substituted Benzenoid -----> 1-substituted-2,3-dihydroxy Benzenoid
21	1	1-Oxo 2- or 3-ene derivative -----> 1-Oxo-3-hydroxy derivative
44	1	Enol -----> Keto
71	1	cyclic Ketone -----> cyclic Ester
72	1	1-Carboxy-2-haloaromatic -----> 1,2-Dihydroxyaromatic
73	1	2-unsubstituted Cyclic ether -----> 2-Hydroxy cyclic ether
158	1	Aromatic ether -----> Aromatic alcohol + Alcohol
193	1	di-[C,O]-substituted Sulfoxide -----> di-[C,O]-substituted Sulfone
333	1	aliphatic Methyl [H1] -----> primary Alcohol
359	1	4-Halobenzoate derivative -----> 4-Hydroxybenzoate derivative
374	1	polynuclear Aromatic system -----> 1,2-dioxygenation and cleavage at connecting atom
375	1	1-unsubstituted Furan derivative -----> 1-Hydroxyfuran derivative
391	1	cyclic Imine -----> Ketone + Amine
420	1	Nitroguanidine derivative -----> Urea derivative
425	1	Saccharin -----> Catechol

149 <sup>a</sup>Lists all rules that were predicted for at least one substance by Eawag-PPS (indicated in Table S5). <sup>b</sup>number of occurrences of  
150 the respective rules in Table S6.

151

## S4 Biotransformation batch experiments

In this chapter, detailed experimental procedures for Exp1, Exp2, ExpOx and ExpTP are provided. Additional details (including information on replication, sampling time points and sample volumes) are provided in Table S8.

**Exp1:** The first biotransformation experiment was performed in the 12 L SBRs. The SBR cycles of the reactors were interrupted after a feed phase, the volume of the three reactors at SRTs of 1, 3 and 5 days was reduced by 50% to increase AS concentration and micropollutants were spiked to final concentrations of 6 µg/L each in each reactor. Stirring was continued, and samples were collected at 12 time points over a period of 90 hours. The samples were centrifuged ( $3345 \times g$ , 10 min), and 1 mL of supernatant was collected in an HPLC vial. The samples were amended with isotope-labeled internal standard, stored at 4 °C and analyzed within 7 days. In parallel, samples were collected for measuring concentrations of  $\text{NH}_3$ ,  $\text{NO}_2^-$  and  $\text{NO}_3^-$  using test cuvettes (Hach Lange, LCK 303, 304, 305, 339, 342). pH was measured (HQ30d Flexi Meter, Hach Lange) at three time points. During the experiment, dissolved oxygen (DO) concentrations were controlled as described in the main text. Prior to the last feed before spiking of the MPs, 300 mL of AS was collected from the reactors at 3 and 10 d SRT for sorption and abiotic control experiments performed in smaller batch reactors. These were done as described by Gulde *et al.*,<sup>5</sup> i.e., autoclaved filtrate and autoclaved activated sludge was used to estimate the fractions that were abiotically degraded and sorbed to AS solids, respectively.

**Exp2:** Activated sludge from the six SBR reactors was collected, and the TSS was adjusted to approximately 2 g/L (Table S5) by cautious centrifugation and decantation. Portions of  $3 \times 50$  mL of AS were filled into three 100-mL glass bottles (Schott) for each SBR reactor. The 18 batch reactors were spiked with micropollutants (final concentration in batches: 6 µg/L) and placed on a circulating shaker table (160 rpm). Caps with two holes were used to avoid DO limitation as described elsewhere.<sup>8</sup> Samples were collected at nine time points over a period of 72 hours, centrifuged ( $21130 \times g$ , 5 min) and 0.5 mL of supernatant was collected in an HPLC vial. The samples were amended with isotope-labeled internal standard, stored (4 °C) and analyzed within 6 days. Concentrations of  $\text{NH}_3$ ,

NO<sub>2</sub><sup>-</sup> and NO<sub>3</sub><sup>-</sup> and values for pH were measured as described for Exp1. Sorption and abiotic control experiments were run as described for Exp1.

**ExpOx:** A volume of 50 µL of the MP stock solution (spiked and analyzed substances identical as for Exp2) was added to six 100-mL glass bottles (Schott). The solvent was allowed to evaporate for 10 min under the fume hood. Activated sludge from the SBR operated at 7 days SRT was collected and filled into the six bottles (50 mL each). Three bottles were closed using lids equipped with rubber septa, and the three remaining bottles were closed using caps with two holes to prevent DO limitation. Using injection needles, the airtight closed bottles were flushed with N<sub>2</sub> to remove remaining oxygen. NH<sub>4</sub>Cl (aq) was spiked to all reactors to augment the NH<sub>4</sub> concentration to an initial value of 10 mg/L, and the reactors were placed on a circulating shaker table (160 rpm). Samples for chemical analysis were collected over a period of 72 hours and processed as described for Exp2. Concentrations of NH<sub>3</sub>, NO<sub>2</sub><sup>-</sup> and NO<sub>3</sub><sup>-</sup> were measured using Hach-Lange test cuvettes (LCK 303, 304, 305, 339, 342), and pH was measured as described above for Exp1 and Exp2.

**ExpTP:** As in Exp2 and in ExpOx, experiments in ExpTP were conducted in 100-mL bottles placed on a circulating shaker table (160 rpm). Samples were collected over a period of 48 hours and processed as described for Exp2, except that no internal standard was added.

195 **Table S8:** Batch experiments conducted.

Experiment	AS	replicates	total <sup>a</sup>	V [L]	initial conc. [µg/L]	sampling points [h]	sample V <sup>b</sup> [mL]	transfer V <sup>c</sup> [µL]	ISTD [µg/L]
Exp1	6 SBRs	1	6	12 (6)	6	0,1,2,3,4,8,12,24,36,48,72,90	20	1000	0.5
Exp1-abiotic control	1 SBRs (SRT 10d) - ACF <sup>d</sup>	3	3	0.05	6	0,25,48,72	2	1000	0.5
Exp1-sorption control	2 SBRs (SRT 3, 10d) - AC <sup>e</sup>	3	6	0.05	6	1.5	2	1000	0.5
Exp2	6 SBRs	3 (4) <sup>f</sup>	18	0.05	6	0,1,2,4,8,12,24,48,72	1.5	500	2
Exp2-abiotic control	1 SBRs (SRT 10d) - ACF <sup>d</sup>	3	3	0.05	6	0,48,73	1.5	500	2
Exp2-sorption control	6 SBRs - AC <sup>e</sup>	3	18	0.05	6	2	1.5	500	2
ExpOx - aerobic	1 SBRs (SRT 7d)	3	3	0.05	6	0,1,2,4,8,12,24,48,72	1.5	500	2
ExpOx - anaerobic	1 SBRs (SRT 7d)	3	3	0.05	6	0,1,2,4,8,12,24,48,72	1.5	500	2
ExpTP - Mix1-6 <sup>g</sup>	1 SBRs (SRT 7d) - mix1-6	1	6	0.05	50	0,2,8,24,48	1.5	500	-
ExpTP - non spiked	1 SBRs (SRT 7d)	1	1	0.05	-	0,2,8,24,48	1.5	500	-

196 <sup>a</sup>The total number of reactors was calculated as the product of different conditions (as indicated in the columns 'AS' and/or 'Experiment') multiplied by the number of replicates. <sup>b</sup>Indicates the volume that  
197 was sampled at each sampling time point and subjected to centrifugation. <sup>c</sup>Indicates the volume of supernatant transferred to HPLC vials after centrifugation. <sup>d</sup>ACF indicates that autoclaved activated  
198 sludge filtrate was used as abiotic control. <sup>e</sup>AC indicates that the activated sludge was autoclaved prior to incubation. <sup>f</sup>A 4<sup>th</sup> replicate was established (and spiked with MPs) for each SRT to sample for  
199 the analysis of NO<sub>3</sub><sup>-</sup>-N, NO<sub>2</sub><sup>-</sup>-N and to measure the oxygen uptake rate. <sup>g</sup>Each of the MP mixes (1-6) was spiked into a separate batch reactor.

## S5 Chemical analysis using LC-HRMS

The sample (100  $\mu$ L) was loaded onto an Atlantis T3 column (particle size 3  $\mu$ m, 3.0  $\times$  150 mm, Waters) equipped with a guard column (Atlantis T3 Sentry Guard Cartridge, particle size 3  $\mu$ m, 3.9  $\times$  20 mm). Nanopure water (Barnstead Nanopure, Thermo Scientific) and methanol (HPLC-grade, Fisher Scientific) both with 0.1% formic acid (98-100%, Merck) were used as mobile phase at a flow rate of 300  $\mu$ L/min. Initial conditions (95:5 water/methanol) were maintained for 5 min, then the methanol fraction was increased over 16 min to 5:95 water/methanol. These conditions were held for 8 min, then the initial conditions were reestablished within 0.1 min and kept for 4.9 min before the next analysis was started. The temperature of the column oven was set to 30  $^{\circ}$ C. Mass spectra were acquired at a capillary temperature of 320  $^{\circ}$ C and spray voltages of + 4 kV and -3 kV in positive and negative ionization mode, respectively.

Samples were measured in full scan mode at a resolution of 140,000 at  $m/z$  200 and a scan range of 50-750  $m/z$  in positive/negative switching mode (Exp2, ExpOx, ExpTP) or in separate injections for positive and negative mode in combination with MS<sup>2</sup> fragmentation spectra acquisition (Exp1, part of samples of Exp2 and ExpTP). Data-dependent MS<sup>2</sup> spectra were recorded at a resolution of 17500 at 200  $m/z$  (isolation window of 1  $m/z$ ). An inclusion list (list of masses corresponding to suspected transformation products as described in the methods section of the main text) was used to trigger the acquisition of fragmentation spectra every time a signal corresponding to a listed mass was detected in the full-scan mass spectrum. An overview of measurement settings for all samples is provided in Table S9.

220 **Table S9:** Measured LC-HRMS/MS samples and analytical parameters.

experiment	samples	matrix	replicates measured	sampling points	ionization mode	injection volume	acquisition mode	resolution (full scan)
				[h]		[μL]		
Exp1	biotransformation (6 SBRs)	AS	1/1	0,1,2,3,4,8,12,24,36,48,72,90	+	100	DD <sup>a</sup>	140000
		AS	1/1	1,2,4,8,12,24,58,72,90	-	100	DD <sup>a</sup>	140000
	sorption control (AS from 2 SBRs)	AS-AC <sup>b</sup>	3/3	1.5	+/-	100	switch	140000
	abiotic control (AS from 1 SBR)	AS-ACF <sup>c</sup>	3/3	0,25,48,72	+/-	100	switch	140000
	calibration samples <sup>d</sup>	water			+/-	100	switch	140000
Exp2	biotransformation	AS	3/3	0,1,2,4,8,12,24,48,72	+/-	100	switch	140000
		AS	1/3	2,8,24,72	+	100	DD <sup>a</sup>	140000
		AS	1/3	2,8,24,72	-	100	DD <sup>a</sup>	140000
	sorption control	AS-AC <sup>b</sup>	3/3	2	+/-	20	switch	140000
	abiotic control	AS-ACF <sup>c</sup>	3/3	0,48,73	+/-	100	switch	140000
	calibration samples <sup>d</sup>	water			+/-	100	switch	140000
ExpOx	biotransformation	AS	3/3	0,1,2,4,8,12,24,48,72	+/-	100	switch	140000
	calibration samples <sup>d</sup>	water	3/3		+/-	100	switch	140000
ExpTP	biotransformation	AS	1/1	0,2,8,24,48	+/-	100	switch	140000
		AS	1/1	2,8,24,48	+	100	DD <sup>a</sup>	140000
		AS	1/1	2,8,24,48	-	100	DD <sup>a</sup>	140000
	calibration samples <sup>e</sup>	water			+/-	100	switch	140000

221 <sup>a</sup>DD indicates data-dependent MS2 acquisition. <sup>b</sup>AC indicates that the activated sludge was autoclaved prior to incubation. <sup>c</sup>ACF indicates that autoclaved activated sludge filtrate was used as abiotic  
222 control. <sup>d</sup>Calibration levels: 50, 100, 200, 350, 500, 1000, 2000, 3500, 5000, 10000 ng/L <sup>e</sup>Calibration levels: 50, 100, 200, 350, 500, 1000, 2000, 3500, 5000, 10000, 20000, 50000 ng/L.

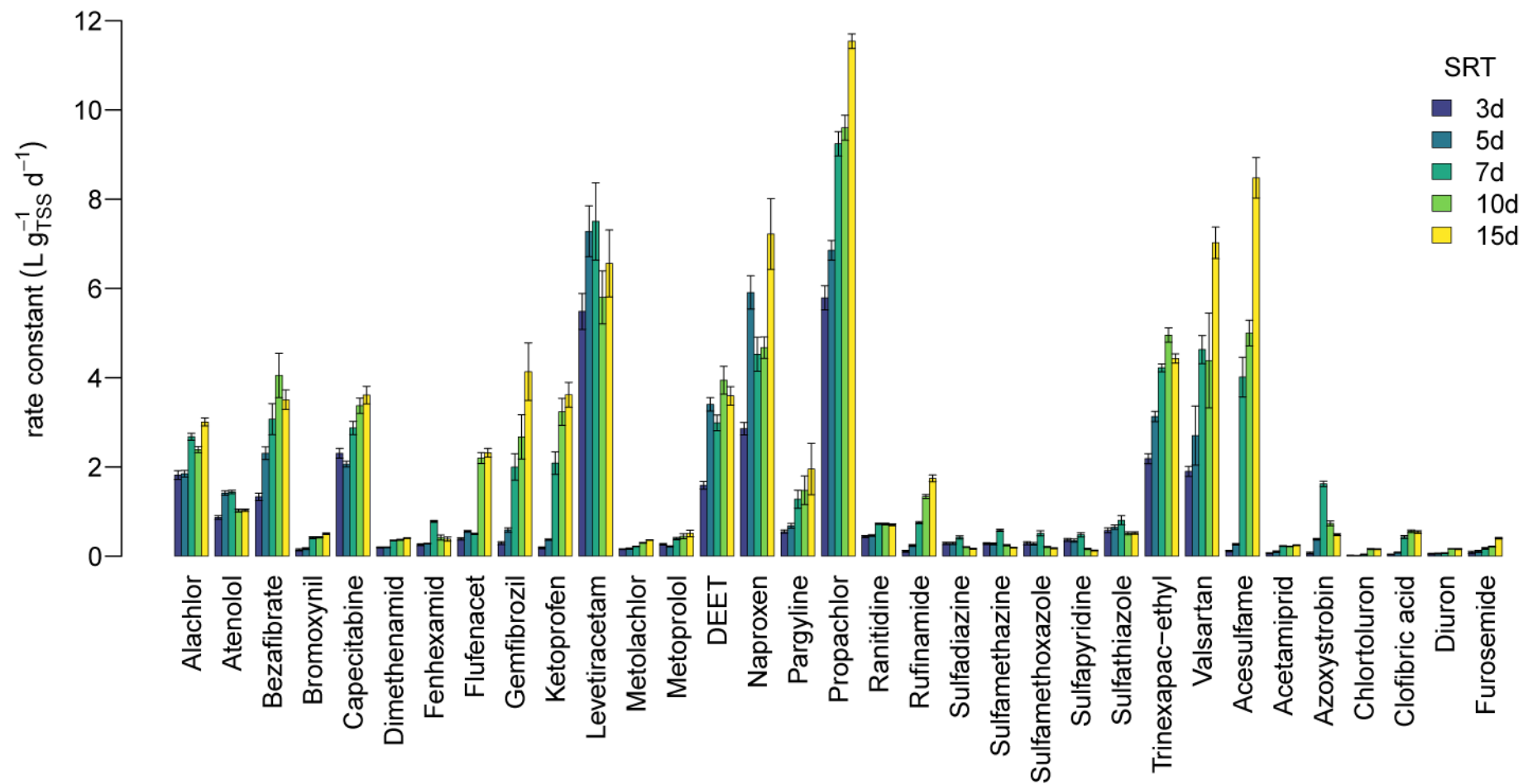


## S6 Biotransformation rate constants

As further detailed in Schwarzenbach *et al.*, enzyme-catalyzed biotransformation reactions are often described as Michaelis-Menten processes.<sup>9</sup> If the substrate concentration is considerably lower than the half-saturation constant, the substrate consumption depends on the enzyme concentration, the substrate concentration and the second-order rate constant  $k_{\text{bio}}$ . Assuming that the enzyme concentration is constant over the time course of the experiment, a pseudo-first order relationship is then typically observed in which the rate depends linearly, i.e., through a pseudo-first order rate constant, on the substrate concentration.

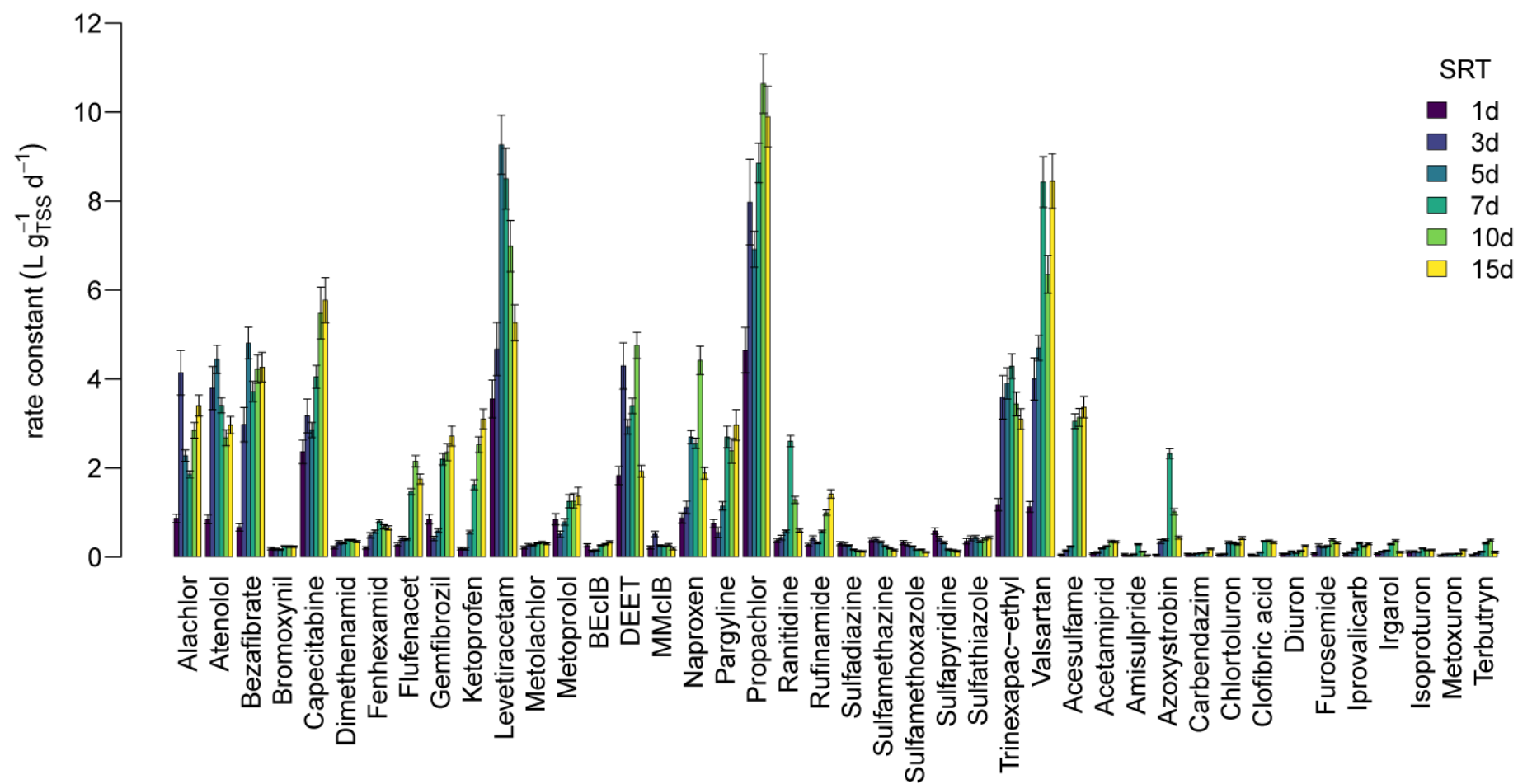
Based on this reasoning, we fitted our concentration-time series data assuming first-order kinetic behavior. However, as detailed in the main text, fitting was not attempted for chemicals that degraded too fast or too slowly to yield accurate degradation information in our experimental window of observation. For the remaining 64 chemicals, first-order rate constants were obtained by linear regression of the logarithmic concentrations against time using R. Through visual inspection and based on the coefficients of determination of the fits ( $r^2$ , observed ranges in  $r^2$ -values are provided in Table S6), substances were identified that did not adhere to first-order kinetic behavior, e.g., substances for which a flattening out of the concentration-time series was observed (mostly amine compounds as described by Gulde *et al.*<sup>7</sup>) or for which no monotonic decline in concentrations was observed. These substances are denoted as “C3” in Table S6 and were not considered for further analyses. For the remaining substances (denoted “A” or “A1” in Table S6), a second-order rate constant  $k_{\text{bio}}$  was obtained through normalization by the measured TSS values. The  $k_{\text{bio}}$  values thus obtained are displayed in Figures S3 and S4.

249



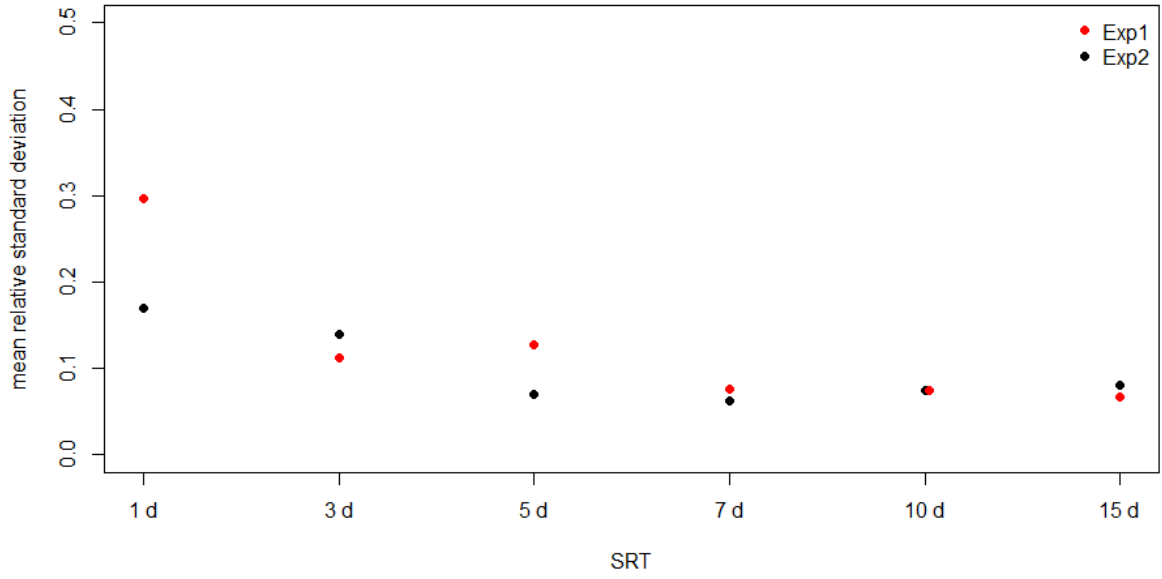
250

251 **Figure S3:** Biomass-normalized rate constants for Exp1 and SRTs from 3 d to 15 d.



252

253 **Figure S4:** Biomass-normalized rate constants for Exp2 and SRTs from 1 d to 15 d.



**Figure S5:** Mean relative standard deviation of rate constants. Considerably higher relative standard deviations were observed for biotransformation rate constants from the reactor operated at 1 d SRT in Exp1.

**Scaling of biotransformation rate constants:** In order to facilitate comparisons of trends exhibited by different MPs independent of absolute biotransformation rate constants, we auto-scaled  $k_{bio}$  values (for each experiment and MP separately). Auto-scaled values are obtained from equation (1), with  $k_{bio,i}$  representing the rate constant obtained for one MP in one experiment at SRT  $i$ , and with  $k_{bio}^m$  and  $k_{bio}^{sd}$  representing mean and standard deviation of rate constants for the same MP and experiment across all SRTs.

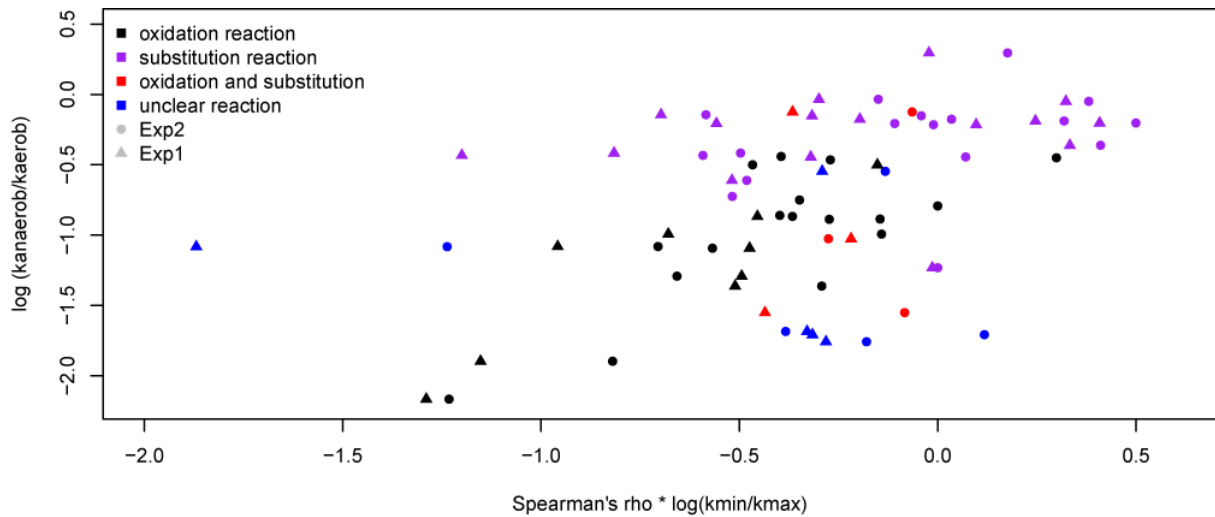
$$k_{bio,i}^{sc} = \frac{k_{bio,i} - k_{bio}^m}{k_{bio}^{sd}} \quad (1)$$

Using the software R (Version: 3.3.0), this transformation was achieved using the command “scale”. Further details are provided elsewhere.<sup>10</sup>

269 **Table S10:** First-order rate constants observed in ExpOx and inhibition experiments.<sup>11</sup>

name	ExpOx k [day <sup>-1</sup> ]		Inhibition k [day <sup>-1</sup> ] <sup>a</sup>		
	k <sub>aerobic</sub>	k <sub>anaerobic</sub>	k <sub>atu</sub>	k <sub>oct</sub>	k <sub>control</sub>
Acesulfame	18.878	1.561	2.954	3.303	3.050
Acetamiprid	0.313	0.077	0.218	0.171	0.438
Alachlor	3.670	2.447	2.758	2.832	2.897
Amisulpride	0.155	<0.053	0.055	0.105	0.107
Atenolol	19.211	37.934	6.867	6.207	5.692
Azoxystrobin	0.471	0.181	0.951	0.885	1.049
BEclB	0.384	<0.053	0.550	0.304	0.710
Bezafibrate	16.479	0.463	9.750	10.420	20.045
Bromoxynil	0.516	0.320	0.438	0.648	0.706
Capecitabine	15.038	1.417	5.674	5.093	17.139
Carbendazim	0.310	0.058	<0.053	0.092	0.110
Chlortoluron	0.657	<0.053	0.271	1.255	1.727
Clofibric acid	1.031	0.085	0.209	0.311	0.624
DEET	8.769	0.172	4.966	5.221	5.377
Dimethenamid	0.805	0.568	0.464	0.480	0.524
Diuron	0.390	<0.053	0.057	0.128	0.215
Fenhexamid	0.986	0.280	0.302	0.482	0.728
Flufenacet	1.434	1.029	0.377	0.398	0.492
Furosemide	0.521	<0.053	0.100	0.392	0.722
Gemfibrozil	4.179	<0.053	3.061	2.393	3.250
Iprovalicarb	1.508	0.268	2.552	3.011	3.241
Irgarol	0.329	<0.053	0.375	0.564	0.825
Isoproturon	0.408	<0.053	0.178	0.188	0.324
Ketoprofen	7.770	<0.053	1.602	2.001	2.251
Levetiracetam	20.229	1.185	8.555	8.627	12.138
Metolachlor	0.590	0.443	0.332	0.325	0.374
Metoprolol	2.566	<0.053	n/d <sup>b</sup>	n/d <sup>b</sup>	n/d <sup>b</sup>
Metoxuron	0.272	0.098	<0.053	<0.053	0.066
MMclB	0.149	<0.053	0.154	<0.053	0.214
Naproxen	8.307	0.145	8.297	8.378	8.037
Pargyline	4.920	0.251	1.275	2.392	4.344
Propachlor	19.256	17.778	12.826	12.570	14.320
Ranitidine	2.166	0.684	0.594	1.844	2.649
Rufinamide	3.829	1.413	1.905	2.570	2.944
Sulfadiazine	0.293	0.190	0.230	0.214	0.207
Sulfamethazine	0.506	0.220	0.317	0.305	0.290
Sulfamethoxazole	0.311	0.278	0.321	0.294	0.269
Sulfapyridine	0.474	0.297	0.532	0.469	0.452
Sulfathiazole	0.937	0.571	0.711	0.854	0.967
Terbutryn	0.409	<0.053	0.329	0.640	0.868
Trinexapac-ethyl	22.561	8.107	3.272	4.402	4.103
Valsartan	13.447	0.584	12.954	9.294	14.420

<sup>a</sup>Rate constants for the inhibition experiments are based on experimental data described previously<sup>11</sup> and were calculated similar as for Exp1, Exp2 and ExpOx. <sup>b</sup>n/d indicates 'not determined'.



**Figure S6:** Values of  $\log(k_{\text{anaer}}/k_{\text{aer}})$  vs. Spearman rank correlation coefficient ( $\rho$ ) multiplied with  $\log(k_{\text{min}}/k_{\text{max}})$  (see Table 1 in main text). The different types of observed reactions (see also Table 1 in main text) are indicated by different colors and data from both Exp1 and Exp2 is shown.

In Figure S6, the relationship between the dependence of  $k_{\text{bio}}$  on redox conditions ( $\log(k_{\text{anaer}}/k_{\text{aer}})$ ) and the correlation ( $\rho$ ) of  $k_{\text{bio}}$  with SRT weighted by the maximal fold change ( $\log(k_{\text{min}}/k_{\text{max}})$ ) are depicted. Most MPs showing strong positive correlation with SRT and high fold changes (low x-axis values), require aerobic conditions for transformation (low y-axis values).

## S7 Transformation products

A suspect screening was performed using Compound Discoverer 2.0. The first part of the workflow comprised retention time (RT) alignment (maximal RT shift: 2 min; mass tolerance 5 ppm) and peak picking (mass tolerance 5 ppm, minimal intensity 10'000, maximal peak width: 0.5 min). Adduct and isotope peaks were componentized to obtain features. Features with less than 5 times higher peak areas in the samples compared to a blank control (measured nanopure water) were not considered for further analysis. The features detected in individual raw files were grouped to generate area-time profiles (mass tolerance 5 ppm, RT tolerance: 0.25 min). Molecular formulas were predicted based on the detected isotopic pattern. As described in the methods section of the main text, a suspect transformation product list was compiled and used in the 'search mass lists'-node in Compound Discoverer (mass tolerance: 5 ppm) to select features potentially representing formed TPs. Candidates for which reasonable area-time trends were observed (data from Exp2) and that were exclusively observed in the batch reactor to which the respective parent chemical was spiked (ExpOx) were further investigated using MS<sup>2</sup> fragmentation spectra. Below, further experimental evidence for the detection and structure elucidation of transformation products that allowed assigning reaction types (Table 1 in the main text) is presented and discussed (Tables S12-S22, Figures S7-S8). Also, for the MPs for which no TPs were detected, the detected parent exact masses are shown (Figure S9). In section S8, measured MS<sup>2</sup> spectra are provided for TPs for which no published MS<sup>2</sup> was found and for which no reference standard was available to confirm the TP or other TPs of the suggested biotransformation pathway. In the text, exact *m/z* values of fragments are rounded and presented as nominal masses. Chromatographic retention time is abbreviated as RT. No analysis of MS<sup>2</sup> fragmentation spectra was performed for TPs that could be confirmed using reference standards (Table S11).

**Table S11:** Transformation products for which references standards were available.

transformation product	parent
2-aminobenzimidazole	carbendazim
acetamiprid-N-desmethyl	acetamiprid
alachlor OXA	alachlor
amisulpride-N-oxide	amisulpride
atenolol acid	atenolol
azoxystrobin acid	azoxystrobin
capecitabine-hydrolyzed	capecitabine
dimethenamid-OXA	dimethenamid
diuron-desmethyl	diuron
diuron-didesmethyl	diuron
flufenacet-OXA	flufenacet
furosemide-N-dealkylated	furosemide
isoproturon-didesmethyl	isoproturon
isoproturon-desmethyl	isoproturon
levetiracetam acid	levetiracetam
metolachlor-OXA	metolachlor
pargyline-N-oxide	pargyline
propachlor-ESA	propachlor
propachlor-OXA	propachlor
ranitidine-N-oxide	ranitidine
ranitidine-S-oxide	ranitidine
trinexapac-acid	trinexapac-ethyl

**Chlortoluron, diuron, isoproturon and metoxuron (Table S12):** For diuron and isoproturon, the formation of mono- and didesmethylated TPs were confirmed by chemical reference standards. Retention time shifts of -0.2 min (monodesmethylated TPs) and -0.7 – -0.8 min (didesmethylated TPs) were observed. Similar retention time shifts were observed for the corresponding desmethylated TPs observed for chlortoluron (-0.2 and -0.9 min) and metoxuron (-0.4 and -1.2 min). The fragments at  $m/z$  72, being replaced by a fragment at  $m/z$  58 in the hypothesized desmethylated TP (difference of  $m/z$  14 corresponding to a loss of  $\text{CH}_2$ ), further supports the proposed structures of desmethylated chlortoluron and metoxuron (see  $\text{MS}^2$  spectra in section S8). For chlortoluron, diuron and metoxuron, TPs were detected corresponding to the masses of dihydroxylated products, all of which showed slightly negative shifts in retention time (-0.2 – -0.4 min) and were detected in negative ionization mode. For isoproturon and chlortoluron, also TPs corresponding to an oxidation of the alkyl group on the aromatic ring were observed.  $\text{MS}^2$  spectra are provided in section S8.



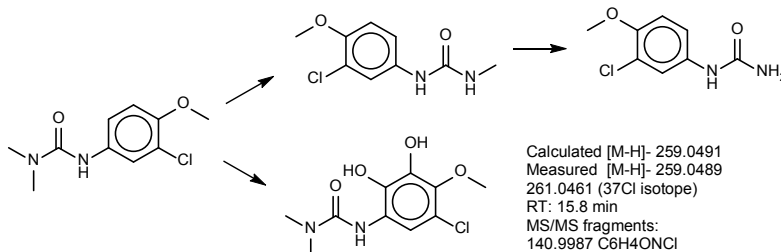
<p><b>Diuron</b></p> <div> <div> <p>Calculated [M+H]<sup>+</sup> 233.0243 Measured [M+H]<sup>+</sup> 233.0241 235.0211 (35Cl37Cl isotope) 237.0181 (37Cl37Cl isotope) RT: 18.9 min</p> </div> <div> <p>Calculated [M+H]<sup>+</sup> 219.0086 Measured [M+H]<sup>+</sup> 219.0084 221.0054 (35Cl37Cl isotope) 223.0024 (37Cl37Cl isotope) RT: 18.7 min confirmed by reference standard</p> </div> <div> <p>Calculated [M+H]<sup>+</sup> 204.9930 Measured [M+H]<sup>+</sup> 204.9928 206.9898 (35Cl37Cl isotope) 208.9870 (37Cl37Cl isotope) RT: 18.1 min confirmed by reference standard</p> </div> <div> <p>Calculated [M-H]<sup>-</sup> 262.9996 Measured [M-H]<sup>-</sup> 262.9995 264.9967 (35Cl37Cl isotope) 266.9936 (37Cl37Cl isotope) RT: 18.7 min MS/MS fragments: 159.9728 C<sub>6</sub>H<sub>4</sub>Cl<sub>2</sub>N</p> </div> </div>	<p><b>Isoproturon</b></p> <div> <div> <p>Calculated [M+H]<sup>+</sup> 207.1492 Measured [M+H]<sup>+</sup> 207.1490 RT: 18.6 min 162.0916 C<sub>10</sub>H<sub>12</sub>NO 134.0963 C<sub>9</sub>H<sub>12</sub>N 72.0444 C<sub>3</sub>H<sub>6</sub>NO</p> </div> <div> <p>Calculated [M+H]<sup>+</sup> 193.1335 Measured [M+H]<sup>+</sup> 193.1334 RT: 18.4 min confirmed by reference standard</p> </div> <div> <p>Calculated [M+H]<sup>+</sup> 179.1179 Measured [M+H]<sup>+</sup> 179.1177 RT: 17.9 min confirmed by reference standard</p> </div> <div> <p>Calculated [M+H]<sup>+</sup> 223.1441 Measured [M+H]<sup>+</sup> 223.1439 RT: 14.7 min MS/MS fragments: 160.0756 C<sub>10</sub>H<sub>10</sub>NO 117.0700 C<sub>9</sub>H<sub>9</sub> 72.0444 C<sub>3</sub>H<sub>6</sub>NO 59.0494 C<sub>3</sub>H<sub>7</sub>O</p> </div> <div> <p>Calculated [M+H]<sup>+</sup> 237.1234 Measured [M+H]<sup>+</sup> 237.1231 RT: 15.0 min MS/MS fragments: 146.0600 C<sub>9</sub>H<sub>8</sub>NO 120.0808 C<sub>8</sub>H<sub>10</sub>N 72.0444 C<sub>3</sub>H<sub>6</sub>NO</p> </div> </div>	<p><b>Chlortoluron</b></p> <div> <div> <p>Calculated [M+H]<sup>+</sup> 199.0633 Measured [M+H]<sup>+</sup> 199.0630 201.0600 (37Cl isotope) RT: 18.2 min MS/MS fragments: 140.0260 C<sub>7</sub>H<sub>7</sub>NCl 125.0152 C<sub>7</sub>H<sub>6</sub>Cl 58.0290 C<sub>2</sub>H<sub>4</sub>NO</p> </div> <div> <p>Calculated [M+H]<sup>+</sup> 185.0476 Measured [M+H]<sup>+</sup> 185.0475 187.0445 (37Cl isotope) RT: 17.5 min MS/MS fragments: 140.0261 C<sub>7</sub>H<sub>7</sub>NCl 125.0152 C<sub>7</sub>H<sub>6</sub>Cl</p> </div> <div> <p>Calculated [M-H]<sup>-</sup> 243.0542 Measured [M-H]<sup>-</sup> 243.0541 245.0512 (37Cl isotope) RT: 18.1 min MS/MS fragments: 140.0274 C<sub>7</sub>H<sub>7</sub>CIN</p> </div> <div> <p>Calculated [M+H]<sup>+</sup> 243.0531 Measured [M+H]<sup>+</sup> 243.0529 245.0499 (37Cl isotope) RT: 15.1 min MS/MS fragments: 197.9948 C<sub>8</sub>H<sub>5</sub>NO<sub>2</sub>Cl 154.0051 C<sub>7</sub>H<sub>5</sub>NOCl 72.0443 C<sub>3</sub>H<sub>6</sub>NO</p> </div> <div> <p>Calculated [M+H]<sup>+</sup> 213.0789 Measured [M+H]<sup>+</sup> 213.0787 215.0757 (37Cl isotope) RT: 18.4 min MS/MS fragments: 140.0261 C<sub>7</sub>H<sub>7</sub>NCl 125.0153 C<sub>7</sub>H<sub>6</sub>Cl 72.0444 C<sub>3</sub>H<sub>6</sub>NO</p> </div> </div>
---	--	--

## Metoxuron

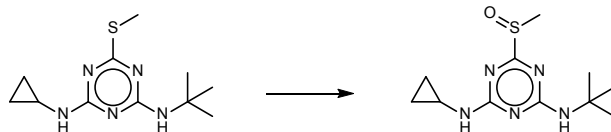
Calculated [M+H]<sup>+</sup> 229.0738  
Measured [M+H]<sup>+</sup> 229.0737  
231.0707 (37Cl isotope)  
RT: 16.2 min  
MS/MS fragments:  
156.0211 C<sub>7</sub>H<sub>7</sub>ONCl  
72.0445 C<sub>3</sub>H<sub>6</sub>NO

Calculated [M+H]<sup>+</sup> 215.0582  
Measured [M+H]<sup>+</sup> 215.0581  
217.0552 (37Cl isotope)  
RT: 15.8 min  
MS/MS fragments:  
158.0367 C<sub>7</sub>H<sub>9</sub>ONCl  
156.0212 C<sub>7</sub>H<sub>7</sub>ONCl  
123.0679 C<sub>7</sub>H<sub>9</sub>ON  
108.0444 C<sub>6</sub>H<sub>6</sub>ON  
58.0290 C<sub>2</sub>H<sub>4</sub>NO

Calculated [M+H]<sup>+</sup> 201.0425  
Measured [M+H]<sup>+</sup> 201.0430  
203.0400 (37Cl isotope)  
RT: 15.0 min  
156.0207 C<sub>7</sub>H<sub>7</sub>ONCl  
123.0678 C<sub>7</sub>H<sub>9</sub>ON  
108.0444 C<sub>6</sub>H<sub>6</sub>ON

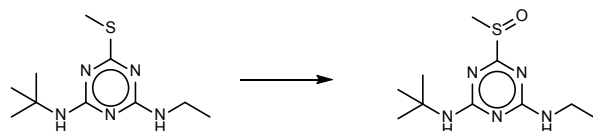


**Irgarol, terbutryn and ranitidine (Table S13):** Formation of ranitidine-S-oxide was confirmed by a reference standard. For irgarol and terbutryn, similar MS<sup>2</sup> fragments were observed as in an earlier study by Luft *et al.*,<sup>12</sup> in which the S-oxides emerged as major TPs in AS, supporting the proposed S-oxide structures. Formation of minor amounts of ranitidine-N-oxide were confirmed by a reference standard.

**Irgarol**

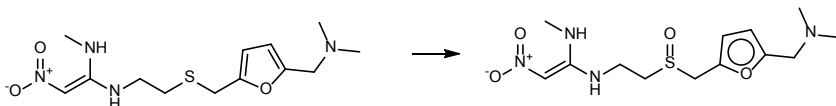
Calculated [M+H]<sup>+</sup> 254.1434  
 Measured [M+H]<sup>+</sup> 254.1433  
 RT: 19.1 min  
 MS/MS fragments:  
 198.0808 C<sub>7</sub>H<sub>12</sub>N<sub>5</sub>S  
 57.0702 C<sub>4</sub>H<sub>9</sub>

Calculated [M+H]<sup>+</sup> 270.1383  
 Measured [M+H]<sup>+</sup> 270.1381  
 RT: 18.9 min  
 MS/MS fragments:  
 214.0757 C<sub>7</sub>H<sub>12</sub>N<sub>5</sub>O<sup>a</sup>  
 196.0652 C<sub>7</sub>H<sub>10</sub>N<sub>5</sub>S<sup>a</sup>  
 168.0880 C<sub>6</sub>H<sub>10</sub>N<sub>5</sub>O<sup>a</sup>  
 57.0702 C<sub>4</sub>H<sub>9</sub>

**Terbutryn**

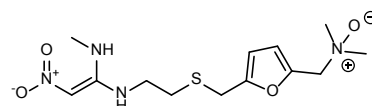
Calculated [M+H]<sup>+</sup> 242.1434  
 Measured [M+H]<sup>+</sup> 242.1432  
 RT: 18.5 min  
 MS/MS fragments:  
 186.0807 C<sub>6</sub>H<sub>12</sub>N<sub>5</sub>S  
 57.0702 C<sub>4</sub>H<sub>9</sub>

Calculated [M+H]<sup>+</sup> 258.1383  
 Measured [M+H]<sup>+</sup> 258.1383  
 RT: 18.6 min  
 MS/MS fragments:  
 202.0756 C<sub>6</sub>H<sub>12</sub>N<sub>5</sub>O<sup>a</sup>  
 184.0651 C<sub>6</sub>H<sub>10</sub>N<sub>5</sub>S<sup>a</sup>  
 156.0881 C<sub>5</sub>H<sub>10</sub>N<sub>5</sub>O<sup>a</sup>  
 57.0702 C<sub>4</sub>H<sub>9</sub>

**Ranitidine**

Calculated [M+H]<sup>+</sup> 315.1485  
 Measured [M+H]<sup>+</sup> 315.1482  
 RT: 9.0 min

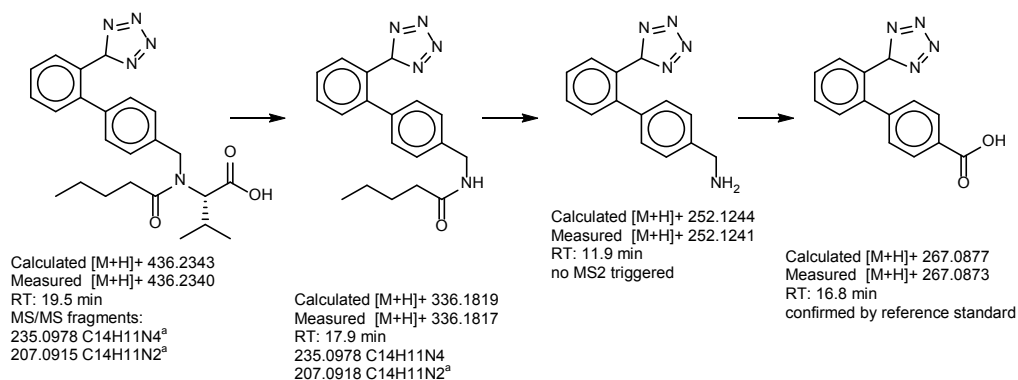
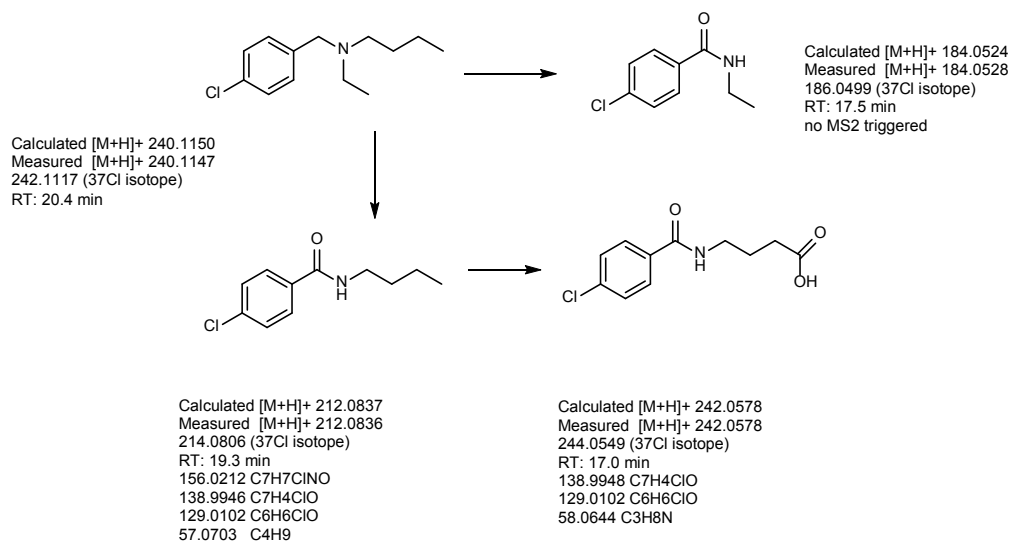
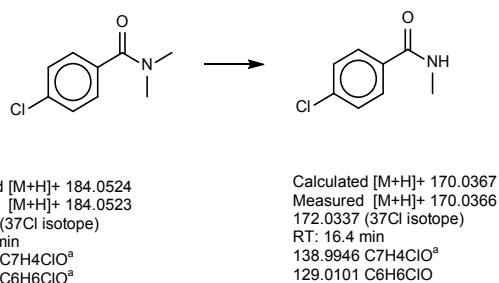
Calculated [M+H]<sup>+</sup> 331.1435  
 Measured [M+H]<sup>+</sup> 331.1431  
 RT: 5.1 min  
 confirmed by reference standard



Calculated [M+H]<sup>+</sup> 331.1435  
 Measured [M+H]<sup>+</sup> 331.1431  
 RT: 9.3 min  
 confirmed by reference standard


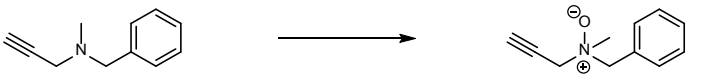
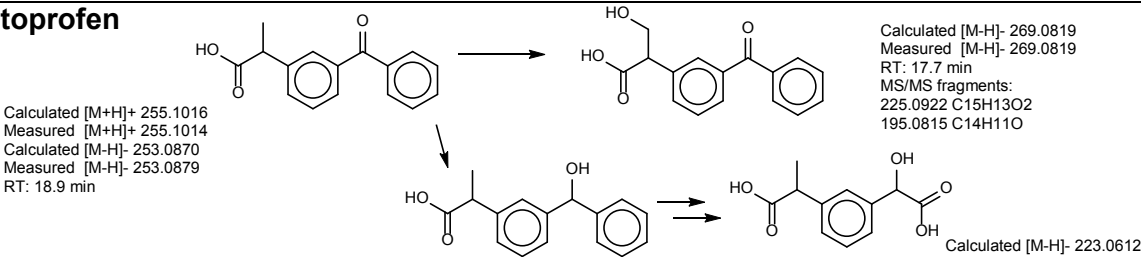
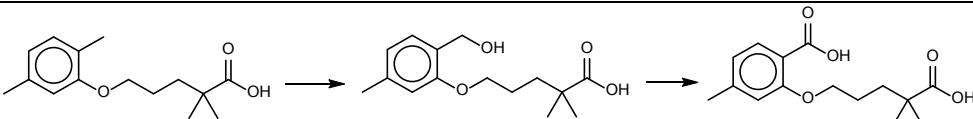
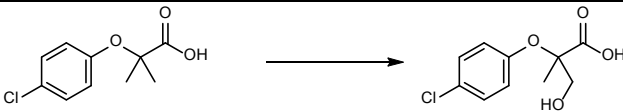
336 <sup>a</sup>Indicates that the respective fragments were reported previously.<sup>12</sup>

**Valsartan, BEclB, MMclB (Table S14):** Valsartan was transformed to valsartan acid (confirmed using a reference standard) via initial N-dealkylation reactions. Also for MMclB, a TP corresponding to an N-dealkylation reaction was detected as previously reported by Helbling *et al.*<sup>13</sup> For BEclB, desethylation was followed by an oxidation to a carboxylic acid. No MS<sup>2</sup> measurement was triggered for the TP observed at *m/z* 184, supposedly corresponding to BEclB without the butyl functional group. MS<sup>2</sup> spectra of desethyl BEclB and the carboxylic acid TP are provided in section S8.

**Valsartan****BEclB****MMclB**<sup>a</sup>Indicates that the respective fragments were reported previously.<sup>13</sup>

**Furosemide (Table S15):** For furosemide, an N-dealkylation reaction was observed and confirmed by a reference standard. For **pargyline (Table S15)**, biotransformation to the corresponding N-oxide was confirmed by a reference standard. **Ketoprofen (Table S15):** A peak was detected at  $m/z$  269, the expected  $m/z$  value of hydroxylated ketoprofen. Analysis of MS<sup>2</sup> fragments supports the proposed TP structure with the hydroxyl group added to the methyl group of ketoprofen (see MS<sup>2</sup> spectrum in section S8). Additional peaks were observed at  $m/z$  values corresponding to TPs reported by Quintana *et al.*<sup>14</sup> In their suggested pathway, the keto-group is first reduced, followed by ring dihydroxylation leading to observable metabolites with one remaining ring structure. No MS<sup>2</sup> measurement was triggered for the first intermediate. For the TP detected at  $m/z$  223, two MS<sup>2</sup> fragments reported by Quintana *et al.*<sup>14</sup> could be confirmed. **Gemfibrozil (Table S15):** For the TP measured at  $m/z$  279, the fragment observed at  $m/z$  151 likely corresponds to the proposed carboxy-gemfibrozil after loss of the carboxyalkyl substituent. The fragment at  $m/z$  107 may arise from further decarboxylation of the fragment at  $m/z$  151, explaining the difference of  $m/z$  14 (CH<sub>2</sub>) to the fragment at  $m/z$  121 observed for the parent molecule (see MS<sup>2</sup> spectrum in section S8). No MS<sup>2</sup> was triggered for the observed TP at  $m/z$  267, presumably corresponding to the intermediate hydroxy-gemfibrozil that has previously been described.<sup>15</sup> **Clofibric acid (Table S15):** The fragments at  $m/z$  85 and 127 of the parent molecule can be explained by a bond cleavage leading to 4-chlorophenol ( $m/z$  127) and the carboxyalkyl group ( $m/z$  85). In case of the transformation product at  $m/z$  229, the fragment at  $m/z$  101 (with a mass shift of  $m/z$  16 compared to the fragment at  $m/z$  85 of the parent molecule) supports the proposed TP structure (see MS<sup>2</sup> spectrum in section S8).

375 **Table S15:** Biotransformation of furosemide, pargyline, ketoprofen, gembrozil and clofibric acid.

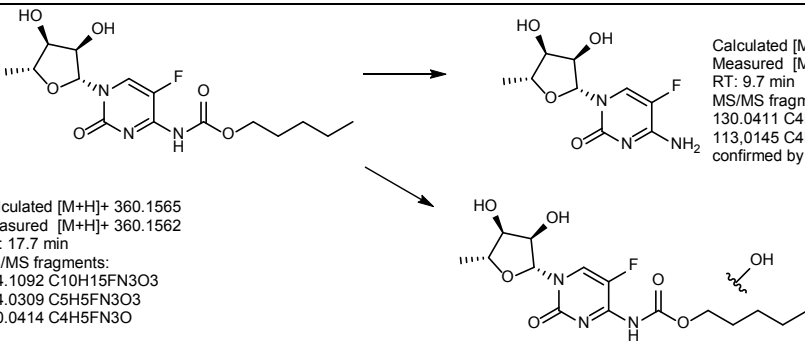
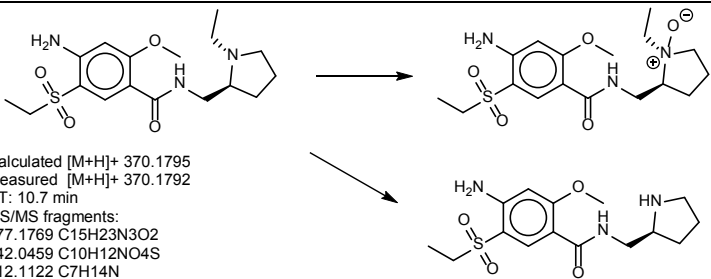
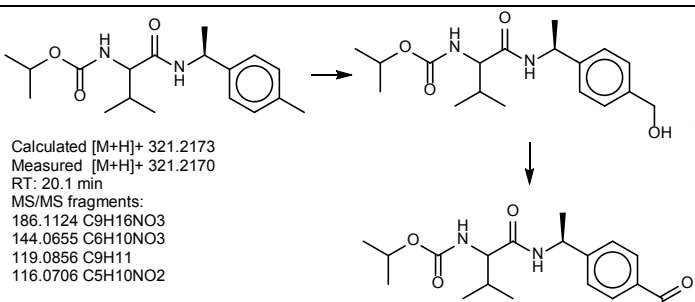
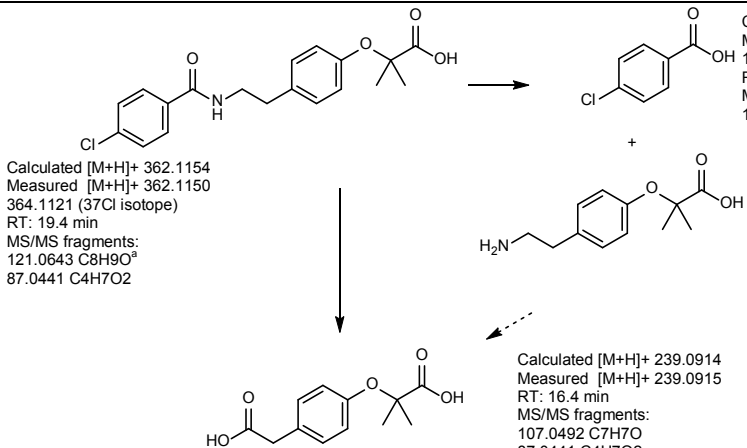
<b>Furosemide</b>	 <p>           Calculated [M+H]<sup>+</sup> 331.0150            Measured [M+H]<sup>+</sup> 331.0148            333.0118 (37Cl isotope)            RT: 16.3 min         </p> <p>           Calculated [M+H]<sup>+</sup> 250.9888            Measured [M+H]<sup>+</sup> 250.9886            252.9856 (37Cl isotope)            RT: 11.6 min            confirmed by reference standard         </p>
<b>Pargyline</b>	 <p>           Calculated [M+H]<sup>+</sup> 160.1121            Measured [M+H]<sup>+</sup> 160.1120            RT: 10.0 min         </p> <p>           Calculated [M+H]<sup>+</sup> 176.1070            Measured [M+H]<sup>+</sup> 176.1068            RT: 10.7 min            confirmed by reference standard         </p>
<b>Ketoprofen</b>	 <p>           Calculated [M+H]<sup>+</sup> 255.1016            Measured [M+H]<sup>+</sup> 255.1014            Calculated [M-H]<sup>-</sup> 253.0870            Measured [M-H]<sup>-</sup> 253.0879            RT: 18.9 min         </p> <p>           Calculated [M-H]<sup>-</sup> 269.0819            Measured [M-H]<sup>-</sup> 269.0819            RT: 17.7 min            MS/MS fragments:            225.0922 C<sub>15</sub>H<sub>13</sub>O<sub>2</sub>            195.0815 C<sub>14</sub>H<sub>11</sub>O         </p> <p>           Calculated [M-H]<sup>-</sup> 255.1027            Measured [M-H]<sup>-</sup> 255.1026            RT: 18.0 min            no MS2 measurement triggered         </p> <p>           Calculated [M-H]<sup>-</sup> 223.0612            Measured [M-H]<sup>-</sup> 223.0611            RT: 17.1 min            MS/MS fragments:            179.0717 C<sub>10</sub>H<sub>11</sub>O<sub>3</sub><sup>a</sup>            135.0819 C<sub>9</sub>H<sub>11</sub>O<sup>a</sup> </p>
<b>Gembrozil</b>	 <p>           Calculated [M+H]<sup>+</sup> 251.1642            [M-H]<sup>-</sup> 249.1496            Measured [M+H]<sup>+</sup> 251.1641            [M-H]<sup>-</sup> 249.1495            RT: 22.0 min            MS/MS fragments (negative ionization mode)            205.1590 C<sub>14</sub>H<sub>21</sub>O            121.0660 C<sub>8</sub>H<sub>9</sub>O         </p> <p>           Calculated [M+H]<sup>+</sup> 267.1591            Measured [M+H]<sup>+</sup> 267.1590            RT: 20.1 min            no MS2 triggered         </p> <p>           Calculated [M-H]<sup>-</sup> 279.1238            Measured [M-H]<sup>-</sup> 279.1236            RT: 20.1 min            MS/MS fragments:            151.0401 C<sub>8</sub>H<sub>7</sub>O<sub>3</sub>            107.0504 C<sub>7</sub>H<sub>7</sub>O         </p>
<b>Clofibric acid</b>	 <p>           Calculated [M-H]<sup>-</sup> 213.0324            Measured [M-H]<sup>-</sup> 213.0323            215.0293 (37Cl isotope)            RT: 19.3 min            MS/MS fragments:            126.9958 C<sub>6</sub>H<sub>4</sub>ClO            85.0295 C<sub>4</sub>H<sub>5</sub>O<sub>2</sub> </p> <p>           Calculated [M-H]<sup>-</sup> 229.0273            Measured [M-H]<sup>-</sup> 229.0272            231.0243 (37Cl isotope)            RT: 17.3 min            MS/MS fragments:            126.9958 C<sub>6</sub>H<sub>4</sub>ClO            101.0241 C<sub>4</sub>H<sub>5</sub>O<sub>3</sub> </p>

<sup>a</sup>Indicates that the respective fragments were reported previously.<sup>14</sup>

**Capecitabine (Table S16):** The TP formed by hydrolysis of the carbamate structure was confirmed by a reference standard. An additional TP was observed at  $m/z$  376. The fragments at  $m/z$  174 and  $m/z$  130 appear in both the parent spectrum and the MS<sup>2</sup> spectrum of the TP. Although the exact position of the hydroxylation is not known, the fragment at  $m/z$  260 can be explained by a hydroxylated alkyl chain still connected to the fluoropyrimidine ring and loss of the tetrahydrofuran structure (see MS<sup>2</sup> spectrum in section S8). **Amisulpride (Table S16):** Formation of the corresponding N-oxide was confirmed by a reference standard. Another TP was observed at  $m/z$  342. The fragment at  $m/z$  242 was observed in both the parent and the TP spectra. In agreement with the suggested deethylation (–C<sub>2</sub>H<sub>4</sub>), a fragment at  $m/z$  84 was observed in the TP spectrum instead of the fragment  $m/z$  112 observed for the parent (see MS<sup>2</sup> spectrum in section S8). **Iprovalicarb (Table S16):** The two observed TPs at  $m/z$  337 and 351 can be explained by a hydroxylation of iprovalicarb, followed by further oxidation to the corresponding carboxylic acid (most likely via an intermediate aldehyde). The fragment at  $m/z$  116 was observed for the parent and both TPs. The fragments  $m/z$  119 in the parent,  $m/z$  135 for hydroxy-iprovalicarb and  $m/z$  149 for carboxy-iprovalicarb likely reflect this step-wise oxidation (see MS<sup>2</sup> spectra and further interpretation of fragments in section S8). **Bezafibrate (Table S16):** TPs at  $m/z$  155 and 224 were detected as previously reported by Helbling *et al.*<sup>13</sup> and result from hydrolysis of the secondary amide. Additionally, a TP at  $m/z$  239 was observed, likely corresponding to an N-dealkylation of bezafibrate, followed by oxidation of the aldehyde. The fragment at  $m/z$  87 was observed for both the parent molecule and the TP (see MS<sup>2</sup> spectra and further interpretation of fragments in section S8). Note that, as predicted by the Eawag-PPS (<http://eawag-bbd.ethz.ch/predict/>), the proposed structure of the TP at  $m/z$  239 could also be formed from the hydrolysis product (TP at  $m/z$  155).



402 **Table S16:** Biotransformation of capecitabine, amisulpride, iprovalicarb and bezafibrate.

<b>Capecitabine</b>	 <p>Calculated [M+H]<sup>+</sup> 246.0885 Measured [M+H]<sup>+</sup> 246.0883 RT: 9.7 min MS/MS fragments: 130.0411 C<sub>4</sub>H<sub>5</sub>FN<sub>3</sub>O 113.0145 C<sub>4</sub>H<sub>2</sub>FN<sub>2</sub> confirmed by reference standard</p> <p>Calculated [M+H]<sup>+</sup> 360.1565 Measured [M+H]<sup>+</sup> 360.1562 RT: 17.7 min MS/MS fragments: 244.1092 C<sub>10</sub>H<sub>15</sub>FN<sub>3</sub>O<sub>3</sub> 174.0309 C<sub>5</sub>H<sub>5</sub>FN<sub>3</sub>O<sub>3</sub> 130.0414 C<sub>4</sub>H<sub>5</sub>FN<sub>3</sub>O</p> <p>Calculated [M+H]<sup>+</sup> 376.1515 Measured [M+H]<sup>+</sup> 376.1512 RT: 13.8 min MS/MS fragments: 260.1043 C<sub>10</sub>H<sub>15</sub>FN<sub>3</sub>O<sub>4</sub> 174.0309 C<sub>10</sub>H<sub>5</sub>FN<sub>3</sub>O 130.0411 C<sub>4</sub>H<sub>5</sub>FN<sub>3</sub>O</p>
<b>Amisulpride</b>	 <p>Calculated [M+H]<sup>+</sup> 370.1795 Measured [M+H]<sup>+</sup> 370.1792 RT: 10.7 min MS/MS fragments: 277.1769 C<sub>15</sub>H<sub>23</sub>N<sub>3</sub>O<sub>2</sub> 242.0459 C<sub>10</sub>H<sub>12</sub>NO<sub>4</sub>S 112.1122 C<sub>7</sub>H<sub>14</sub>N</p> <p>Calculated [M+H]<sup>+</sup> 386.1744 Measured [M+H]<sup>+</sup> 386.1742 RT: 11.5 min MS/MS fragments: 242.0471 C<sub>10</sub>H<sub>12</sub>NO<sub>4</sub>S 128.1072 C<sub>7</sub>H<sub>14</sub>NO confirmed by reference standard</p> <p>Calculated [M+H]<sup>+</sup> 342.1482 Measured [M+H]<sup>+</sup> 342.1482 RT: 10.5 min MS/MS fragments: 242.0480 C<sub>10</sub>H<sub>12</sub>NO<sub>4</sub>S 84.0808 C<sub>5</sub>H<sub>10</sub>N</p>
<b>Iprovalicarb<sup>b</sup></b>	 <p>Calculated [M+H]<sup>+</sup> 321.2173 Measured [M+H]<sup>+</sup> 321.2170 RT: 20.1 min MS/MS fragments: 186.1124 C<sub>9</sub>H<sub>16</sub>NO<sub>3</sub> 144.0655 C<sub>6</sub>H<sub>10</sub>NO<sub>3</sub> 119.0856 C<sub>9</sub>H<sub>11</sub> 116.0706 C<sub>5</sub>H<sub>10</sub>NO<sub>2</sub></p> <p>Calculated [M+H]<sup>+</sup> 337.2122 Measured [M+H]<sup>+</sup> 337.2119 RT: 17.5 min MS/MS fragments: 251.1753 C<sub>14</sub>H<sub>23</sub>N<sub>2</sub>O<sub>2</sub> 186.1125 C<sub>9</sub>H<sub>16</sub>NO<sub>3</sub> 144.0656 C<sub>6</sub>H<sub>10</sub>NO<sub>3</sub> 135.0805 C<sub>9</sub>H<sub>11</sub>O 116.0706 C<sub>5</sub>H<sub>10</sub>NO<sub>2</sub></p> <p>Calculated [M+H]<sup>+</sup> 351.1914 Measured [M+H]<sup>+</sup> 351.1914 RT: 18.0 min MS/MS fragments: 265.1537 C<sub>14</sub>H<sub>21</sub>O<sub>3</sub>N<sub>2</sub> 149.0594 C<sub>9</sub>H<sub>9</sub>O<sub>2</sub> 116.0704 C<sub>5</sub>H<sub>10</sub>NO<sub>2</sub></p>
<b>Bezafibrate</b>	 <p>Calculated [M+H]<sup>+</sup> 362.1154 Measured [M+H]<sup>+</sup> 362.1150 RT: 19.4 min MS/MS fragments: 121.0643 C<sub>8</sub>H<sub>9</sub>O<sup>a</sup> 87.0441 C<sub>4</sub>H<sub>7</sub>O<sub>2</sub></p> <p>Calculated [M-H]<sup>-</sup> 154.9905 Measured [M-H]<sup>-</sup> 154.9906 156.9875 (37Cl isotope) RT: 18.4 min MS/MS fragments: 111.0008 C<sub>6</sub>H<sub>4</sub>Cl<sup>a</sup></p> <p>Calculated [M+H]<sup>+</sup> 224.1281 Measured [M+H]<sup>+</sup> 224.1280 RT: 11.9 min MS/MS fragments: 121.0648 C<sub>8</sub>H<sub>9</sub>O<sup>a</sup> 87.0443 C<sub>4</sub>H<sub>7</sub>O<sub>2</sub> 59.0495 C<sub>3</sub>H<sub>7</sub>O</p> <p>Calculated [M+H]<sup>+</sup> 239.0914 Measured [M+H]<sup>+</sup> 239.0915 RT: 16.4 min MS/MS fragments: 107.0492 C<sub>7</sub>H<sub>7</sub>O 87.0441 C<sub>4</sub>H<sub>7</sub>O<sub>2</sub> 59.0494 C<sub>3</sub>H<sub>7</sub>O</p>

<sup>a</sup>Indicates that the respective fragments were reported previously.<sup>13</sup> <sup>b</sup>the position of hydroxylation and carboxylation was not unequivocally determined from the fragments and only one possible structural isomer is shown for each TP.

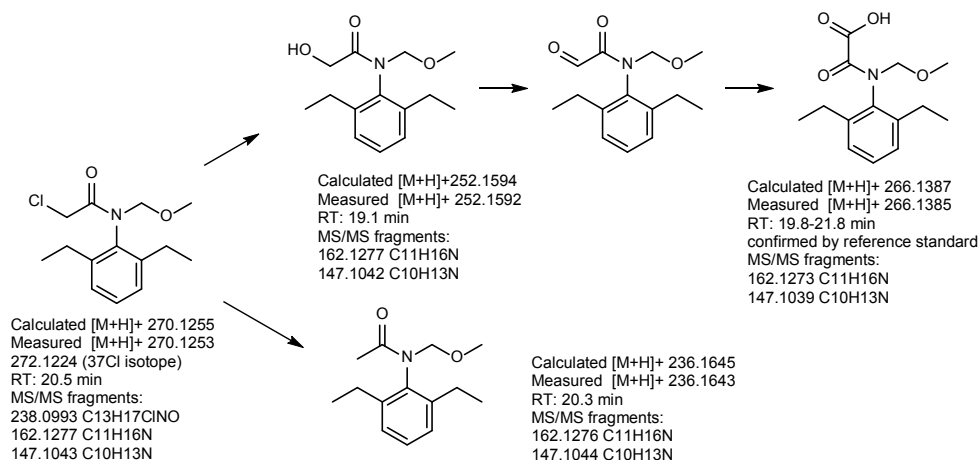
**Atenolol, levetiracetam and rufinamide (Table S17):** Formation of the hydrolysis products atenolol acid and levetiracetam acid was confirmed by reference standards. Analogously, a TP at the expected mass of the corresponding rufinamide hydrolysis product ( $m/z$  240) was detected. In the MS<sup>2</sup> spectra of both rufinamide and the TP at  $m/z$  240, one dominant fragment at  $m/z$  127 emerged, likely representing the 2,6-difluorotoluene moiety of rufinamide (see MS<sup>2</sup> spectrum in section S8).

**Table S17:** Biotransformation of atenolol, levetiracetam and rufinamide.

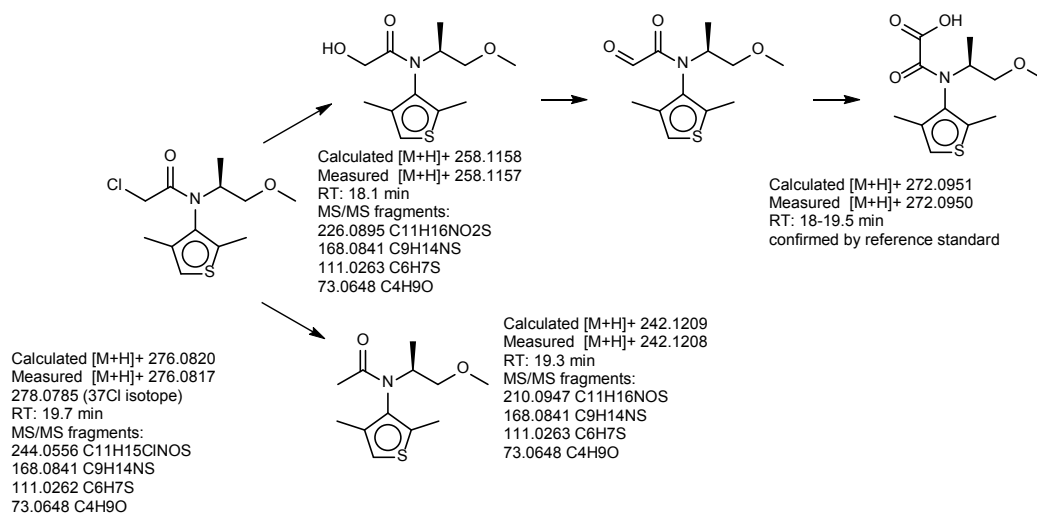
<p><b>Atenolol</b></p> <div style="text-align: center;"> </div> <div style="display: flex; justify-content: space-around; margin-top: 10px;"> <div style="text-align: center;"> <p>Calculated [M+H]<sup>+</sup> 267.1703 Measured [M+H]<sup>+</sup> 267.1701 RT: 8.9 min</p> </div> <div style="text-align: center;"> <p>Calculated [M+H]<sup>+</sup> 268.1543 Measured [M+H]<sup>+</sup> 268.1540 RT: 11.0 min confirmed by reference standard</p> </div> </div>
<p><b>Levetiracetam</b></p> <div style="text-align: center;"> </div> <div style="display: flex; justify-content: space-around; margin-top: 10px;"> <div style="text-align: center;"> <p>Calculated [M+H]<sup>+</sup> 171.1128 Measured [M+H]<sup>+</sup> 171.1127 RT: 11.3 min</p> </div> <div style="text-align: center;"> <p>Calculated [M+H]<sup>+</sup> 172.0968 Measured [M+H]<sup>+</sup> 172.0967 RT: 13.4 min confirmed by reference standard</p> </div> </div>
<p><b>Rufinamide</b></p> <div style="text-align: center;"> </div> <div style="display: flex; justify-content: space-around; margin-top: 10px;"> <div style="text-align: center;"> <p>Calculated [M+H]<sup>+</sup> 239.0739 Measured [M+H]<sup>+</sup> 239.0737 RT: 14.4 min MS/MS fragments: 127.0353 C7H5F2</p> </div> <div style="text-align: center;"> <p>Calculated [M+H]<sup>+</sup> 240.0579 Measured [M+H]<sup>+</sup> 240.0576 RT: 14.8 min MS/MS fragments: 127.0352 C7H5F2</p> </div> </div>

**Dimethenamid, alachlor, metolachlor, propachlor and flufenacet (Table S18):** For all five acetanilides, formation of the OXA-transformation products was confirmed using reference standards. The proposed pathway via substitution of the chlorine (or the thiadiazole moiety in the case of flufenacet) was supported by the detection of hydroxy-acetanilides for all 5 substances. The hydroxylated intermediates showed negative retention time shifts (-1.4 – -3 min) and revealed similarities in MS<sup>2</sup> fragmentation with their respective parent spectra (see Table S18). As additional pathway, reductive dehalogenation was observed for all 4 chloro-substituted acetanilides. For propachlor, the observed fragments at *m/z* 94 und 136 (that were also observed in the spectrum of the parent) have been reported previously.<sup>16</sup> For all reduction products, similar shifts in retention time (-0.2 – -0.6) and similar fragmentations as for the respective parents were observed (see MS<sup>2</sup> spectra in section S8). A peak corresponding to the *m/z* value of the expected analogous reduced flufenacet was observed but no MS<sup>2</sup> fragmentation spectrum was obtained. For propachlor and metolachlor, additional TPs were detected: For propachlor, formation of propachlor-ESA was confirmed by a reference standard. For metolachlor, a TP at *m/z* 270 with a mass shift corresponding to a methylene group (-CH<sub>2</sub>, *m/z* 14) was observed, suggesting that an O-demethylation reaction had occurred. The fragments at *m/z* 176, 134 already observed in the spectrum of the parent remained unaltered and a fragment at *m/z* 59 (C<sub>3</sub>H<sub>7</sub>O) appeared instead of the fragment at *m/z* 73 (C<sub>4</sub>H<sub>9</sub>O) observed for the parent molecule (see MS<sup>2</sup> spectrum in section S8).

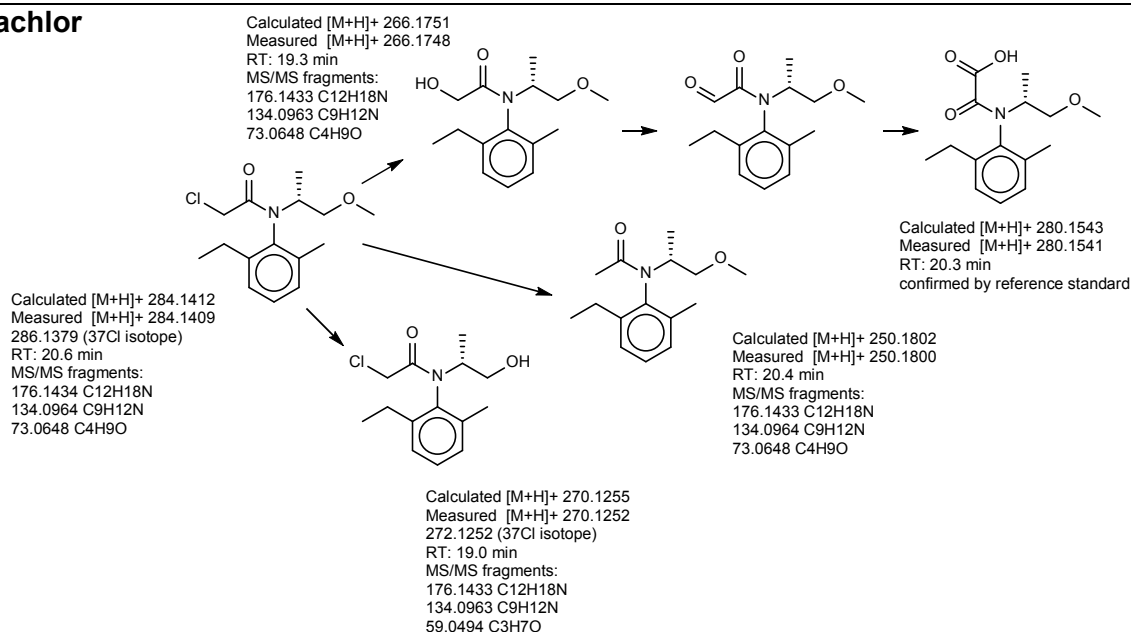
### Alachlor



### Dimethenamid



### Metolachlor

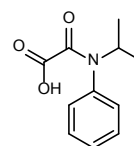
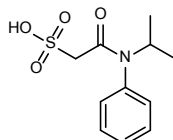
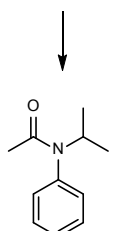
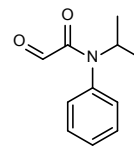
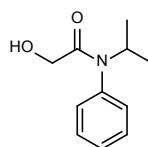
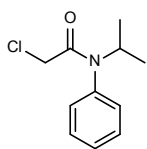


## Propachlor

Calculated [M+H]<sup>+</sup> 212.0837  
Measured [M+H]<sup>+</sup> 212.0836  
214.0806 (37Cl isotope)  
RT: 18.6 min  
MS/MS fragments:  
134.0600 C<sub>8</sub>H<sub>8</sub>NO  
94.0652 C<sub>6</sub>H<sub>8</sub>N<sup>a</sup>

Calculated [M+H]<sup>+</sup> 194.1176  
Measured [M+H]<sup>+</sup> 194.1175  
RT: 16.9 min  
MS/MS fragments:  
152.0705 C<sub>8</sub>H<sub>10</sub>NO<sub>2</sub><sup>a</sup>  
134.0600 C<sub>8</sub>H<sub>8</sub>NO<sup>a</sup>  
106.0651 C<sub>7</sub>H<sub>8</sub>N<sup>a</sup>  
94.0652 C<sub>6</sub>H<sub>8</sub>N<sup>a</sup>

Calculated [M+H]<sup>+</sup> 192.1019  
Measured [M+H]<sup>+</sup> 192.1017  
RT: 17.5 min  
MS/MS fragments:  
104.0494 C<sub>6</sub>H<sub>8</sub>N<sup>a</sup>  
94.0651 C<sub>6</sub>H<sub>8</sub>N<sup>a</sup>



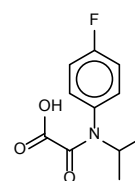
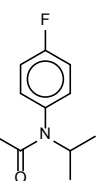
Calculated [M+H]<sup>+</sup> 178.1226  
Measured [M+H]<sup>+</sup> 178.1225  
RT: 18.2 min  
MS/MS fragments:  
136.0754 C<sub>8</sub>H<sub>10</sub>NO<sup>a</sup>  
94.0649 C<sub>6</sub>H<sub>8</sub>N<sup>a</sup>

Calculated [M-H]<sup>-</sup> 256.0649  
Measured [M-H]<sup>-</sup> 256.0651  
RT: 17.3-18.5 min  
confirmed by reference standard

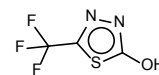
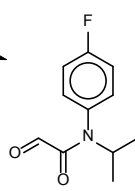
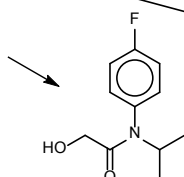
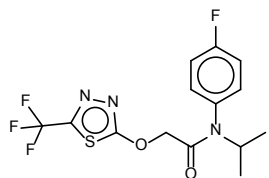
Calculated [M+H]<sup>+</sup> 208.0968  
Measured [M+H]<sup>+</sup> 208.0967  
RT: 16.8-17.8 min  
confirmed by reference standard

## Flufenacet

Calculated [M+H]<sup>+</sup> 196.1132  
Measured [M+H]<sup>+</sup> 196.1131  
RT: 18.2 min  
no MS2 triggered



Calculated [M-H]<sup>-</sup> 224.0728  
Measured [M-H]<sup>-</sup> 224.0728  
RT: 17.5-18.5 min  
confirmed by reference standard



Calculated [M+H]<sup>+</sup> 364.0737  
Measured [M+H]<sup>+</sup> 364.0735  
RT: 20.1 min  
MS/MS fragments:  
194.0975 C<sub>11</sub>H<sub>13</sub>FNO  
152.0506 C<sub>8</sub>H<sub>7</sub>FNO  
124.0551 C<sub>7</sub>H<sub>7</sub>FN

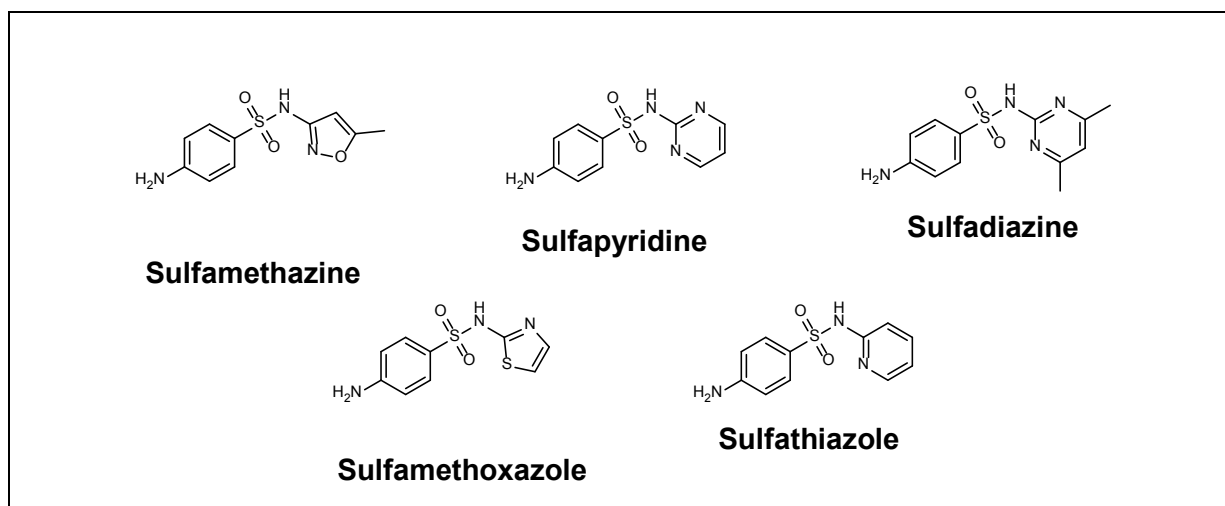
Calculated [M+H]<sup>+</sup> 212.1081  
Measured [M+H]<sup>+</sup> 212.1080  
RT: 17.1 min  
MS/MS fragments:  
152.0506 C<sub>8</sub>H<sub>7</sub>FNO  
124.0557 C<sub>7</sub>H<sub>7</sub>FN  
122.0400 C<sub>7</sub>H<sub>5</sub>FN  
97.0448 C<sub>6</sub>H<sub>6</sub>F

Calculated [M+H]<sup>+</sup> 210.0925  
Measured [M+H]<sup>+</sup> 210.0923  
RT: 17.7 min  
MS/MS fragments:  
150.0350 C<sub>8</sub>H<sub>5</sub>FNO  
122.0401 C<sub>7</sub>H<sub>5</sub>FN  
95.0292 C<sub>6</sub>H<sub>4</sub>F

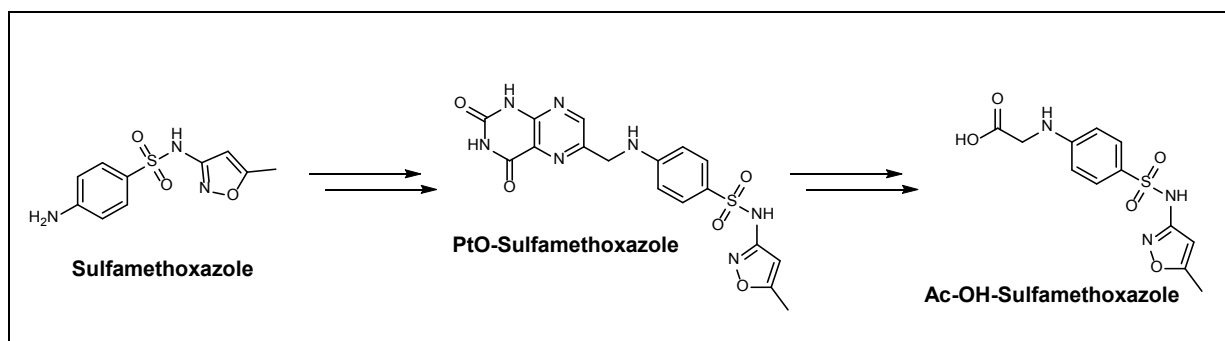
434 <sup>a</sup>Indicates that the fragments were measured previously.<sup>13</sup>

435

**Sulfamethoxazole, sulfadiazine, sulfamethazine, sulfapyridine and sulfathiazole:** For all five investigated sulfonamide antibiotics (Figure S7), TPs of the recently reported pterin-conjugate pathway<sup>17</sup> were detected, namely the conjugates PtO-sulfonamide and Ac-OH-sulfonamide (Figure S8). The detected *m/z* values are provided in Table S19. Because the same measurement method was applied, we could directly compare the obtained retention times with the retention times reported in the study in which the pterin-conjugate pathway was investigated.<sup>17</sup> Although all retention times measured here were shifted to higher values due to changes in dead volume, the differences in retention time between the TPs and the corresponding parents were conserved ( $\pm 0.1$  min).



**Figure S7:** Molecular structures of the 5 sulfonamide antibiotics investigated in this study.



**Figure S8:** In the recently reported pterin-conjugate pathway,<sup>17</sup> two of the major metabolites were PtO-sulfamethoxazole and Ac-OH-sulfamethoxazole.

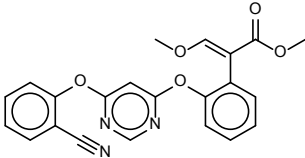

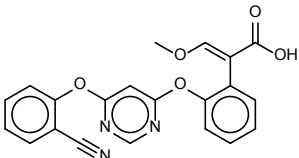
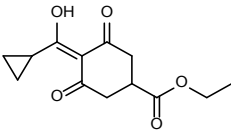

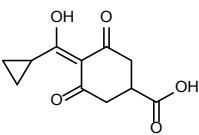
**Table S19:** Detected  $m/z$  values and RTs of the parent sulfonamides and the PtO and Ac-OH TPs.

TP		Sulfamethazine	Sulfapyridine	Sulfadiazine	Sulfamethoxazole	Sulfathiazole
Parent	$m/z$ calculated $[M+H]^+$	279.0910	250.0645	251.0597	254.0594	256.0209
	$m/z$ observed $[M+H]^+$	279.0908	250.0642	251.0595	254.0591	256.0207
	RT observed	12.6	11.2	10.5	13.4	10.8
PtO-SA	$m/z$ calculated $[M+H]^+$	455.1250	426.0984	427.0937	430.0934	432.0549
	$m/z$ observed $[M+H]^+$	455.1254	426.0989	427.0941	430.0937	432.0551
	RT observed	13.6	12.7	12.3	14.1	12.3
	RT shift <sup>a</sup>	1.0	1.5	1.8	0.7	1.5
Ac-OH-SA	$m/z$ calculated $[M+H]^+$	337.0971	308.0705	309.0658	312.0654	314.0269
	$m/z$ observed $[M+H]^+$	337.0967	308.0701	309.0653	312.0648	314.0264
	RT observed	13.6	12.4	11.9	14.1	12.1
	RT shift <sup>a</sup>	1.0	1.2	1.4	0.7	1.3

<sup>a</sup>Indicates the retention time differences to the peaks of the respective parent sulfonamides.

**Azoxystrobin and trinexapac-ethyl (Table S20):** Biotransformation to the corresponding carboxylic acids (azoxystrobin acid and trinexapac) was confirmed using analytical standards.

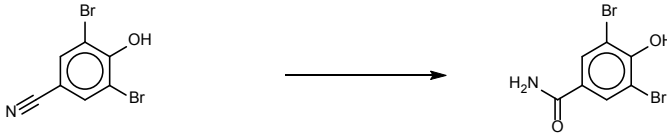
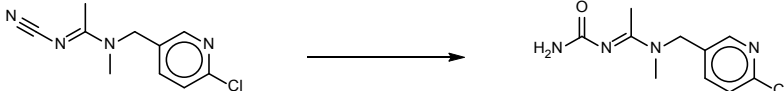
**Table S20:** Detected TPs of azoxystrobin and trinexapac-ethyl.

<p><b>Azoxystrobin</b></p> <div style="text-align: center;">    </div> <div style="display: flex; justify-content: space-around;"> <div style="text-align: center;"> <p>Calculated [M+H]<sup>+</sup> 404.1241 Measured [M+H]<sup>+</sup> 404.1237 RT: 18.9 min</p> </div> <div style="text-align: center;"> <p>Calculated [M+H]<sup>+</sup> 390.1084 Measured [M+H]<sup>+</sup> 390.1081 RT: 18.0 min confirmed by reference standard</p> </div> </div>
<p><b>Trinexapac-ethyl</b></p> <div style="text-align: center;">    </div> <div style="display: flex; justify-content: space-around;"> <div style="text-align: center;"> <p>Calculated [M+H]<sup>+</sup> 253.1070 Measured [M+H]<sup>+</sup> 253.1068 RT: 18.9 min</p> </div> <div style="text-align: center;"> <p>Calculated [M+H]<sup>+</sup> 225.0757 Measured [M+H]<sup>+</sup> 225.0756 RT: 16.8 min confirmed by reference standard</p> </div> </div>



**Bromoxynil (Table S21):** For bromoxynil, formation of a TP at  $m/z$  292 was observed, suggesting that the nitrile was hydrated and the corresponding amide thus formed. The characteristic isotope pattern (2 Br atoms) served as clear indication that the TP originated from bromoxynil. The MS<sup>2</sup> spectrum is provided in section S8. For **acetamiprid (Table S21)**, a TP at  $m/z$  241 was observed, presumably again representing the amide formed by a nitrile hydration reaction. Fragments at  $m/z$  56 (C<sub>3</sub>H<sub>6</sub>N) and 126 (C<sub>8</sub>H<sub>5</sub>ClN) were observed in both the parent and the TP spectrum, representing structural moieties that remained unchanged by the biological transformation. See MS<sup>2</sup> spectra and further interpretation of fragments in section S8. No evidence was detected indicating further transformation of the observed primary amides to the corresponding carboxylic acids.

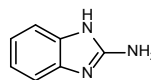
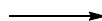
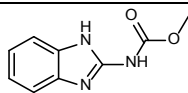
**Table S21:** Biotransformation of bromoxynil and acetamiprid.

<p><b>Bromoxynil</b></p> <div style="text-align: center;">  </div> <div style="display: flex; justify-content: space-around;"> <div data-bbox="526 1216 866 1361"> <p>Calculated [M-H]<sup>-</sup>: 273.8509  Measured [M-H]<sup>-</sup>: 273.8508 (79Br79Br isotope)  275.0485 (79Br81Br isotope)  277.8465 (81Br81Br isotope)  RT: 18.6 min  MS/MS fragments:  193.9247 C<sub>7</sub>HONBr  78.9188 Br</p> </div> <div data-bbox="1050 1216 1390 1361"> <p>Calculated [M-H]<sup>-</sup>: 291.8614  Measured [M-H]<sup>-</sup>: 291.8613 (79Br79Br isotope)  293.8594 (79Br81Br isotope)  295.8571 (81Br81Br isotope)  RT: 15.1 min  MS/MS fragments:  248.8557 C<sub>6</sub>H<sub>3</sub>OBr<sub>2</sub>  78.9189 Br</p> </div> </div>
<p><b>Acetamiprid</b></p> <div style="text-align: center;">  </div> <div style="display: flex; justify-content: space-around;"> <div data-bbox="659 1765 866 1933"> <p>Calculated [M+H]<sup>+</sup>: 223.0745  Measured [M+H]<sup>+</sup>: 223.0745  225.0715 (<sup>37</sup>Cl isotope)  RT: 14.6 min  MS/MS fragments:  126.0105 C<sub>8</sub>H<sub>5</sub>ClN  81.0335 C<sub>3</sub>H<sub>3</sub>N<sub>3</sub>  56.0498 C<sub>3</sub>H<sub>6</sub>N  55.0394 C<sub>2</sub>H<sub>3</sub>N<sub>2</sub></p> </div> <div data-bbox="1121 1753 1329 1921"> <p>Calculated [M+H]<sup>+</sup>: 241.0851  Measured [M+H]<sup>+</sup>: 241.0849  243.0820 (<sup>37</sup>Cl isotope)  RT: 9.1 min  MS/MS fragments:  198.0791 C<sub>9</sub>H<sub>13</sub>ClN<sub>3</sub>  157.0530 C<sub>7</sub>H<sub>10</sub>ClN<sub>2</sub>  126.0105 C<sub>8</sub>H<sub>5</sub>ClN  56.0498 C<sub>3</sub>H<sub>6</sub>N</p> </div> </div>

471 **Carbendazim (Table S22):** Formation of 2-aminobenzimidazole, presumably formed via hydrolysis  
472 of the carbamate moiety, was confirmed using a reference standard.

473 **Table S22:** Biotransformation of carbendazim.

**Carbendazim**

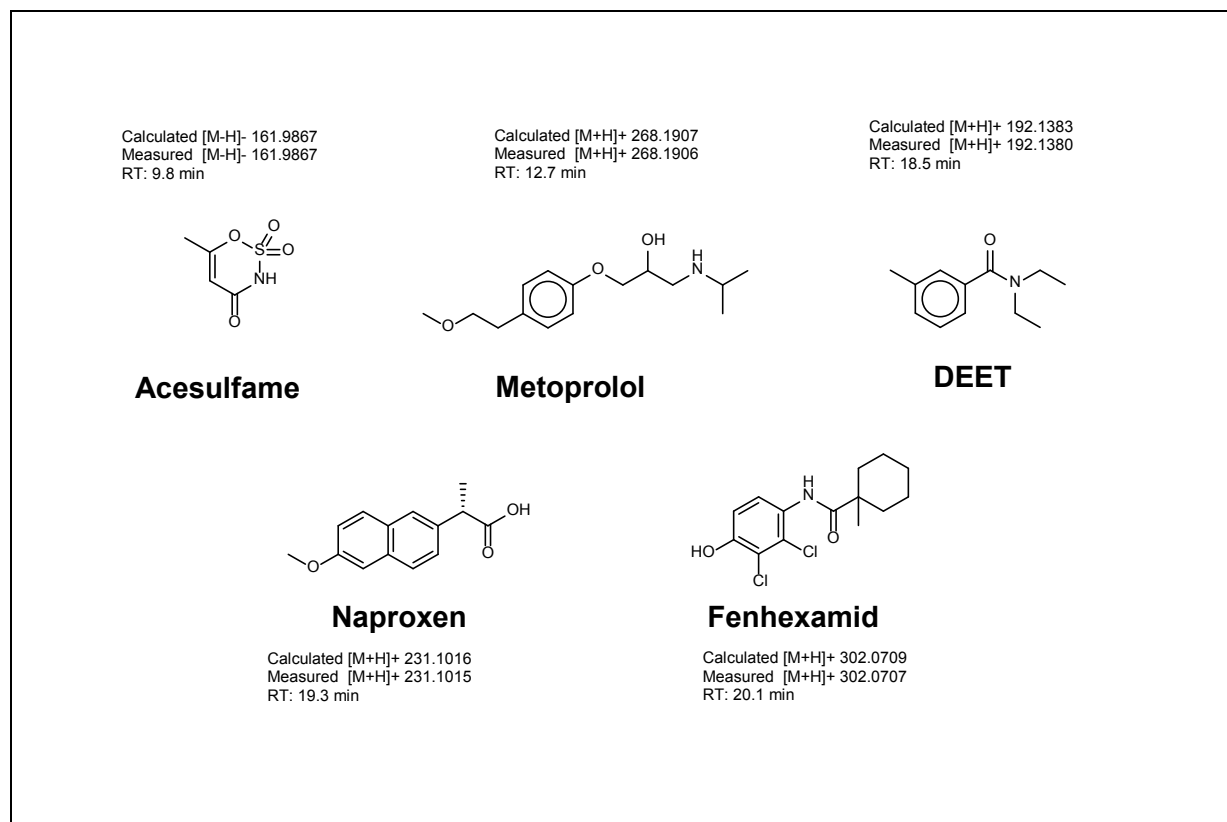


Calculated [M+H]<sup>+</sup> 192.0768  
Measured [M+H]<sup>+</sup> 192.0766  
RT: 11.3 min

Calculated [M+H]<sup>+</sup> 134.0713  
Measured [M+H]<sup>+</sup> 134.0712  
RT: 10.1 min  
confirmed by reference standard

474

**Acesulfame, metoprolol, DEET, naproxen and fenhexamid (Figure S9):** No TPs were detected for the MPs described here. **Acesulfame:** Chromatographic peaks corresponding to the expected  $m/z$  value of sulfamic acid, the main acesulfame TP observed by Castronovo *et al.*, were observed. However, because negative area-time trends were observed, it remained unclear whether there was a formation of sulfamic acid from acesulfame or whether the detected sulfamic acid originated exclusively from other sources. **Metoprolol:** Metoprolol was not spiked and could only be analyzed due to its presence in the influent. In previous studies, O-demethylation to atenolol acid was observed.<sup>18</sup> Due to the low concentrations, the majority of formed atenolol acid could unambiguously be attributed to formation from atenolol. Whether metoprolol was transformed to atenolol acid too, remained elusive. For **DEET, naproxen and fenhexamid**, none of the TPs on our suspect list was detected.



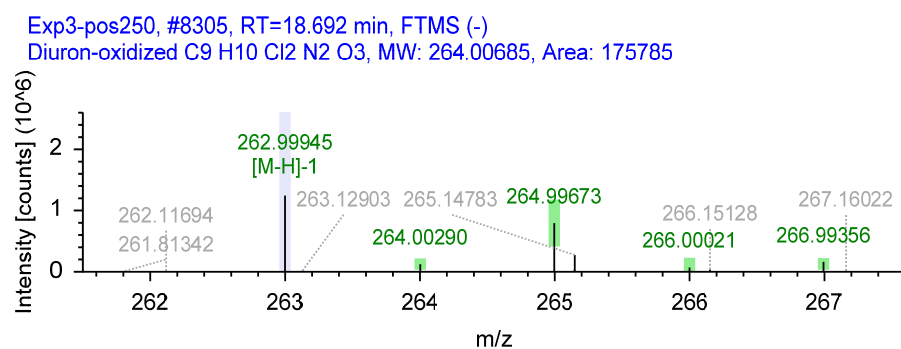
**Figure S9:** Molecular structures and detected  $m/z$  values of acesulfame, metoprolol, DEET, naproxen and fenhexamid.

## **S8 MS2 spectra**

As indicated in the preceding chapters, MS<sup>2</sup> spectra are provided here. On each page, the MS<sup>1</sup> spectrum, the MS<sup>2</sup> spectrum and the proposed molecular structure of one TP is shown. Spectra were obtained from Compound Discoverer 2.0 or Xcalibur Qualbrowser 3.0 (Thermo Scientific). Information on chromatographic retention times and ionization modes are contained in each spectrum. The green rectangles encircling isotope peaks indicate that the observed peaks match the predicted isotope peaks (with 5 ppm mass tolerance and 30% tolerance in peak intensity). For the MS<sup>2</sup> spectra, additionally, the applied collision energies and, in most cases, structural suggestions for fragments are given. Because some MS<sup>2</sup> spectra were obtained in later measurements, the retention time in these measurements was shifted towards lower RTs (due to difference in dead volume in the otherwise identical measurement setups).

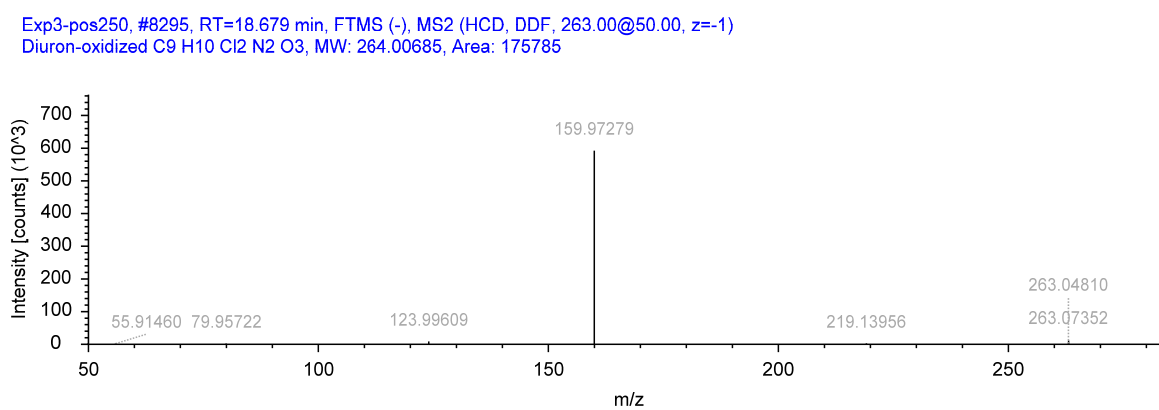
500 **Diuron: dihydroxy-diuron**

501 MS spectrum



502

503 MS<sup>2</sup> spectrum

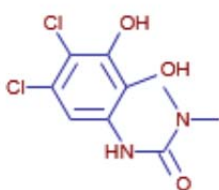


504

505 proposed structure

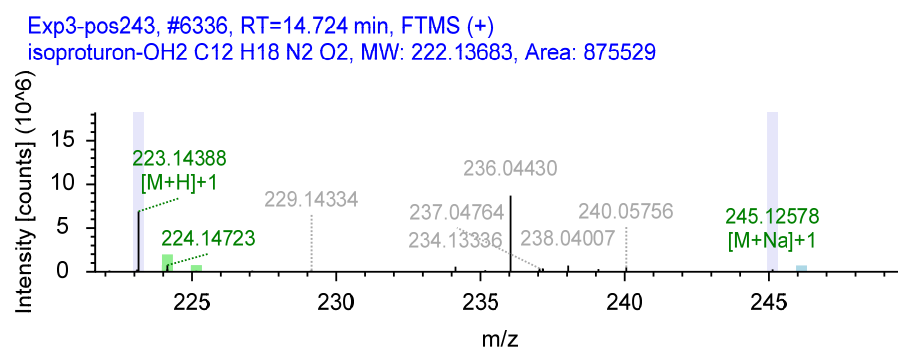
506

507



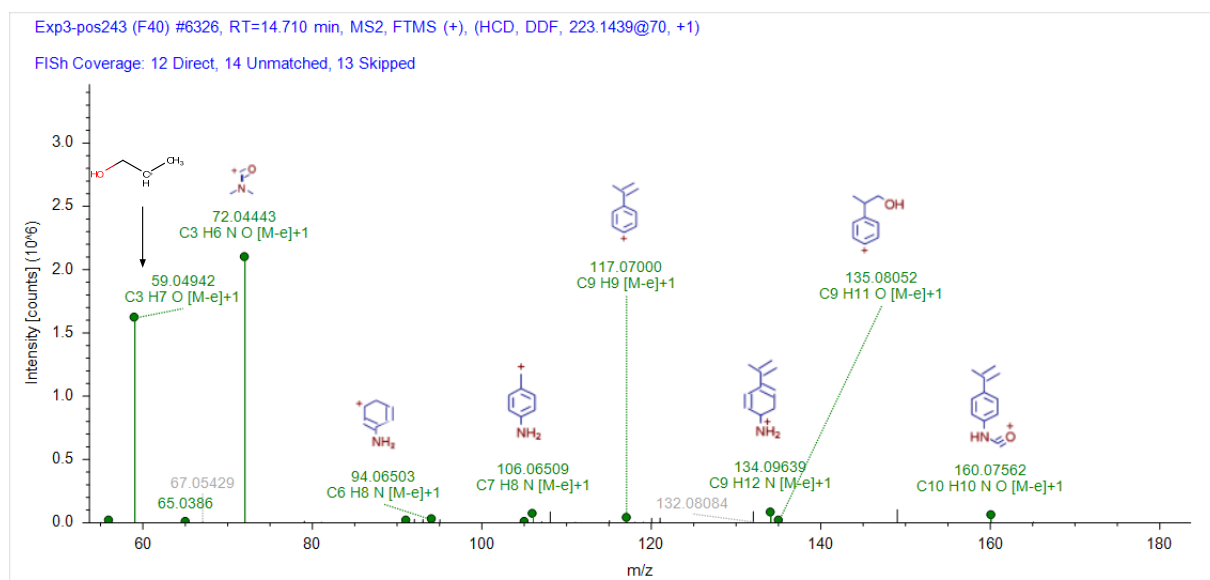
508 **Isoproturon: hydroxy-isoproturon**

509 MS spectrum



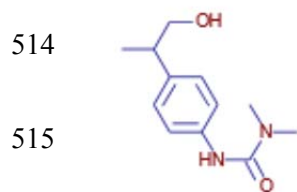
510

511 MS<sup>2</sup> spectrum



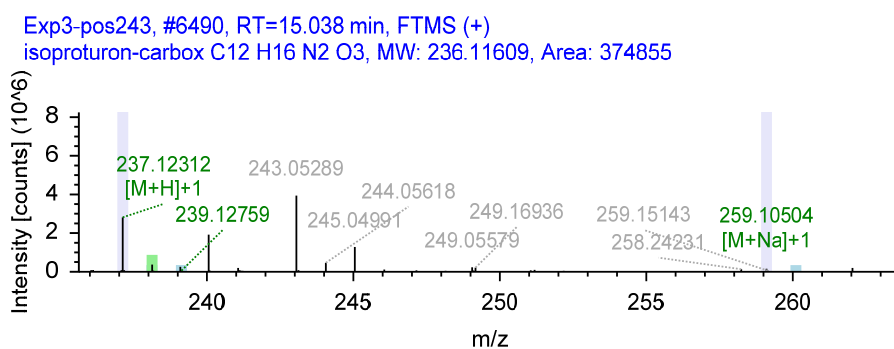
512

513 proposed structure



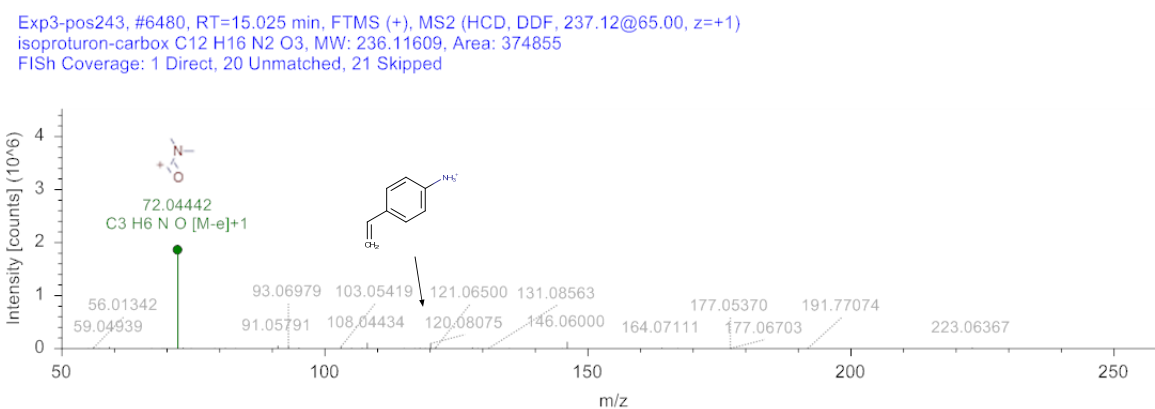
520 **Isoproturon: carboxy-isoproturon**

521 MS spectrum



522

523 MS<sup>2</sup> spectrum



524

525 proposed structure

526

527

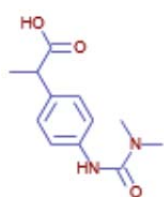
528

529

530

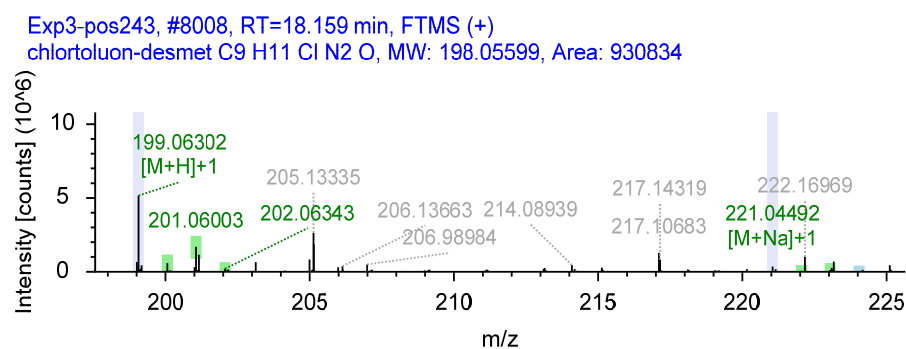
531

532



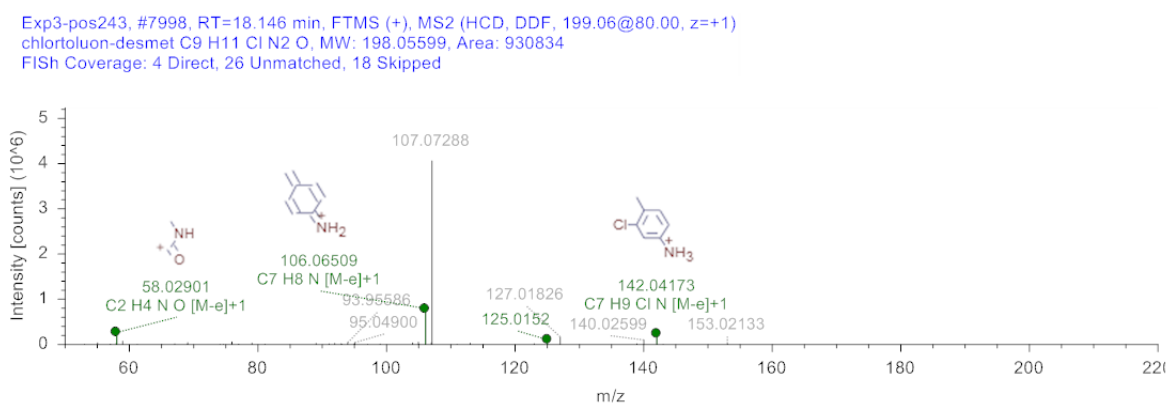
533 **Chlortoluron: chlortoluron desmethyl**

534 MS spectrum



535

536 MS<sup>2</sup> spectrum



537

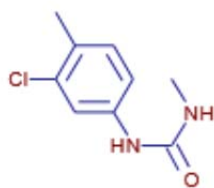
538 proposed structure

539

540

541

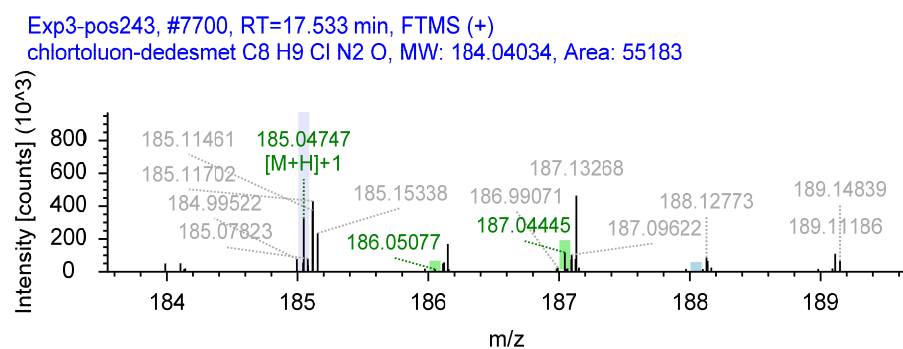
542





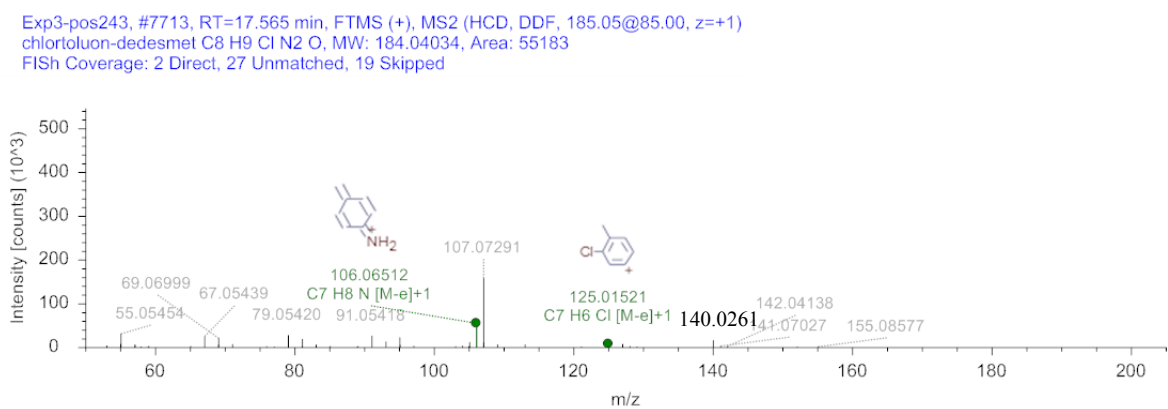
543 **Chlortoluron: chlortoluron didesmethyl**

544 MS spectrum



545

546 MS<sup>2</sup> spectrum



547

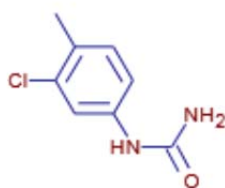
548 proposed structure

549

550

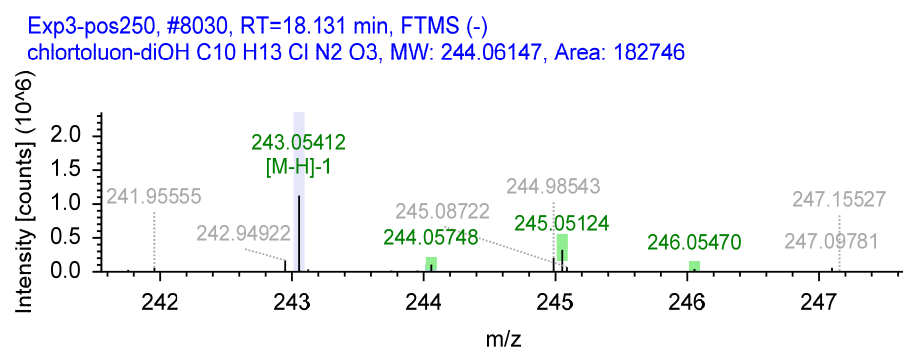
551

552



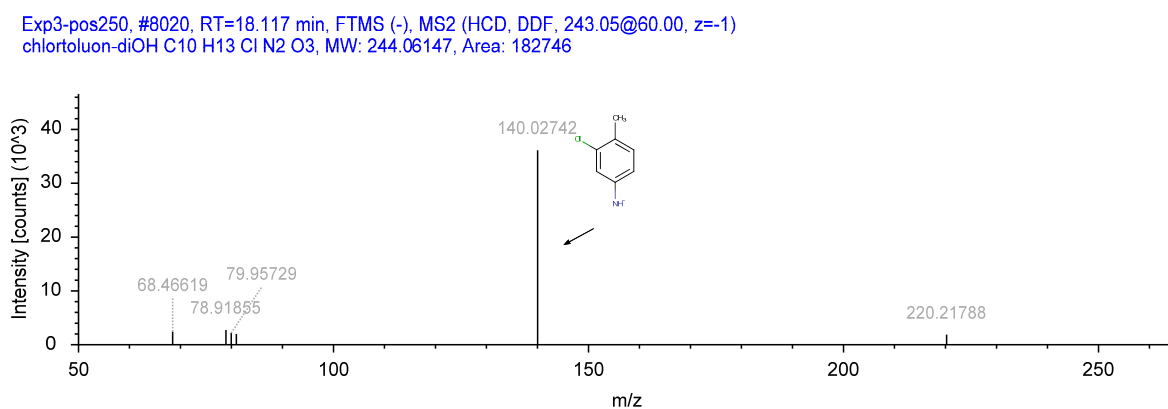
553 **Chlortoluron: dihydroxy-chlortoluron**

554 MS spectrum



555

556 MS<sup>2</sup> spectrum



557

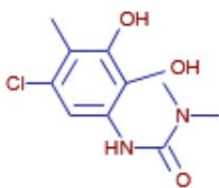
558 proposed structure

559

560

561

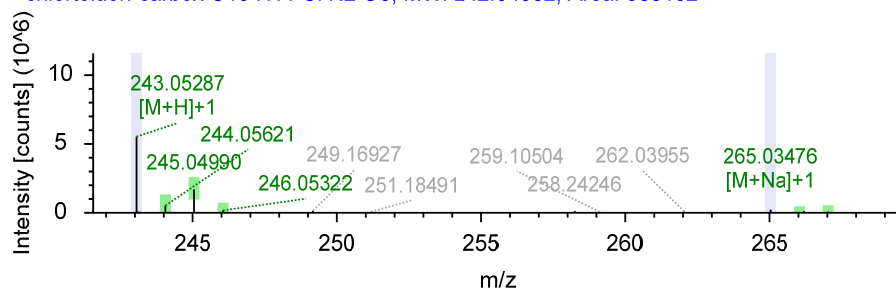
562



563 **Chlortoluron: carboxy-chlortoluron**

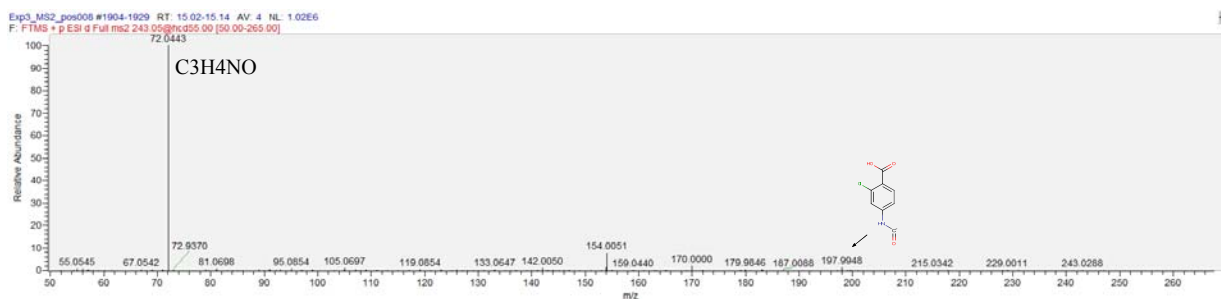
564 MS spectrum

Exp3-pos243, #6512, RT=15.083 min, FTMS (+)  
chlortoluron-carbox C10 H11 Cl N2 O3, MW: 242.04582, Area: 983102



565

566 MS<sup>2</sup> spectrum



567

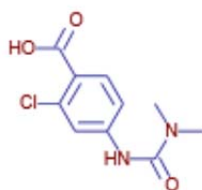
568

569 proposed structure

570

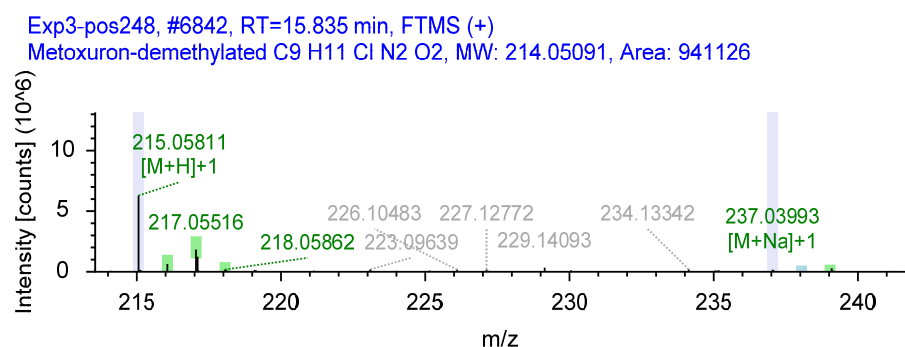
571

572



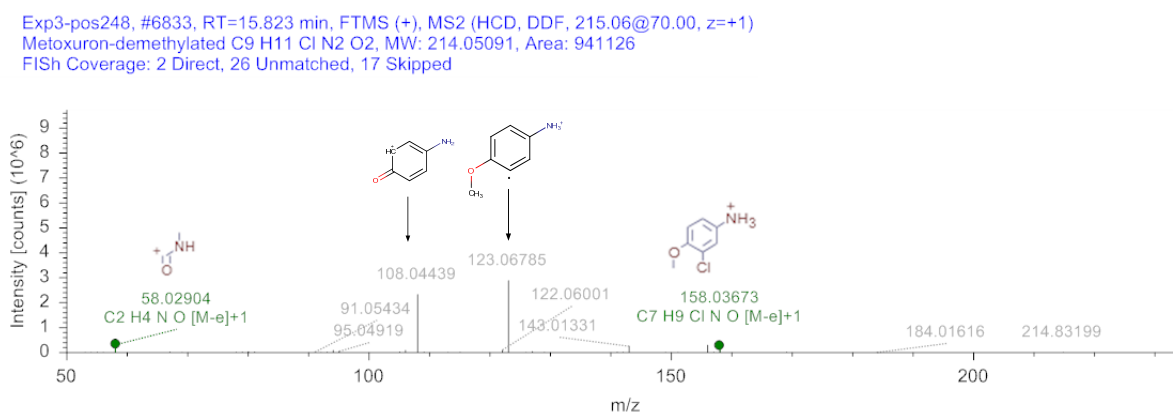
573 **Metoxuron: metoxuron desmethyl**

574 MS spectrum



575

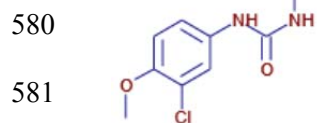
576 MS<sup>2</sup> spectrum



577

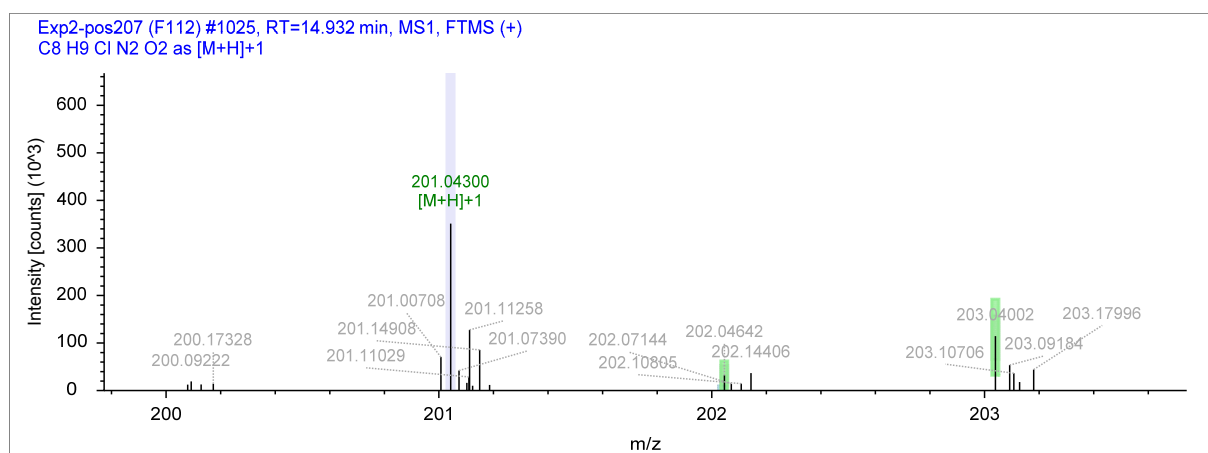
578 proposed structure

579



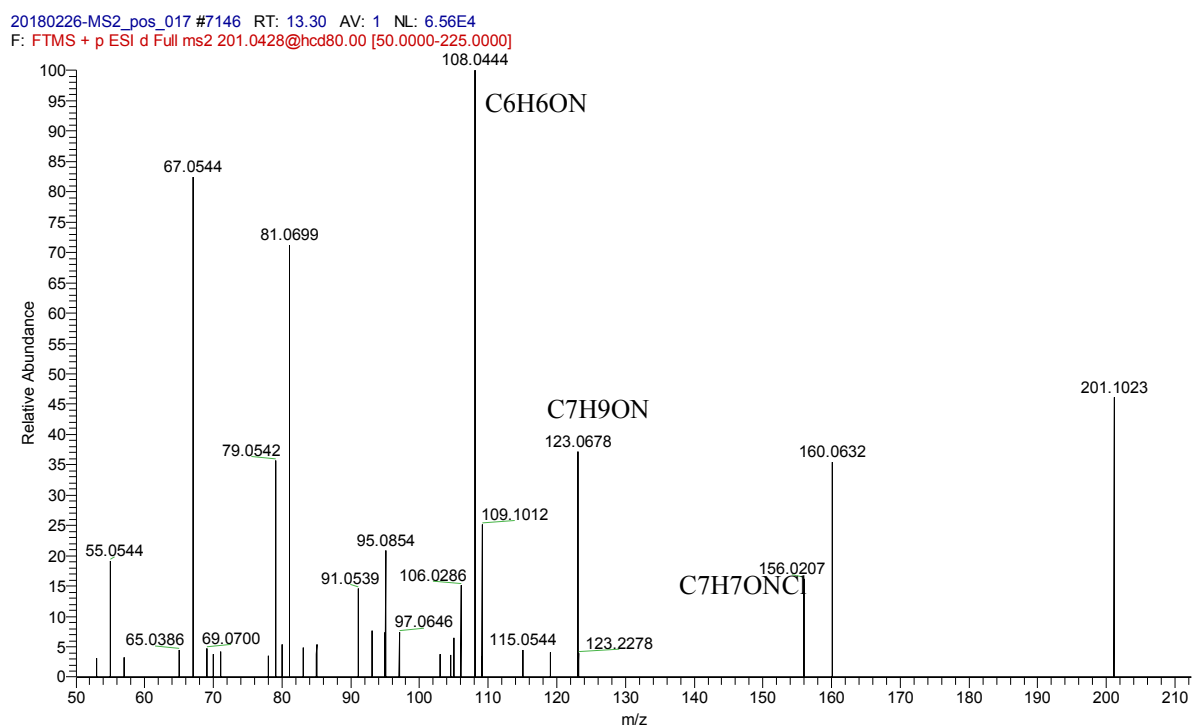
583 **Metoxuron: metoxuron didesmethyl**

584 MS spectrum



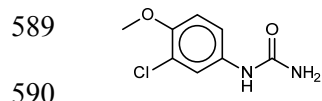
585

586 MS<sup>2</sup> spectrum



587

588 proposed structure



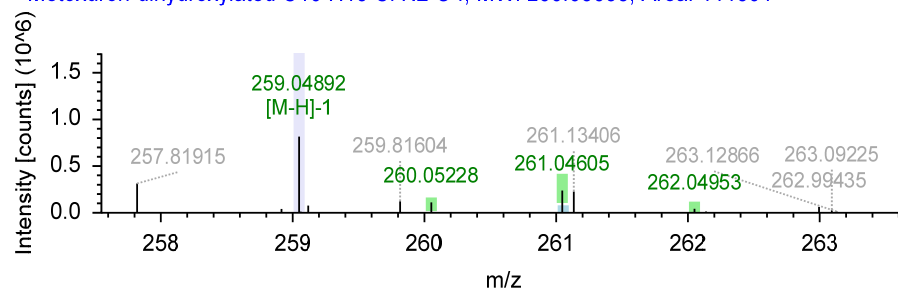
591

592

593 **Metoxuron: dihydroxy-metoxuron**

594 MS spectrum

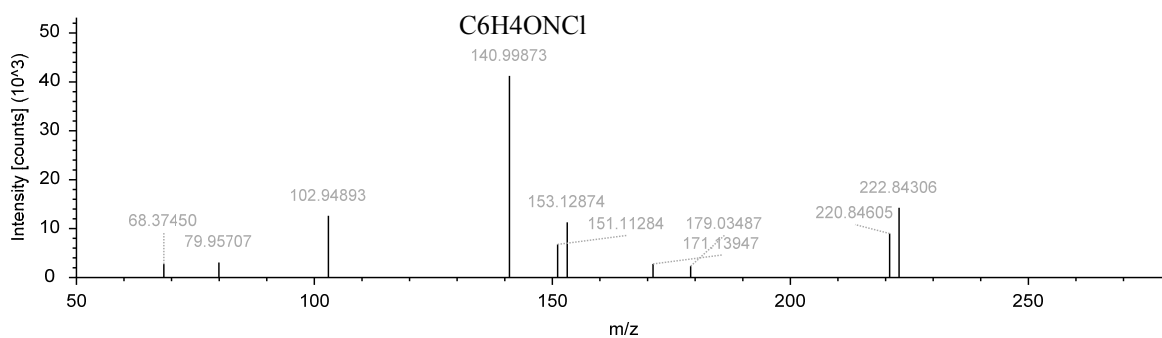
Exp3-pos255, #6908, RT=15.783 min, FTMS (-)  
Metoxuron-dihydroxylated C10 H13 Cl N2 O4, MW: 260.05638, Area: 111591



595

596 MS<sup>2</sup> spectrum

Exp3-pos255, #6931, RT=15.836 min, FTMS (-), MS2 (HCD, DDF, 259.05@55.00, z=-1)  
Metoxuron-dihydroxylated C10 H13 Cl N2 O4, MW: 260.05638, Area: 111591



597

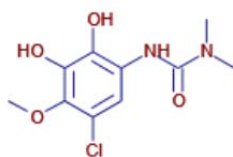
598 proposed structure

599

600

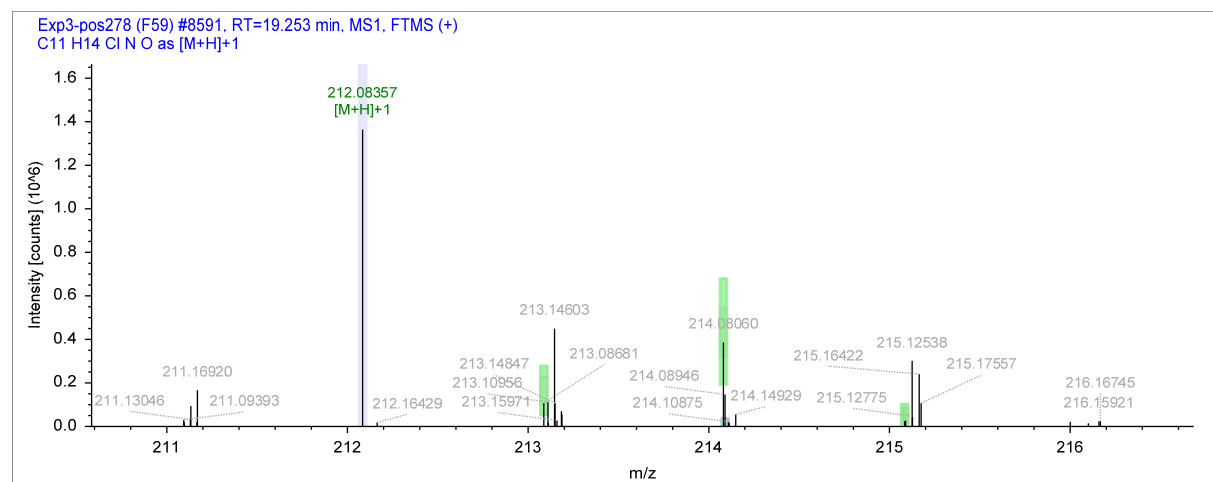
601

602

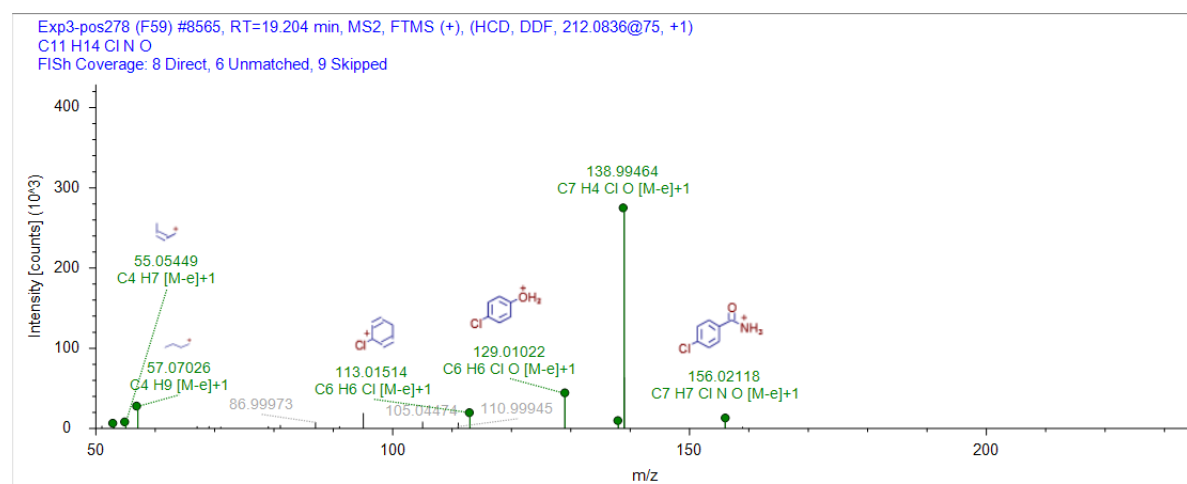


# **BEclB: BEclB desethyl**

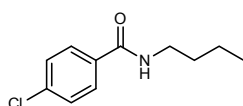
## MS spectrum



## MS<sup>2</sup> spectrum

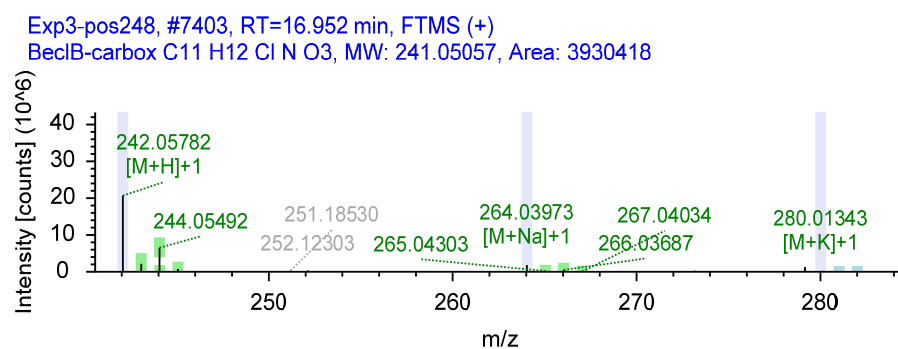


## proposed structure



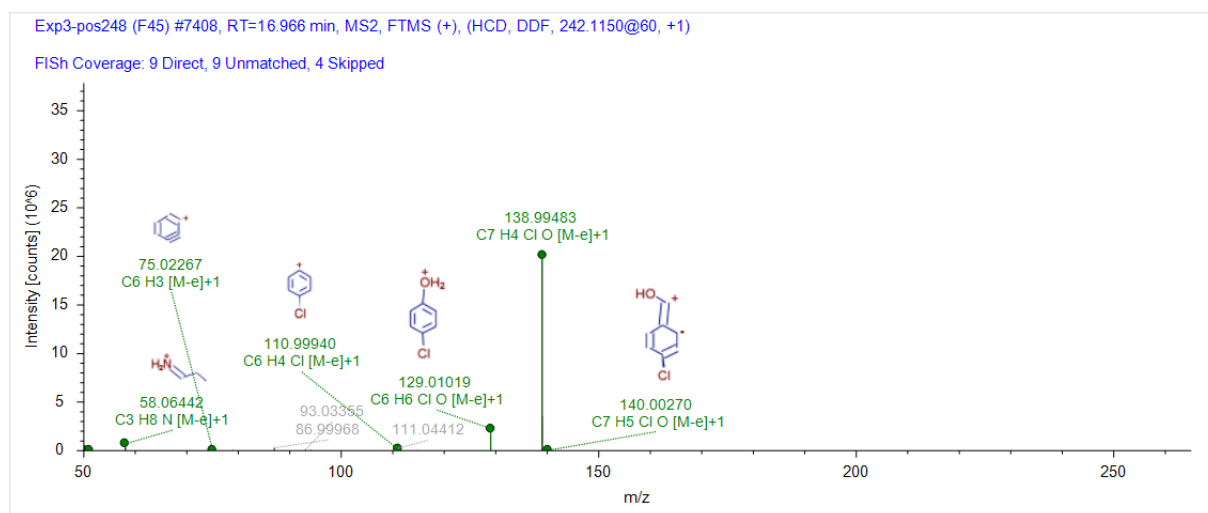
615 **BEclB: BEclB-TP242**

616 MS spectrum



617

618 MS<sup>2</sup> spectrum



619

620

621 proposed structure

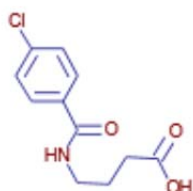
622

623

624

625

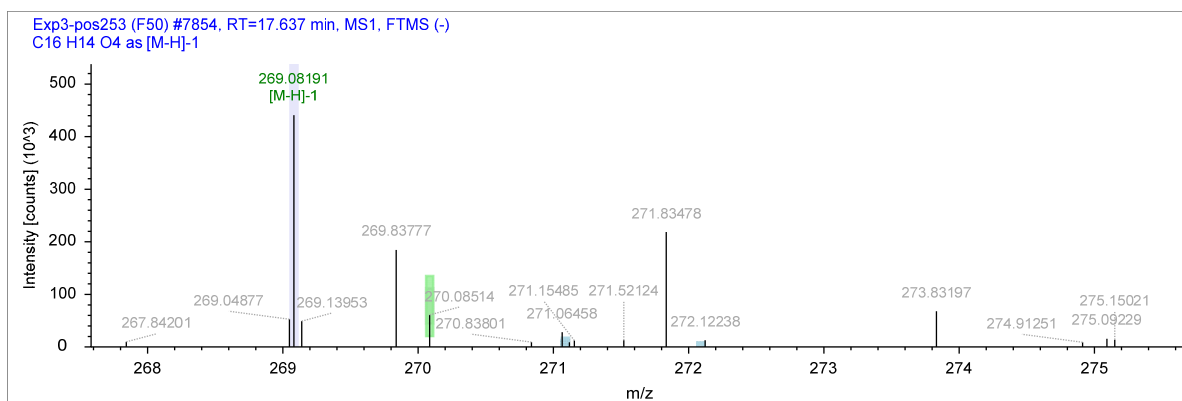
626





627 Ketoprofen: hydroxy-ketoprofen

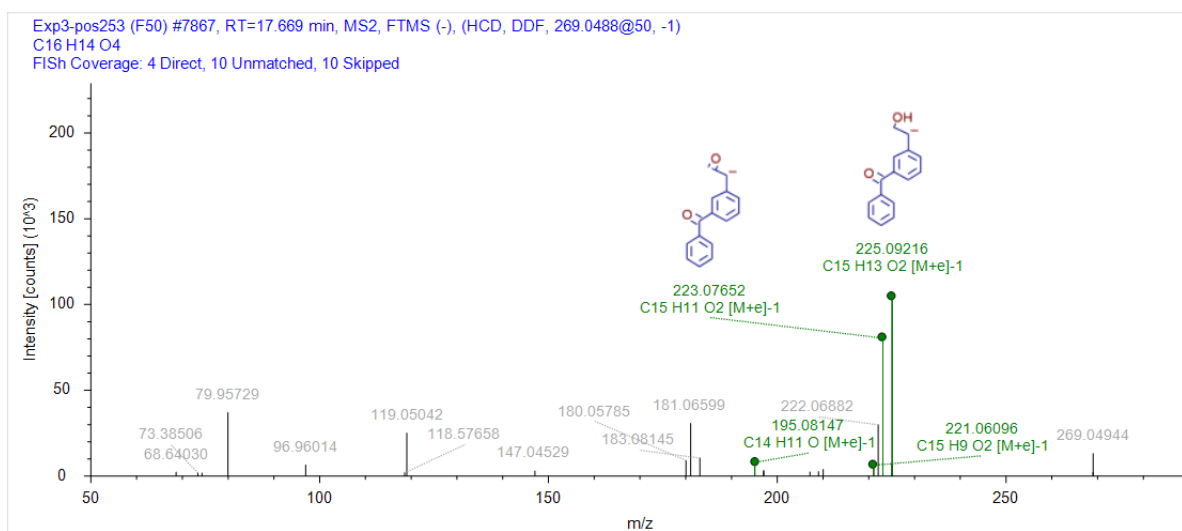
628 MS spectrum



629

630

631 MS<sup>2</sup> spectrum



632

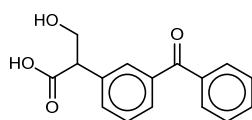
633

634 proposed structure

635

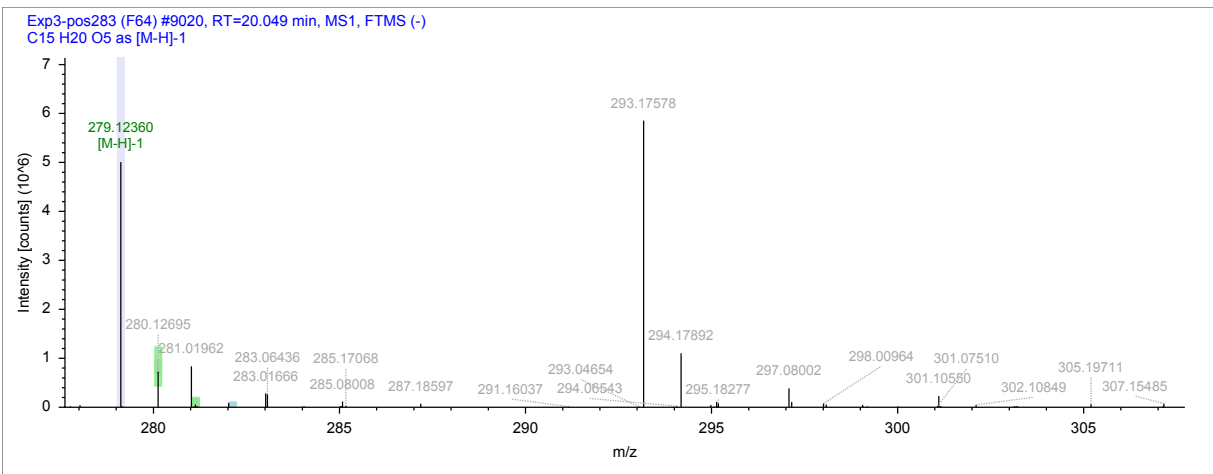
636

637

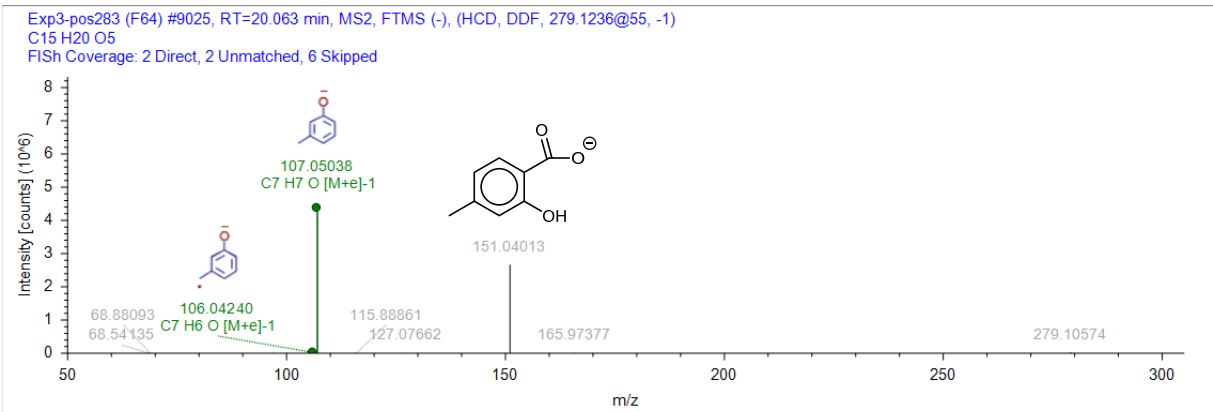


**Gemfibrozil: carboxy-gemfibrozil**

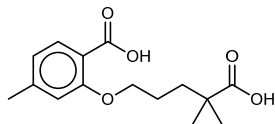
**MS spectrum**



**MS<sup>2</sup> spectrum**

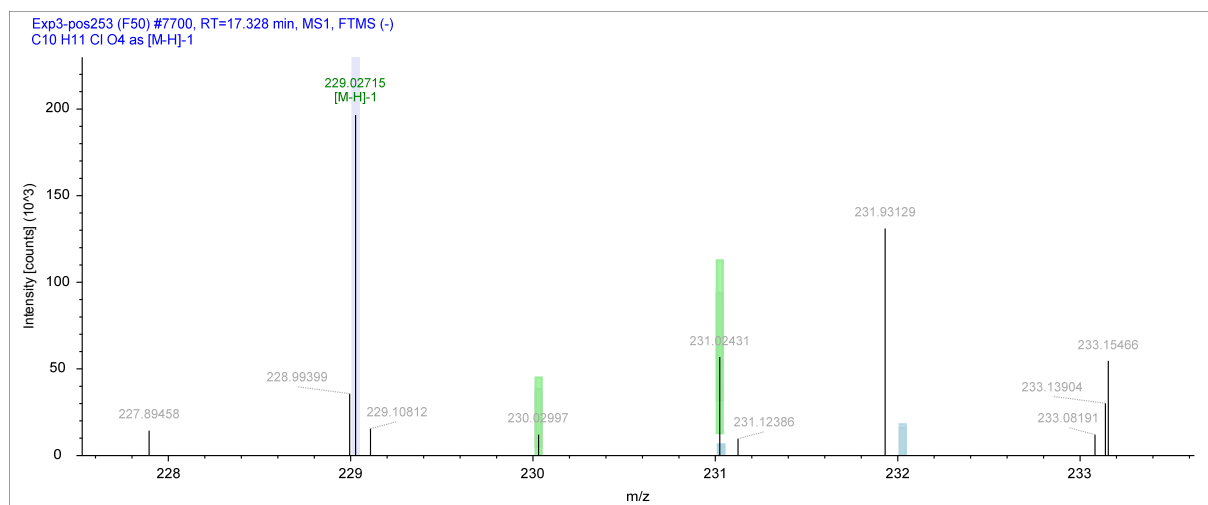


**proposed structure**



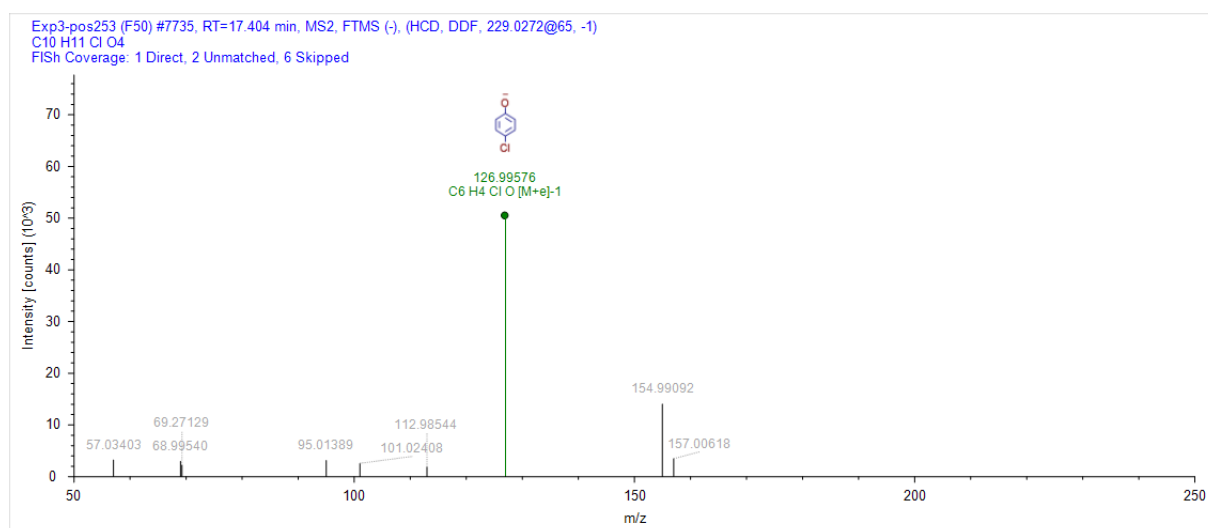
648 **Clofibric acid: hydroxy-clofibric acid**

649 MS spectrum



650

651 MS<sup>2</sup> spectrum



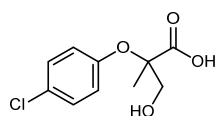
652

653

654 proposed structure

655

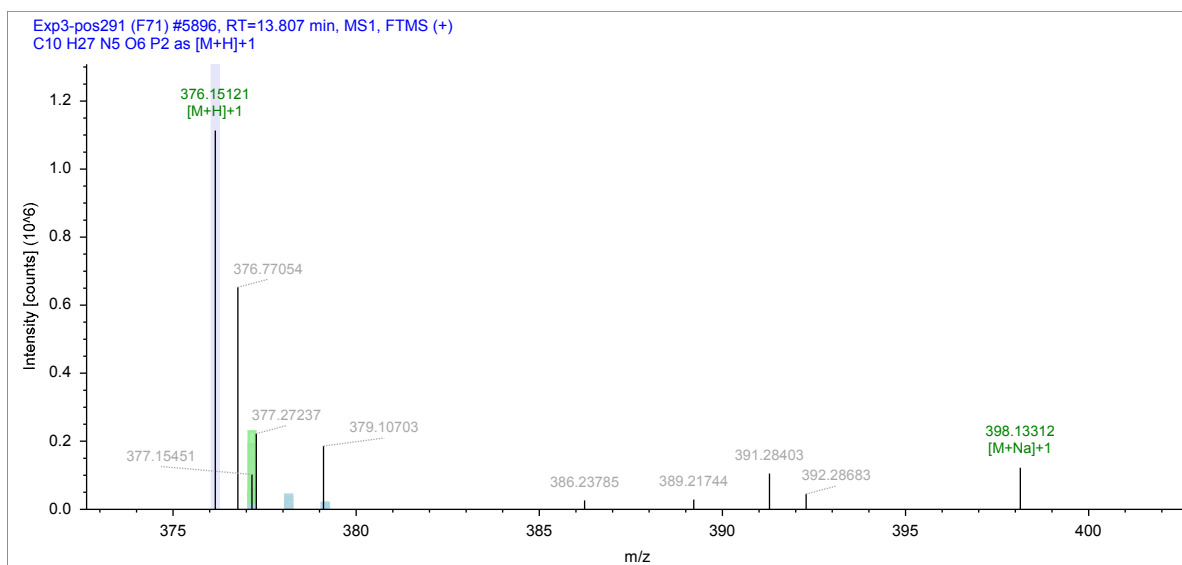
656



657

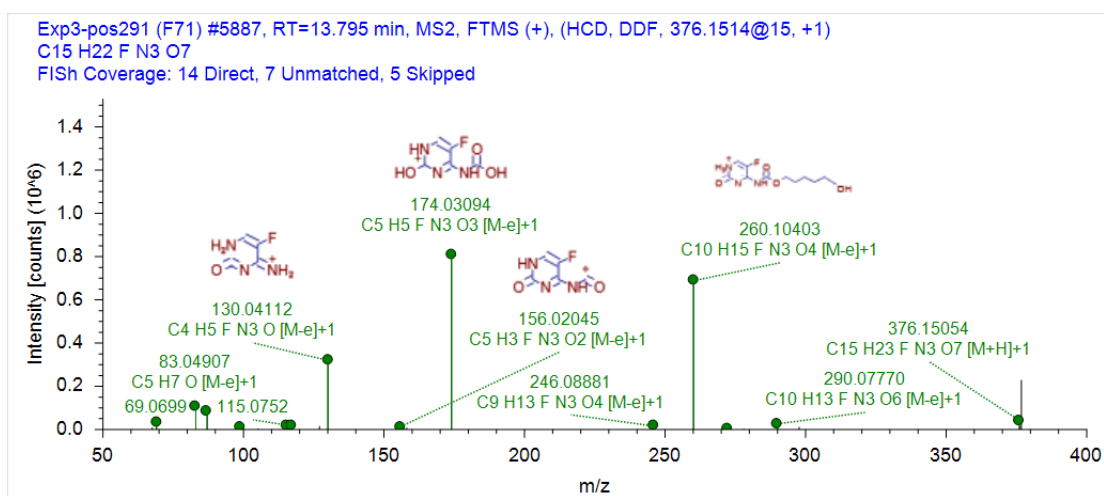
658 **Capecitabine: hydroxy-capecitabine**

659 MS spectrum



660

661 MS<sup>2</sup> spectrum



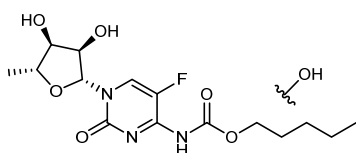
662

663 proposed structure

664

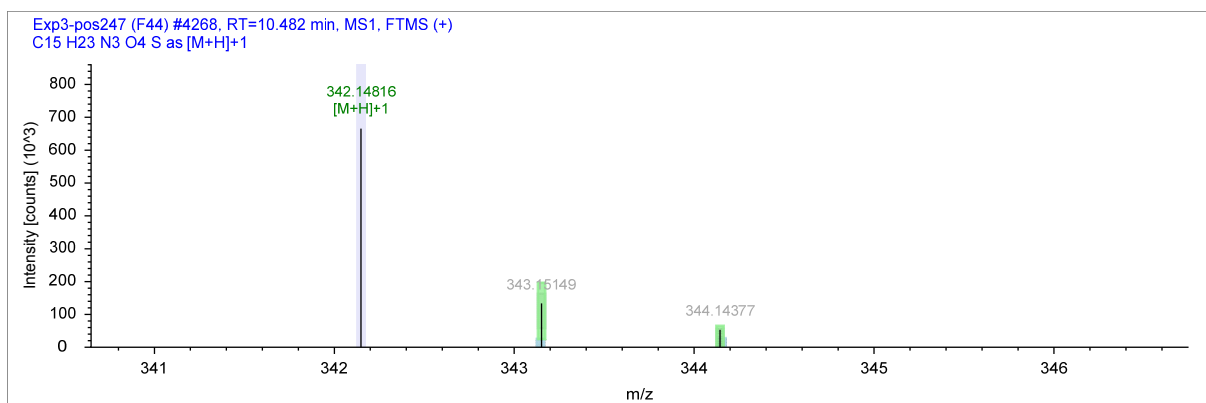
665

666



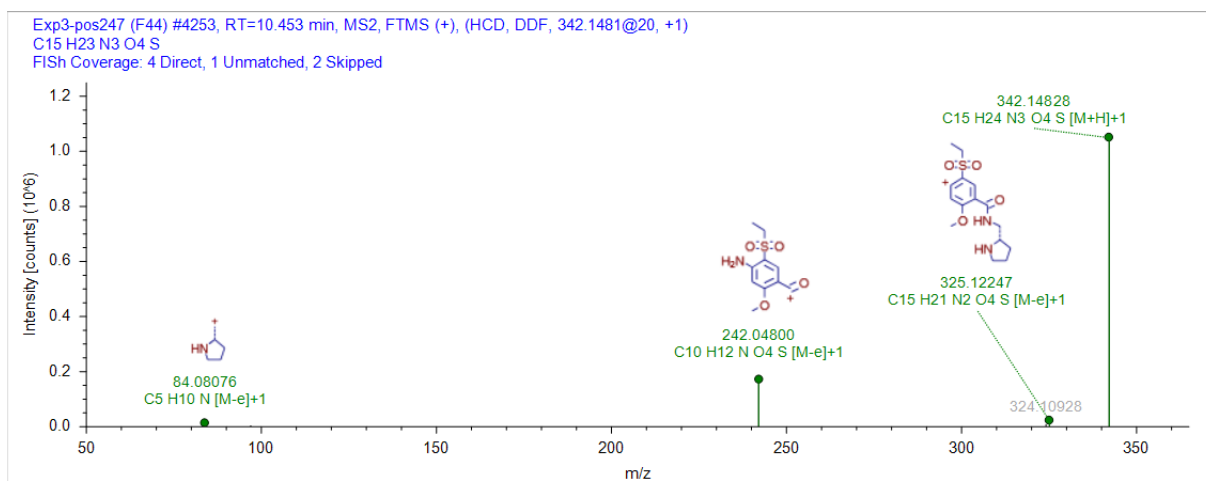
667 Amisulprid: amisulprid desethyl

668 MS spectrum



669

670 MS<sup>2</sup> spectrum



671

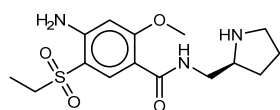
672

673 proposed structure

674

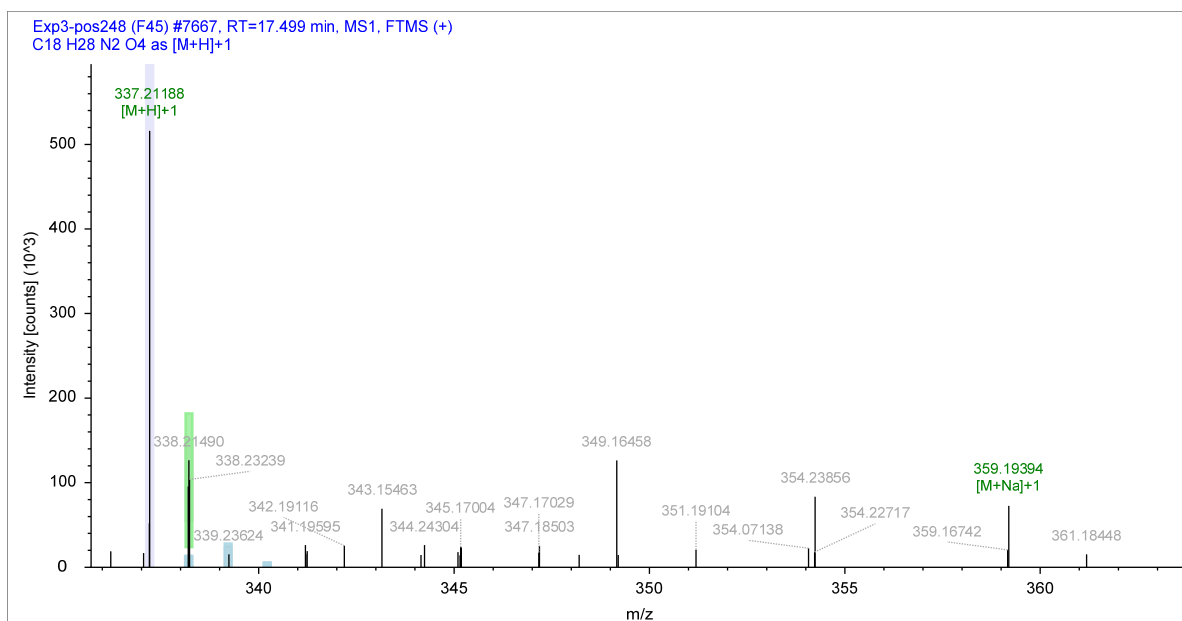
675

676



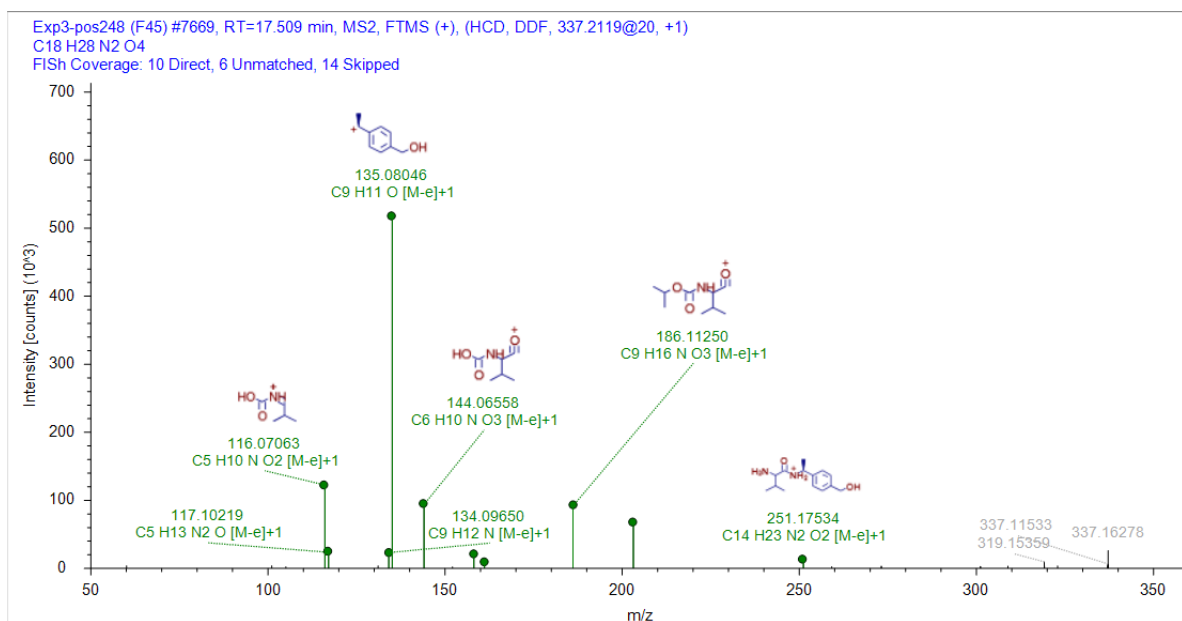
677 Iprovalicarb: hydroxy-iprovalicarb

678 MS spectrum



679

680 MS<sup>2</sup> spectrum



681

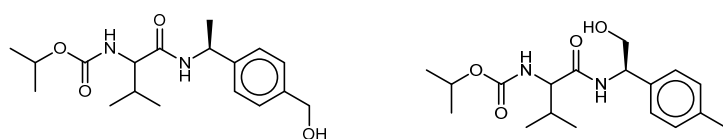
682 proposed structure (2 possible regioisomers)

683

684

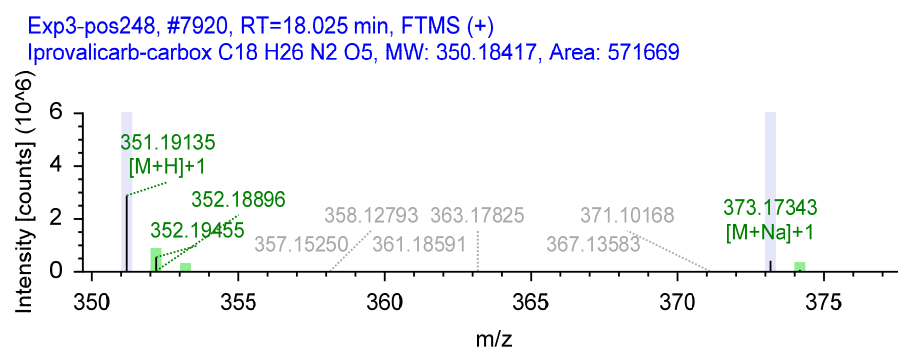
685

686



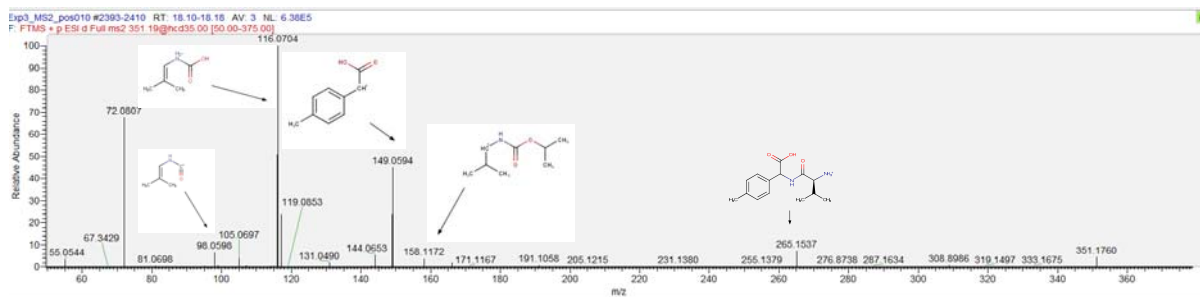
687 Iprovalicarb: carboxy-iprovalicarb

688 MS spectrum



689

690 MS<sup>2</sup> spectrum



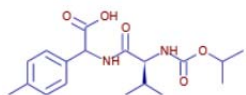
691

692

693 proposed structure (2 possible regioisomers)

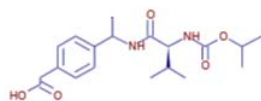
694

695



696

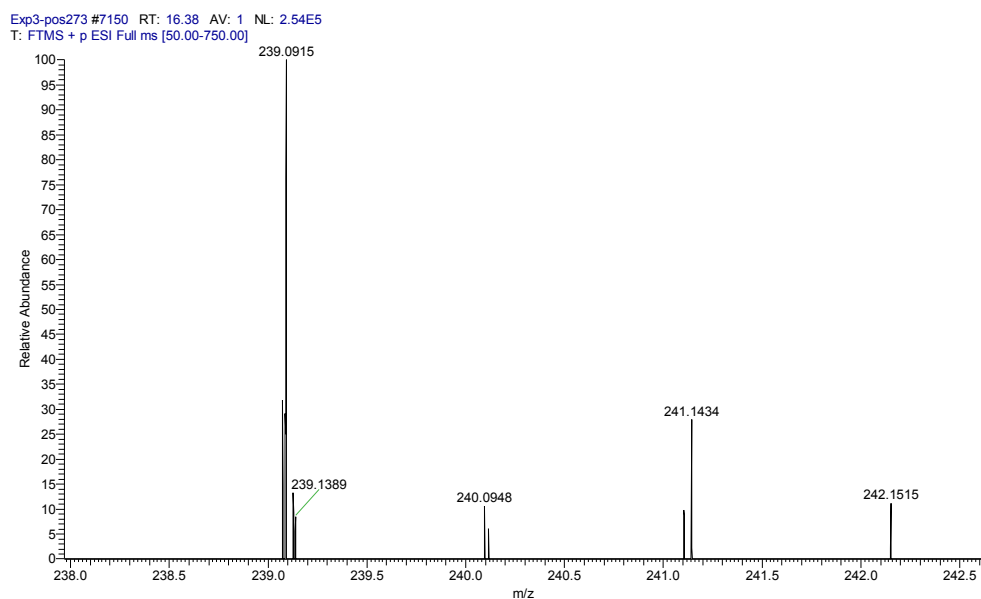
697



698

699 **Bezafibrate: N-dealkylation of amide, oxidation**

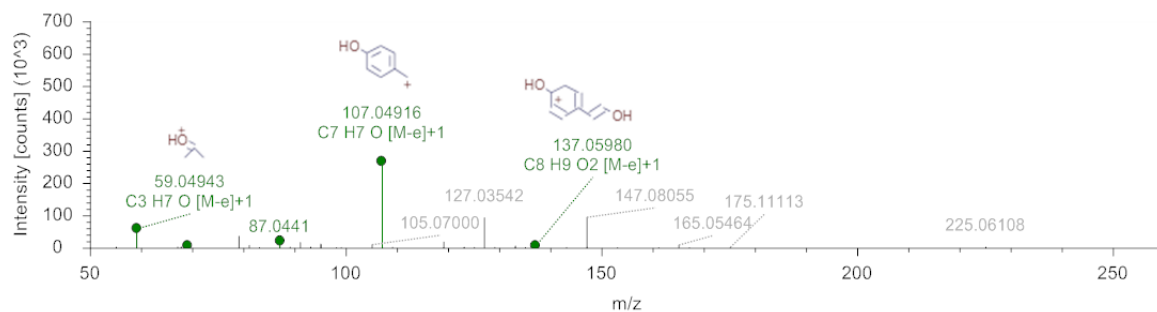
700 MS spectrum



701

702 MS<sup>2</sup> spectrum

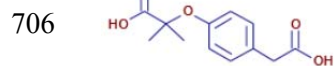
Exp3-pos273, #7167, RT=16.407 min, FTMS (+), MS2 (HCD, DDF, 239.07@60.00, z=+1)  
Bezafibrate-hydrolyzed-carbox C12 H14 O5, MW: 238.08412, Area: 308791  
FISH Coverage: 5 Direct, 16 Unmatched, 22 Skipped



703

704 proposed structure

705



707

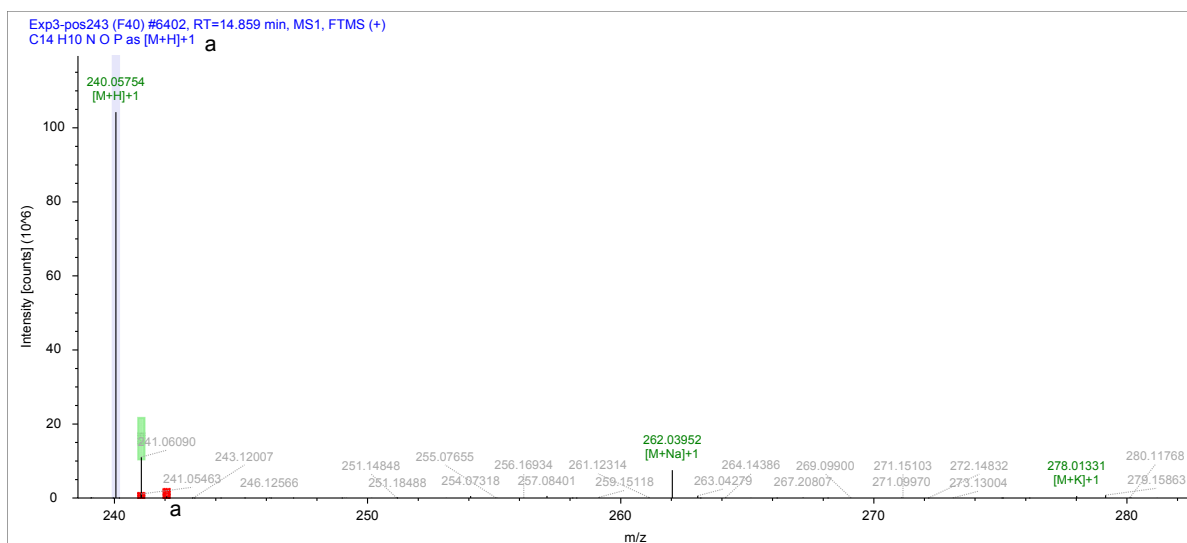
708

709



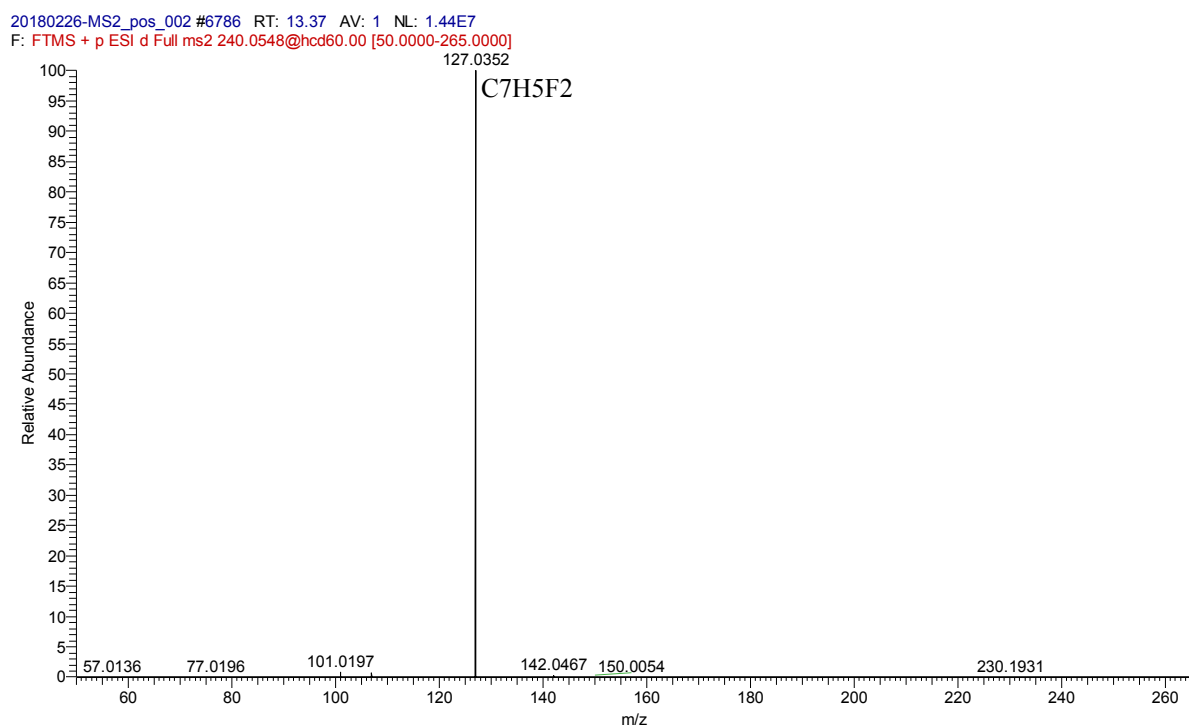
710 **Rufinamide: rufinamide acid**

711 MS spectrum



<sup>a</sup>Because no F-atoms were included in the list of expected elements, the molecular formula and the isotope pattern could not correctly be predicted for this transformation product. The correct molecular formula is C<sub>10</sub>H<sub>7</sub>F<sub>2</sub>N<sub>3</sub>O<sub>2</sub>

716 MS<sup>2</sup> spectrum

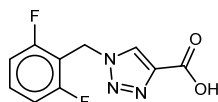


717

718 proposed structure

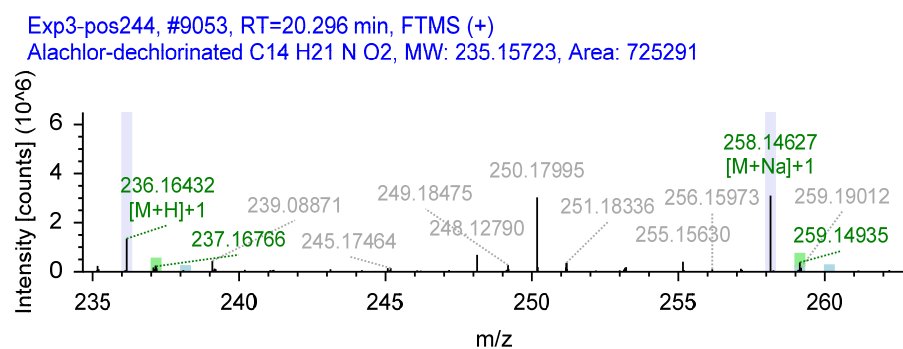
719

720



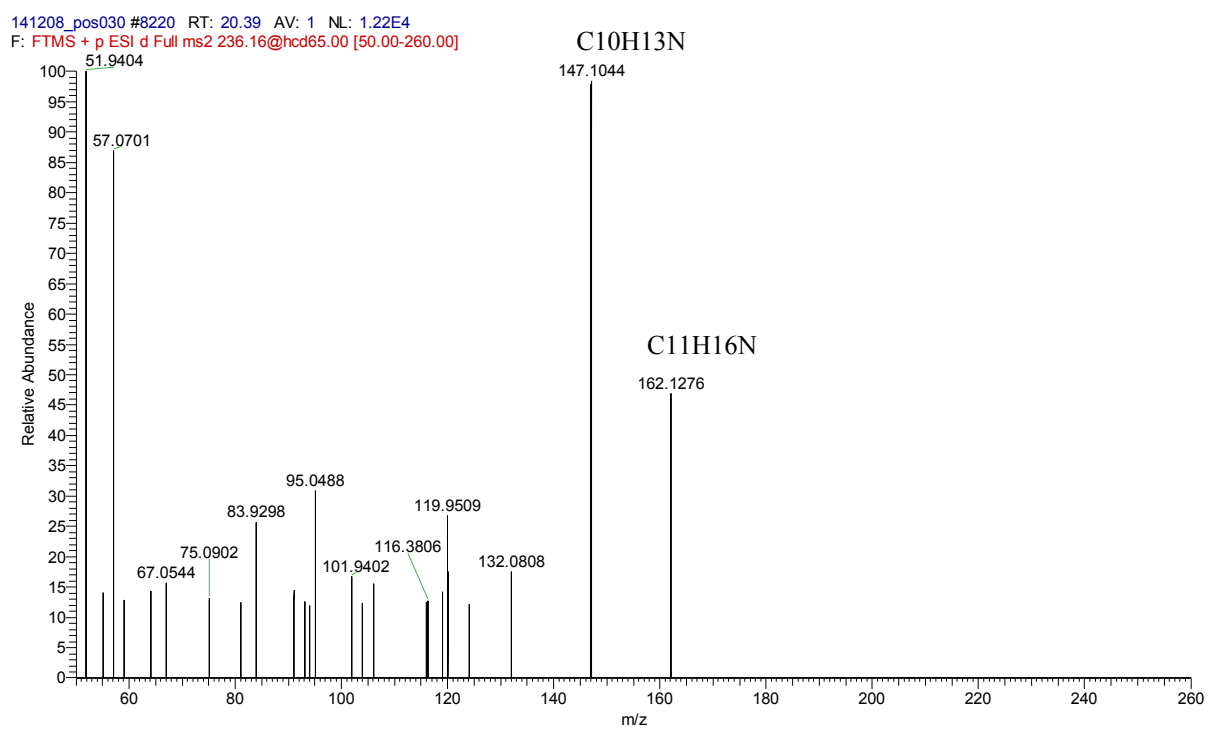
721 Alachlor: dehalogenated alachlor

722 MS spectrum



723

724 MS<sup>2</sup> spectrum

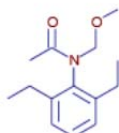


725

726 proposed structure

727

728

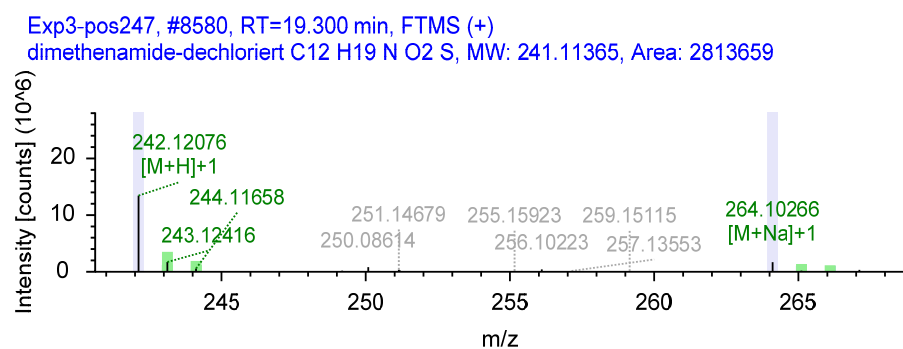


729

730

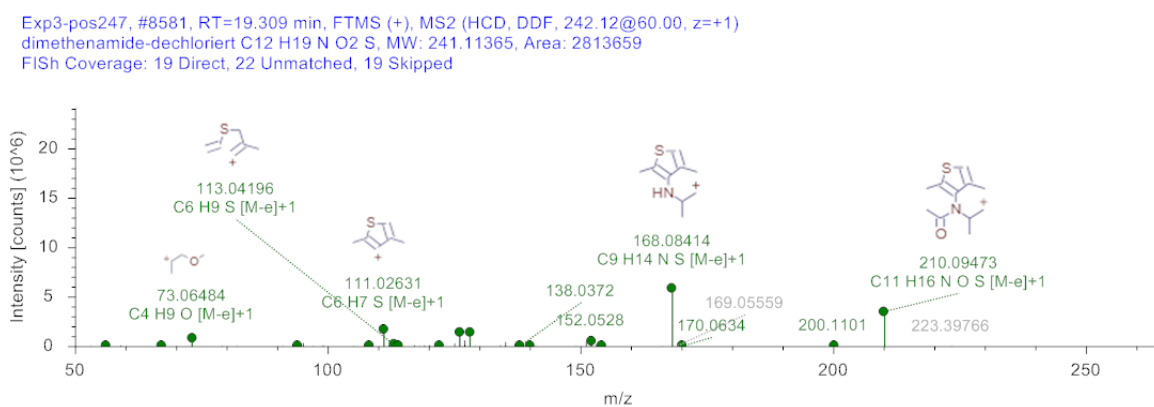
731 **Dimethenamid: dehalogenated dimethenamid**

732 MS spectrum



733

734 MS<sup>2</sup> spectrum



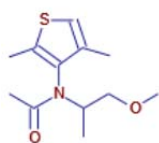
735

736 proposed structure

737

738

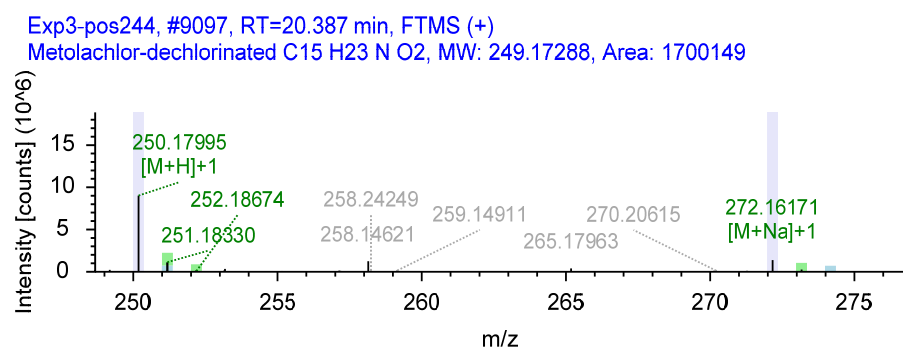
739



740

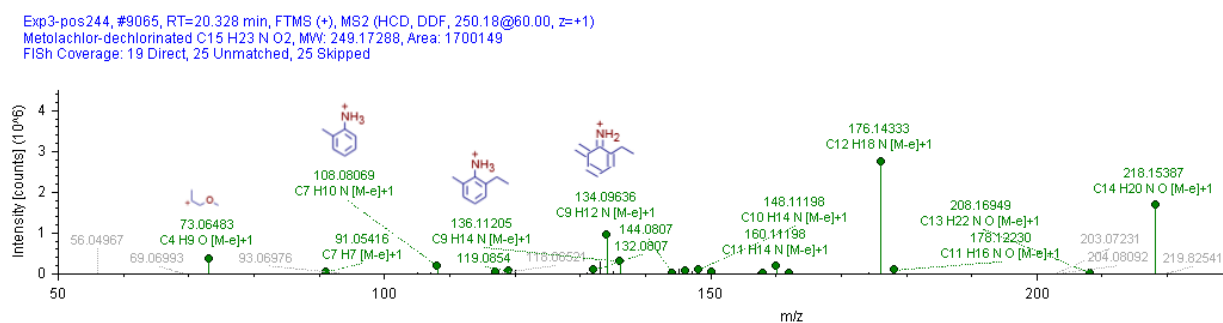
741 **Metolachlor: dehalogenated metolachlor**

742 MS spectrum



743

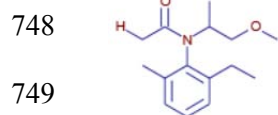
744 MS<sup>2</sup> spectrum



745

746 proposed structure

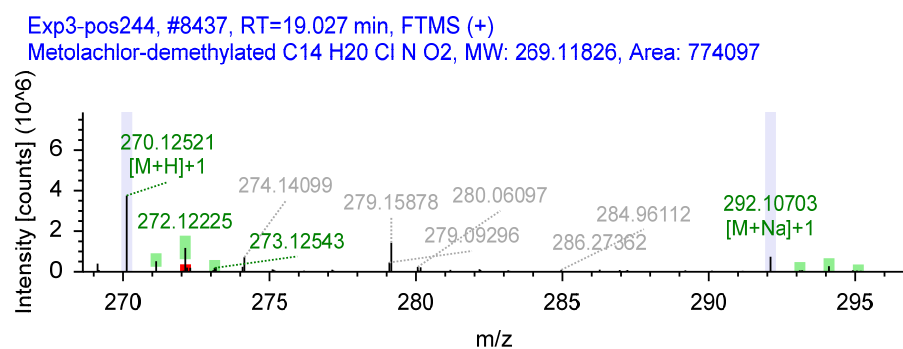
747



750

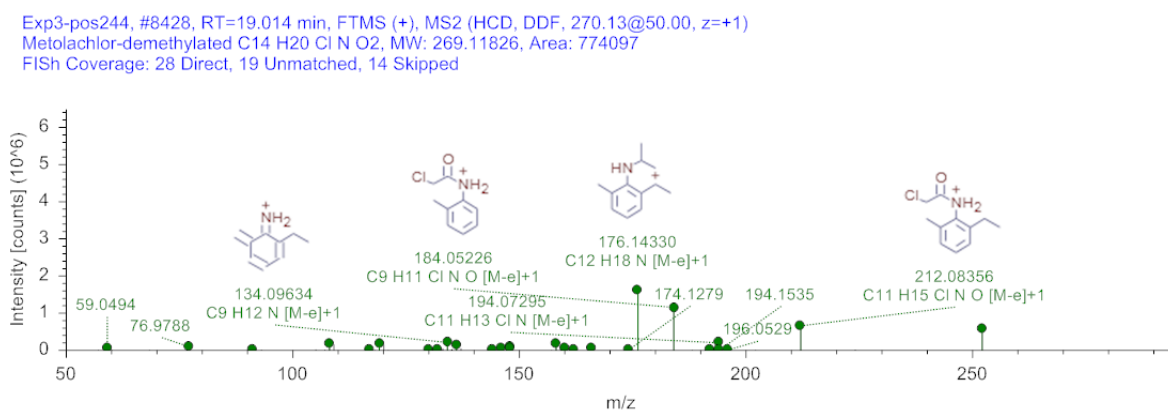
751 **Metolachlor: metolachlor desmethyl**

752 MS spectrum



753

754 MS<sup>2</sup> spectrum



755

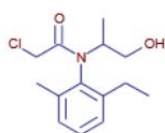
756 proposed structure

757

758

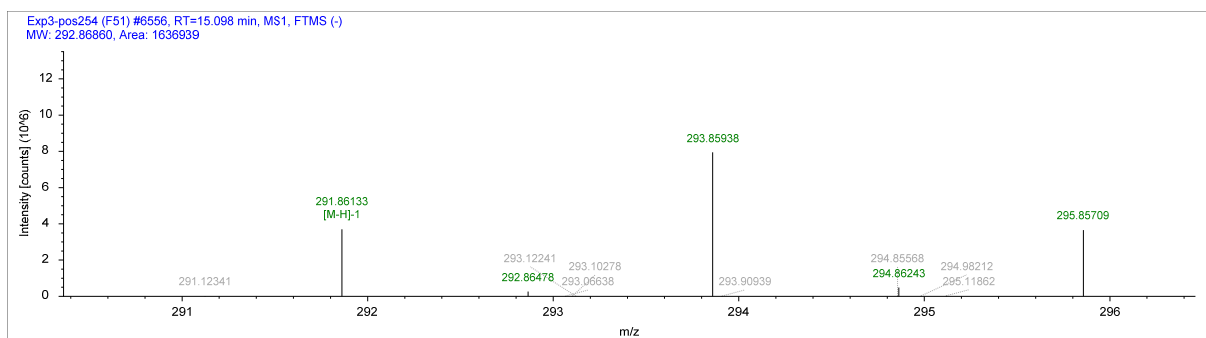
759

760



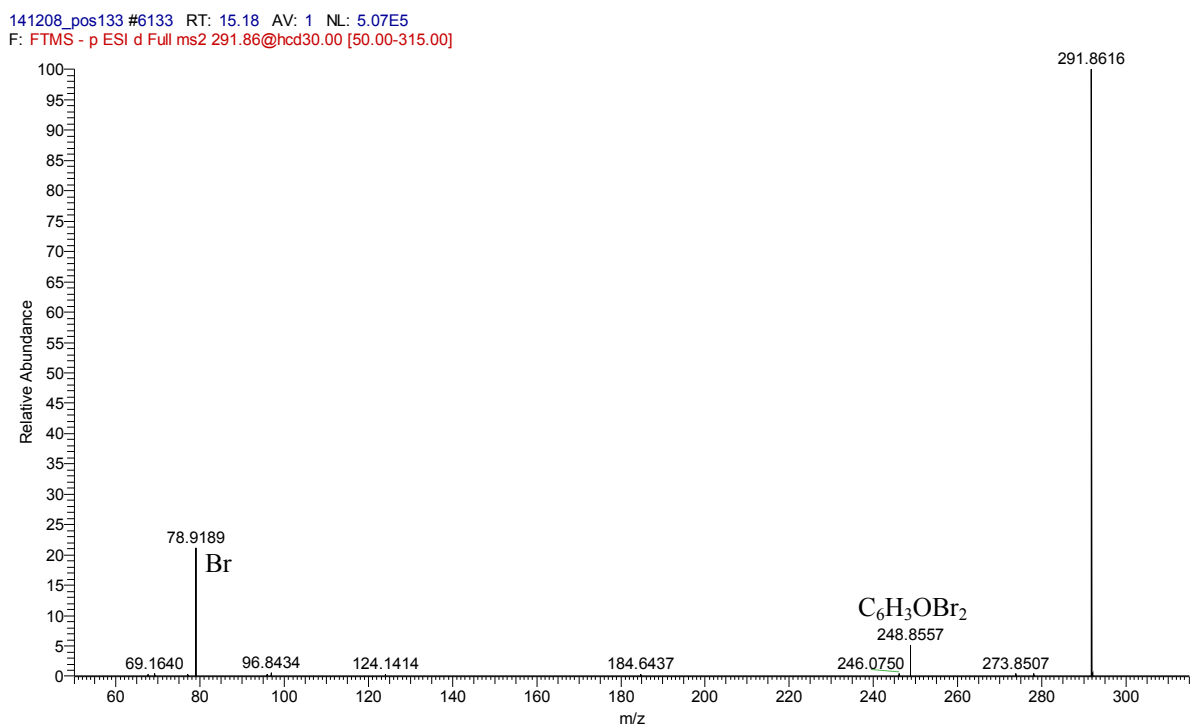
761 **Bromoxynil: bromoxynil-TP291**

762 MS spectrum



763

764 MS<sup>2</sup> spectrum



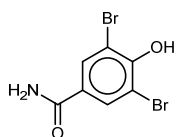
765

766 proposed structure

767

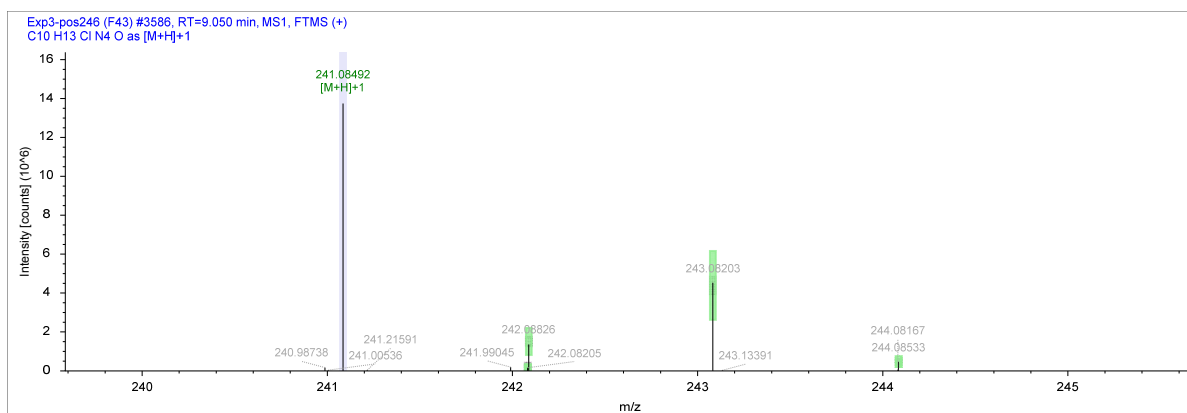
768

769

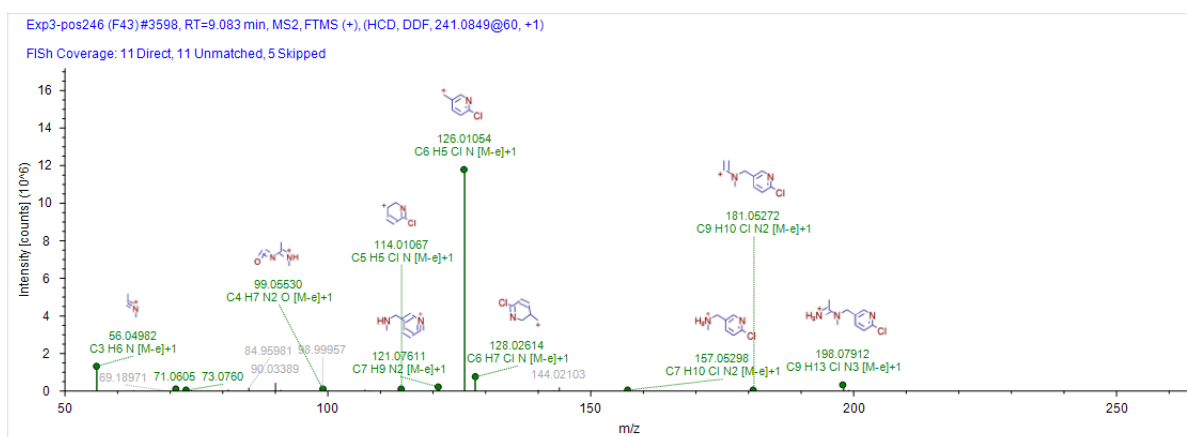


# Acetamiprid: acetamiprid TP241

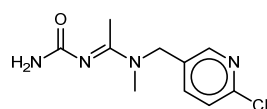
## MS spectrum



## MS<sup>2</sup> spectrum



## proposed structure



## 781    **References**

- 782    1.     Fan, H.; Liu, X.; Wang, H.; Han, Y.; Qi, L.; Wang, H., Oxygen transfer dynamics and activated  
783        sludge floc structure under different sludge retention times at low dissolved oxygen  
784        concentrations. *Chemosphere* **2017**, *169*, 586-595.
- 785    2.     *Standard methods for the examination of water and wastewater*. 21th Edition ed.; American  
786        Public Health Association: 2005.
- 787    3.     Joss, A.; Zabczynski, S.; Göbel, A.; Hoffmann, B.; Löffler, D.; McArdell, C. S.; Ternes, T. A.;  
788        Thomsen, A.; Siegrist, H., Biological degradation of pharmaceuticals in municipal wastewater  
789        treatment: proposing a classification scheme. *Water Res.* **2006**, *40*, 1686-1696.
- 790    4.     Maeng, S. K.; Choi, B. G.; Lee, K. T.; Song, K. G., Influences of solid retention time, nitrification  
791        and microbial activity on the attenuation of pharmaceuticals and estrogens in membrane  
792        bioreactors. *Water Res.* **2013**, *47*, 3151-3162.
- 793    5.     Gulde, R.; Helbling, D. E.; Scheidegger, A.; Fenner, K., pH-dependent biotransformation of  
794        ionizable organic micropollutants in activated sludge. *Environ. Sci. Technol.* **2014**, *48*, 13760-  
795        13768.
- 796    6.     Gao, J.; Ellis, L. B.; Wackett, L. P., The University of Minnesota Pathway Prediction System:  
797        multi-level prediction and visualization. *Nucleic Acids Res.* **2011**, *39*, W406-411.
- 798    7.     Gulde, R.; Anliker, S.; Kohler, H. E.; Fenner, K., Ion Trapping of Amines in Protozoa: A Novel  
799        Removal Mechanism for Micropollutants in Activated Sludge. *Environ. Sci. Technol.* **2018**, *52*,  
800        52-60.
- 801    8.     Gulde, R.; Meier, U.; Schymanski, E. L.; Kohler, H. P.; Helbling, D. E.; Derrer, S.; Rentsch, D.;  
802        Fenner, K., Systematic Exploration of Biotransformation Reactions of Amine-Containing  
803        Micropollutants in Activated Sludge. *Environ. Sci. Technol.* **2016**, *50*, 2908-2920.
- 804    9.     Schwarzenbach, R. P.; Gschwend, P. M.; Imboden, D. M., *Environmental organic chemistry*.  
805        John Wiley & Sons: 2005.
- 806    10.    van den Berg, R. A.; Hoefsloot, H. C.; Westerhuis, J. A.; Smilde, A. K.; van der Werf, M. J.,  
807        Centering, scaling, and transformations: improving the biological information content of  
808        metabolomics data. *BMC Genom.* **2006**, *7*, 1.
- 809    11.    Men, Y.; Achermann, S.; Helbling, D. E.; Johnson, D. R.; Fenner, K., Relative contribution of  
810        ammonia oxidizing bacteria and other members of nitrifying activated sludge communities to  
811        micropollutant biotransformation. *Water Res.* **2016**, *109*, 217-226.
- 812    12.    Luft, A.; Wagner, M.; Ternes, T. A., Transformation of Biocides Irgarol and Terbutryn in the  
813        Biological Wastewater Treatment. *Environ. Sci. Technol.* **2013**, *48*, 244-254.
- 814    13.    Helbling, D. E.; Hollender, J.; Kohler, H.-P. E.; Fenner, K., Structure-Based Interpretation of  
815        Biotransformation Pathways of Amide-Containing Compounds in Sludge-Seeded Bioreactors.  
816        *Environ. Sci. Technol.* **2010**, *44*, 6628-6635.
- 817    14.    Quintana, J. B.; Weiss, S.; Reemtsma, T., Pathways and metabolites of microbial degradation  
818        of selected acidic pharmaceutical and their occurrence in municipal wastewater treated by a  
819        membrane bioreactor. *Water Res.* **2005**, *39*, 2654-2664.
- 820    15.    Kjeldal, H.; Zhou, N. A.; Wissenbach, D. K.; von Bergen, M.; Gough, H. L.; Nielsen, J. L.,  
821        Genomic, Proteomic, and Metabolite Characterization of Gemfibrozil-Degrading Organism  
822        *Bacillus* sp. GeD10. *Environ. Sci. Technol.* **2016**, *50*, 744-755.
- 823    16.    Helbling, D. E.; Johnson, D. R.; Honti, M.; Fenner, K., Micropollutant Biotransformation  
824        Kinetics Associate with WWTP Process Parameters and Microbial Community Characteristics.  
825        *Environ. Sci. Technol.* **2012**, *46*, 10579-10588.
- 826    17.    Achermann, S.; Bianco, V.; Mansfeldt, C. B.; Vogler, B.; Kolvenbach, B. A.; Corvini, P. F. X.;  
827        Fenner, K., Biotransformation of Sulfonamide Antibiotics in Activated Sludge: The Formation  
828        of Pterin-Conjugates Leads to Sustained Risk. *Environ. Sci. Technol.* **2018**, *52*, 6265-6274.
- 829    18.    Kern, S.; Baumgartner, R.; Helbling, D. E.; Hollender, J.; Singer, H.; Loos, M. J.;  
830        Schwarzenbach, R. P.; Fenner, K., A tiered procedure for assessing the formation of



831 biotransformation products of pharmaceuticals and biocides during activated sludge  
832 treatment. *J. Environ. Monit.* **2010**, *12*, 2100-2111.  
833